UNIVERSITY OF OKLAHOMA

GRADUATE COLLEGE

BIOSURFACTANTS: CHARACTERIZATION, MICROEMULSION FORMATION AND POTENTIAL APPLICATIONS

A DISSERTATION

SUBMITTED TO THE GRADUATE FACULTY

in partial fulfillment of the requirements for the

Degree of

DOCTOR OF PHILOSOPHY

By

THU THI LE NGUYEN
Norman, Oklahoma
2009

Downloaded from SHAREOK. Persistent Handle URL: https://hdl.handle.net/11244/318566

BIOSURFACTANTS: CHARACTERIZATION, MICROEMULSION FORMATION AND POTENTIAL APPLICATIONS

A DISSERTATION APPROVED FOR THE
SCHOOL OF CHEMICAL, BIOLOGICAL AND MATERIALS ENGINEERING

BY

_____

Dr. Jeffrey H. Harwell, Chair

_____

Dr. David A. Sabatini

_____

Dr. John F. Scamehorn

_____

Dr. Tohren C. G. Kibbey

_____

Dr. Lance L. Lobban

© Copyright by THU THI LE NGUYEN 2009
All Rights Reserved.

DEDICATION

This dissertation is dedicated to my loving parents, Hung Vu and Quyet Nguyen, and sisters, Tam and Huong, my dear husband, Dung Tran, and son, Minh Tran.

ACKOWLEDGEMENTS

I would like to express my deep gratitude to all the people who have helped me with their kindness and generosity throughout my graduate years, who have made this dissertation possible and because of whom my graduate life has become one of the most enjoyable and memorable experiences that I will cherish forever.

My deepest gratitude goes to my advisor, Dr. Sabatini, who has played a great role in making me become who I am today. With his guidance from the beginning of my graduate study and his faith in my ability, I have become more independent and confident. I also would like to thank his wife, Frances Sabatini, for all the support and encouragement that she has given me, especially since I had my baby son. Their kindness has meant a lot to my whole family and has kept my work life and family life enjoyable.

I would also like to express my gratitude to Dr. Jeffrey Harwell, Dr. John Scamehorn, Dr. Tohren Kibbey and Dr. Lance Lobban for being my committee members, for helpful advice and discussion from the beginning to the completion of my dissertation. Besides, I would like to thank Dr. Edgar Acosta for all the advice and suggestion he has given me in both family and research matters.

Most importantly, this dissertation would not be possible without the encouragement, the love and the support of my parents, my parents-in-law, my sisters, my husband and my son, to whom this dissertation is dedicated and who have been giving me all the love and strength to move every step in my life.

I have found myself grateful to have known and become a part of Sherry and Dan Glenn's family, who have been like parents to my little family and have loved us as their children and grandchild, especially when we are not in our home country. Without them, we may not have become who we are today.

My graduate study would not be so enjoyable and memorable without my host family, student colleagues and friends at the University of Oklahoma. I would like to thank Ha and Larry Flanagan family, Linh, Anh, Oat, Ha, Huong, Son, Pan, Tri, Sezin, Laura, Chris, Damon, Khwan, Him, Mink and Emma for their encouragement and support. My special thank is sent to my undergraduate research assistants Ashley Edelen and Bridgett Neighbors for their lab-assistant, hard work and friendship.

I would like to thank all the staff members of both Civil Engineering and Environmental Science Department and the Chemical, Biological, and Materials Engineering Department for their kind assistance during my years of study.

Finally, I would like acknowledge the Integrated Petroleum and Environment Consortium (IPEC), the Oklahoma Center for Advancement of Science and Technology (OCAST), the Oklahoma Department of Energy (OK DOE) and the Institute of Applied Surfactant Research (IASR) at the University of Oklahoma for financial supports.

TABLE OF CONTENTS

	Page
ACKNOWLEDGEMENTS	iv
TABLE OF CONTENT	vi
LIST OF TABLES	viii
LIST OF FIGURES	xiv
ABSTRACT	
CHAPTER 1. Introduction	1
References	3
CHAPTER 2. Rhamnolipid Biosurfactant Mixtures for Environmental Remediation	6
Abstract	6
Introduction	7
Materials and Methods	10
Results and Discussion	15
Conclusions	29
Acknowledgements	30
References	30
CHAPTER 3. Formulating Alcohol-Free Microemulsions Using Rhamnolipid Biosurfactant and Rhamnolipid Mixtures	35
Abstract	35
Introduction	36
Materials and Methods	38
Results and Discussion	41
Acknowledgements	52
References	52

CHAPTER 4. Biodiesel Production via Peanut Oil Extraction Using Diesel-Based Reverse Micellar Microemulsions 57

Abstract 57
Introduction 58
Materials and Methods 61
Results and Discussion 67
Conclusions 77
Acknowledgements 78
References 78

CHAPTER 5. Biocompatible Lecithin-Based Microemulsions with Rhamnolipid and Sophorolipid Biosurfactants: Potential Applications 83

Abstract 83
Introduction 84
Materials and Methods 87
Results and Discussion 93
Conclusions 104
Acknowledgements 105
References 105

CHAPTER 6. Conclusions 112

APPENDIX A. Rhamnolipid Biosurfactant Mixtures for Environmental Remediation (Chapter 2) 115

APPENDIX B. Formulating Alcohol-Free Microemulsions Using Rhamnolipid Biosurfactant and Rhamnolipid Mixtures (Chapter 3) 116

APPENDIX C. Biocompatible Lecithin-Based Microemulsions with Rhamnolipid and Sophorolipid Biosurfactants: Potential Applications (Chapter 5) 117

LIST OF TABLES

Table 2.1. Properties of oils used. 12

Table 2.2. Optimum formulations of surfactant mixtures for different hydrocarbons. 29

Table 3.1. Solubilization parameters and fraction of JBR in the middle phase microemulsion at optimum formulations of rhamnolipid microemulsions (at 23 ± 1 ^{o}C). 43

Table 4.1. Surfactants used in this work. 63

Table 5.1. Surfactants used in this work. 89

Table 5.2. Oils used in this work. 90

LIST OF FIGURES

Figure 2.1. Structures of the rhamnolipids: (a) monorhamnolipid (α-L-rhamnopyranosyl-β-hydroxydecanoyl-β-hydroxydecanoate) and (b) dirhamnolipid (2-O-α-L-rhamnopyranosyl-α-L-rhamnopyranosyl-β-hydroxydecanoyl-β-hydroxydecanoate) (adapted from ref [4] and [18]). 11

Figure 2.2. Correlation between optimal salinity (S*) (□) and EACN as determined by optimum equilibrium IFT (IFT*) (▲). The rhamnolipid concentration was 0.1w/w% for all oils. Data points for IFTs represent the average from three to five measurements; error bars are included but at times are smaller than the data symbols. 16

Figure 2.3. Phase diagram of rhamnolipid with toluene (CMC of 0.001 w/w%). The boundary lines (solid for 23 ± 1 °C; dashed for 55 ± 1 °C) connect all the points where a transition for microemulsion type was observed. The line labeled optimum salinity, which cuts through the interior of the phase diagram, corresponds to the optimum salinity at each surfactant concentration, as further studied in Figure 2.4. The phase diagrams were drawn based on averages of triplicate experiments. 19

Figure 2.4. Optimum equilibrium IFT for toluene versus rhamnolipid concentration (below the CμC, salinity is constant at 14.5 w/w% as represented by vertical line in Figure 2.3; above the CμC, salinity varies to correspond to optimum salinity in the center of phase boundaries as represented by the slanted line in Figure 2.3). Data points represent the average from triplicate measurements, error bars are included but are at times smaller than the data points. 21

Figure 2.5. IFT of mixtures of rhamnolipid and C12,13–8PO sulfate for toluene (♦), hexane (◊), decane (▲), and hexadecane (Δ) at optimum salinity (S*) for each system. The total surfactant concentration was 0.1 w/w%. The IFT shown in this figure was the optimum IFT for each formulation. Data points represent the average from triplicate measurements, error bars are included but are at times smaller than the data points. 23

Figure 2.6. IFT of mixtures of rhamnolipid and C16–10.7PO sulfate for toluene (♦), hexane (◊), decane (▲), and hexadecane (Δ). The total surfactant concentration was 0.1 w/w%. The ratio of rhamnolipid to C16–10.7PO sulfate was fixed at 1:1 by weight percent basis (or 2:1 by molar basis). Data points represent the average from triplicate measurements, error bars are included but are at times smaller than the data points. 25

Figure 2.7. Optimum IFT (m) and optimum salinity (S*) (&) of a mixture of rhamnolipid and C16–18PO–2EO sulfate versus EACN (EACN values of 1 for toluene, 6 for hexane, 10 for decane, and 16 for hexadecane). The total surfactant concentration was 0.1 w/w%. The ratio of rhamnolipid to C16–18PO–2EO sulfate was fixed at 3:7 by weight basis (or 1:1 by molar basis). Data points represent the average from triplicate measurements, error bars are included but are at times smaller than the data points. 27

Figure 3.1. Molecular structures of the rhamnolipids: (a) monorhamnolipid, (b) dirhamnolipid (adapted from ref. [3]). 36

Figure 3.2. Microemulsion formulations (Winsor Types I, II and III) with (a) limonene and (b) diesel using two surfactant mixtures containing rhamnolipid: SBDHS/JBR (open squares) and SBDHS/JBR/OA (filled circles) (at 23 ± 1 ^{o}C). 42

Figure 3.3. Shift in optimum electrolyte concentration [ln (S^*/S_1^*)] for SDHS-JBR-benzene at 23 ± 1 ^{o}C microemulsions as a function of the fraction of JBR in the system. 46

Figure 3.4. Phase diagram of formulation (Winsor Types I, II and III) composed of SMEE3EO, JBR and OA with limonene at fixed ratio of SMEE3EO/JBR/OA = 4/1.75/2.5 by wt.%. The phase boundary connects all the points where a transition for microemulsion type was observed. The line labeled optimum salinity, which cuts through the interior of the phase diagram, corresponds to the optimum salinity at each surfactant concentration, as further studied in Figure 3.5 (at 23 ± 1 ^{o}C). 48

Figure 3.5. Interfacial tensions at optimum formulations of surfactant-limonene microemulsions from Figure 3.4 (below CμC, salinity is constant at 13 wt.% as presented by the vertical dashed line in Figure 3.4; above the CμC, salinity varies to correspond to optimum salinity in the center of the phase boundaries as represented by the slanted dashed line in Figure 3.4) (at 23 ± 1 ^{o}C). 50

Figure 4.1. Structures of the rhamnolipids: (a) monorhamnolipid, (b) dirhamnolipid (adapted from [25]) and (c) Sophorolipid (Ac = Acetyl) (adapted from [26]). 62

Figure 4.2. Schematic diagram of the extraction process. 64

Figure 4.3. Partial fish phase diagrams with diesel of two surfactant systems: (a) Lecithin/SPL/JBR = 1/1/0.628 by wt. and (b) SBDHS/JBR/OA = 1.11/1.44/0.67 by wt. 68

Figure 4.4. Effect of extraction solvent on oil extraction efficiency at 60 minute extraction time and 200 rpm shaking speed. 70

Figure 4.5. Effect of solid-to-solvent ratio on oil extraction efficiency at 40 minute extraction time and 200 rpm shaking speed using formulation of AOT/JBR/OA = 0.0125/0.0125/0.0125 M diesel-based reverse micellar microemulsion. 72

Figure 4.6. Effect of extraction time on oil extraction efficiency at 200 rpm shaking speed, solid-to-solvent ratio of 1:5 using the formulation of AOT/JBR/OA = 0.0125/0.0125/0.0125 M diesel-based reverse micellar microemulsion. 73

Figure 4.7. Fraction of peanut oil in extracted oil blend at various solid-to-solvent ratios and 200 rpm shaking speed for 40 minutes using the formulation of AOT/JBR/OA = 0.0125/0.0125/0.0125 M diesel-based reverse micellar microemulsion. 75

Figure 4.8. Kinematic viscosity of extracted oil blend at different solid-to-solvent ratios and temperatures, 200 rpm shaking speed and 40 minute extraction using the formulation of AOT/JBR/OA = 0.0125/0.0125/0.0125 M diesel-based reverse micellar microemulsion. 76

Figure 5.1. Structures of the rhamnolipids: (a) monorhamnolipid and (b) dirhamnolipid (adapted from ref. [3]) 88

Figure 5.2. Structures of the sophorolipids (Ac = Acetyl): (a) lactone form and (b) acidic form (adapted from ref. [4]). 88

Figure 5.3. Optimum salinity (S^*) for varying fraction of rhamnolipid in mixtures with SDHS (♦), SDBHS (■), SPL-P (▲) and SPL-O (×) in microemulsion formulation with benzene. Total surfactant concentration is kept constant at 0.1 M for all mixtures and surfactant ratios. 95

Figure 5.4. Phase behavior diagrams for biocompatible IPM-based microemulsions at different formulation conditions: (A) Effect of temperature (10 ^{o}C, 25 ^{o}C and 40 ^{o}C) and (B) Effect of electrolyte concentration (0.9% and 4.0% w/v). Microemulsions were prepared at Lecithin/SPL weight ratio = 1/1. 98

Figure 5.5. Phase behavior diagram for IPM and Limonene microemulsions at 25 ^{o}C, JBR/Lecithin weight ratio = 1/1, 0.9% w/v NaCl. 100

Figure 5.6. Interfacial tension and microemulsion for four different oils: limonene (♦), IPM (■), decane (Δ) and hexadecane (×). Formulations were prepared with Lecithin/SPL concentration of 4/4% w/v and 0.9% w/v NaCl. 101

Figure 5.7. Detergency performance (A) and dynamic IFT (B) of our formulation vs. commercial detergent at different total surfactant active concentration. Our formulation has Lecithin/SPL/JBR = 1.0/1.0/0.3 by wt. ratio and 0.9% w/v NaCl. 103

ABSTRACT

Biosurfactants, which are produced from microorganisms, have become of interest due to their non-toxic nature, their biodegradability and their production from renewable resources. Research has evaluated the use of biosurfactants in a wide variety of potential applications such as environmental bioremediation, biomedical applications, cosmetics, personal care products and perfume and fragrance industry. However, limited research has evaluated microemulsion formulations using biosurfactants. Microemulsions are thermodynamically stable dispersions of oil and water stabilized by surfactant films. Microemulsions possess ultralow interfacial tension and high solubilization capacity, making them desirable in enhanced oil recovery, drug delivery, cosmetic and pharmaceutical applications. Therefore, in this work we characterized the hydrophobicity/hydrophilicity of biosurfactants, specifically rhamnolipid and sophorolipid biosurfactant, and evaluated their ability to formulate alcohol-free microemulsions with a range of oils (both oil types and oil EACNs). We also demonstrated the feasibility of vegetable oil extraction using diesel-based reverse micellar microemulsion; as a result, blends of diesel and vegetable oil were produced and evaluated for biofuel used in diesel engines. Biocompatible lecithin-based microemulsions using rhamnolipid and sophorolipid biosurfactants formulated with limonene and isopropyl myristate were shown to be insensitive to temperature and salinity changes, making them desirable in cosmetic and drug delivery applications. In addition, this work showed that the hexadecane detergency

performance of our biocompatible formulation was better than that of commercial detergency and comparable to formulations reported in the literature.

CHAPTER 1

Introduction

The surfactant industry has recently exceeded US $9 billion a year, and the demand for surfactants is still increasing [1, 2] due to their potential for application in a wide variety of industries. The surfactants currently in widespread use are mostly synthetic petroleum-based surfactants. There has been growing interest in biosurfactants to replace synthetic surfactants due to their relatively non-toxic and biodegradable properties, their diversity and their production from renewable resources.

Biosurfactants are produced from microorganisms with diverse structures such as glycolipids, phospholipids, polysaccharide-lipid complexes and lipopeptides [3, 4]. Biosurfactants have been evaluated as potentials in various applications such as environmental bioremediation, removal of heavy metals from contaminated soil, biomedical applications [5-7], cosmetics and personal care products [8] and in the perfume and fragrance industry [9]. However, none of these studies applied the use of biosurfactants in microemulsion form. Therefore, this dissertation explores the use of biosurfactants in formulating microemulsions which can be used in different applications.

Microemulsions are thermodynamically stable dispersions of oil and water stabilized by surfactant films [10], which makes them desirable in enhanced oil recovery (EOR), drug delivery, cosmetic and pharmaceutical applications [1, 11, 12]. These applications take advantage of the ultralow interfacial tension property and high

solubilization capacity of microemulsions [13]. Microemulsions can exist in four forms, known as Winsor Type microemulsions [10, 14]. Type I and Type II microemulsions exhibit two phase systems. Type I microemulsion solubilizes oil in spherical normal micelles within the water-continuous phase while Type II microemulsion solubilizes water in reverse micelles within the oil-continuous phase. Type III microemulsion is three-phase system in which the middle phase microemulsion is in equilibrium with the excess oil and excess water phases. As the surfactant concentration increases, the volume of the middle phase microemulsion increases until the surfactant concentration is high enough to solubilize all the excess oil and excess water into a single phase microemulsion system, known as Type IV microemulsion.

Limited studies have evaluated biosurfactant-based microemulsions, with the addition of alcohols being necessary to form microemulsions [15, 16]. The framework of this dissertation is divided into two areas: (1) characterizing biosurfactants, specifically rhamnolipid and sophorolipid biosurfactants, by their hydrophobicity/hydrophilicity and evaluating their ability in formulating microemulsions without the aid of alcohol; and (2) evaluating the performance of biosurfactant-based microemulsions in many applications such as vegetable oil extraction, cosmetics, drug delivery and detergency. Chapters 2 and 3 report on studies of rhamnolipid biosurfactant while chapters 4 and 5 focus on the study of sophorolipid biosurfactants and application of biosurfactant-based microemulsions.

In the first study of rhamnolipid (Chapter 2), rhamnolipid biosurfactant was found to be relatively hydrophilic and its ability to formulate microemulsions with a wide range of petroleum-based n-alkane oils was evaluated in mixtures with synthetic surfactants. Further studies reported in Chapter 3 confirmed the finding of the hydrophilicity of rhamnolipid from Chapter 2 and were able to replace synthetic surfactants with biorenewable surfactants in forming microemulsions with different kinds of oils (limonene and diesel). Next the research was extended to the study of sophorolipid biosurfactants in Chapter 4 with more fundamental characterization in Chapter 5. Both of these last chapters evaluated the application of biosurfactant-based microemulsions. Chapter 4 proposed a new approach to vegetable oil extraction using diesel-based reverse micellar microemulsions to produce vegetable oil/diesel blends for biodiesel application and successfully demonstrated the high oil extraction efficiency obtained with this extraction method. Chapter 5 investigated the potentials of biocompatible lecithin-based microemulsions in cosmetic and drug delivery applications. Chapter 5 also demonstrated the detergency power of the biosurfactant formulations on hexadecane removal.

References

1. Desai, J. D.; Banat, I. M. 1997. Microbial Production of Surfactants and Their Commercial Potential. Microbiol. Molecular Biol. Rev. 61 (1), 47-64.

2. Maier, R. M.; Soberón-Chávez. 2000. *Pseudomonas Aeruginosa* Rhamnolipids: Biosynthesis and Potential Applications. Appl. Microbiol. Biotechnol. 54, 625-633.
3. Lin, S. C.; Minton, M. A.; Sharma, M. M., Georgiou, G. 1994. Structural and Immunological Characterization of a Biosurfactant Produced by *Bacillus Lichenisformis JF-2*. Appl. Environ. Microbiol. 60 (1), 31-38.
4. Urum, K. and Pekdemir, T. 2004. Evaluation of Biosurfactants for Crude Oil Contaminated Soil Washing. Chemosphere 57, 1139-1150.
5. Kitamoto, D.; Isoda, H.; Nakahara, T. 2002. Functions and Potential Applications of Glycolipid Biosurfactants – from Energy-saving Materials to Gene Delivery Carriers. J Biosci Bioeng 94 (3), 187-201.
6. Miller R. M. 1995. Biosurfactant-Facilitated Remediation of Metal-Contaminated Soils. Environ Health Perspect 103 (Suppl 1), 59-62.
7. Herman, D. C.; Lenhard, R. J.; Miller, R. M. 1997. Formation and Removal of Hydrocarbon Residual in Porous Media: Effects of Attached Bacteria and Biosurfactants. Environ Sci Technol 31, 1290-1294.
8. Mager, H.; Röthlisberger, R.; Wzgner, F. 1987. Use of Sophorose-lipid Lactone for the Treatment of Dandruffs and Body Odour. European Patent 0,209,783.
9. Inoue, S. and Miyamoto, N. 1980. Process for Producing a Hydroxyfatty Acid Ester. US Patent 4,201,844.
10. Rosen, M. J. 1989. Surfactants and Interfacial Phenomena, 2nd ed. Wiley, New York.

11. McCray, J. E.; Bai, G.; Maier, R. M.; Brusseau, M. L. 2001. Biosurfactant-Enhanced Solubilization of NAPL mixtures. J. Contam. Hydrol. 48 (1-2), 45-68.
12. Acosta, E.; Tran, S.; Uchiyama, H.; Sabatini, D. A.; Harwell, J. H. 2002. Formulating Chlorinated Hydrocarbon Microemulsions Using Linker Molecules. Environ. Sci. Technol. 36, 4618-4624.
13. Acosta, E.; Do, P. M.; Harwell, J. H.; Sabatini, D. A. 2003. Linker-Modified Microemulsions for a Variety of Oils and Surfactants. J. Surfactants Deterg. 6 (4), 353-363.
14. Bourrel, M. and Schechter, R. S. 1988. Microemulsions and Related Systems: Formulation, Solvency, and Physical Properties. Surfactant series 30. Marcel Dekker, New York.
15. Xie, Y.; Li, Y.; Ye, R. 2005. Effect of Alcohols on the Phase Behavior of Microemulsions Formed by a Biosurfactant – Rhamnolipid. J. Despers. Sci. Technol. 26, 455-461.
16. Xie, Y.; Ye, R.; Liu, H. 2007. Microstructure Studies on Biosurfactant – Rhamnolipid/n-Butanol/Water/n-Heptane Microemulsion System. Colloid Surf. A Physicochem. Eng. Asp. 292: 189-195.

CHAPTER 2

Rhamnolipid Biosurfactant Mixtures for Environmental Remediation[1]

Abstract

This study investigated the efficiency of rhamnolipid biosurfactant and synthetic surfactant mixtures for improving the interfacial activity of the surfactant system against several light non-aqueous-phase liquids (LNAPLs). Since the rhamnolipid biosurfactant proved to be relatively hydrophilic, we hypothesized that mixtures of rhamnolipid biosurfactants with more hydrophobic synthetic surfactants would produce lower interfacial tensions (IFTs) than an individual rhamnolipid biosurfactant. The minimum IFT observed for rhamnolipid alone and toluene (0.03 mN/m) was one order of magnitude lower than for hexane, decane, and hexadecane, demonstrating the relatively hydrophilic nature of the rhamnolipid. The low IFTs even at the low surfactant concentration used suggest mobilization as the dominant oil-removal mechanism versus supersolubilization. The critical micelle concentration (CMC) and critical microemulsion concentration (CμC) of the rhamnolipid were found to be 0.001 w/w% (0.019 mM) and 0.01 w/w% (0.19 mM), respectively. Three alkyl propoxylated (PO) sulfate synthetic surfactants were individually mixed with the rhamnolipid. As the hydrophobicity of the surfactant mixture approached that of the hydrocarbon, IFT values decreased by one to two orders of magnitude below that

[1] This chapter or portions thereof has been published previously in *Water Research* under the title "Rhamnolipid Biosurfactant Mixtures for Environmental Remediation", Water Research, 2008, 42, 1735-1743. This current version has been formatted for this dissertation.

achieved with individual surfactants. This work shows that the rhamnolipid has excellent phase behavior at low concentrations and can be used in surfactant mixtures to achieve the low IFT values needed for environmental remediation, enhanced oil recovery (EOR), and other applications.

Key words: biosurfactant, alkyl propoxylated sulfate surfactants, hydrophobicity, interfacial tension, petroleum hydrocarbons, environmental remediation

Introduction

Surfactants are amphiphilic molecules having both hydrophilic and hydrophobic moieties, which causes them to accumulate at the interface between immiscible fluid phases (e.g., oil/water or air/water interfaces) [1] and reduce the interfacial tension (IFT) [2]. Surfactants are categorized by their head groups as nonionic, anionic or cationic (negatively or positively charge), or amphoteric (both positive and negative charges) [3, 4].

Whereas synthetic surfactants are produced from petroleum feedstock, biosurfactants are produced from renewable resources. There are several types of substrates used for biosurfactant production such as water-soluble carbon sources (glycerol, glucose, and ethanol), water-immiscible substrates (n-alkanes and olive oil), and nitrogen sources (ammonium salts and urea) [2; 5]. Microorganisms produce biosurfactants with diverse structures including glycolipids, phospholipids, polysaccharide–lipid complexes, lipopeptides, and hydroxylated and cross-linked fatty

acids [4, 6]. While nonionic and anionic biosurfactants have been reported, cationic biosurfactants have not been found [7]. Biosurfactant head groups usually consist of mono-, di-, or polysaccharides, carboxylic acids, amino acids, or peptides. The hydrophobic tail can be saturated, unsaturated, or hydroxylated fatty acids. Biosurfactants are readily biodegradable, making them well suited for environmental and industrial applications [6, 8]. In addition, biosurfactant-based systems are biorenewable as compared with petroleum-based surfactants. However, to date, biosurfactants are more expensive with production costs of about 3–10 times higher than that of the chemical counterparts [9], making it critical to maximize the performance of biosurfactant-based systems.

Above the critical micelle concentration (CMC), surfactant monomers aggregate to form micelles [1]. Many system properties remain unchanged above the CMC since additional surfactant forms micelles rather than increasing the surfactant aqueous activity [1, 4]. Depending on system properties, micellar configurations can be spherical; elongated, cylindrical, rod-like micelles; large, flat, lamellar micelles; and large vesicles. Micelle formation also plays an important role in understanding microemulsions. Microemulsions are thermodynamically stable emulsions that contain water and oil domains separated by surfactant films [1]. Microemulsions are used in enhanced oil recovery (EOR), drug delivery, cosmetic and pharmaceutical applications, and enhanced aquifer remediation [2, 10, 11]. These applications take advantage of a microemulsion's ability to produce ultralow IFT values (< 0.1mN/m) [12].

The concentration at which a microemulsion first forms is called the critical microemulsion concentration [1]. Microemulsions can exist in four forms. While Type I microemulsions solubilize oil into spherical, normal micelles within the water phase, Type II microemulsions solubilize water in reverse micelles, which occur in the oil phase. Type III microemulsions exhibit three phases, excess oil and water phases and a bicontinuous phase. Type III (middle-phase) microemulsions occur when lamellar micelles are formed in the system [13]. In the presence of a low level of electrolyte (NaCl), ionic surfactant monomers aggregate and form spherical micelles (Type I microemulsions). As more electrolyte is added, the electrical double layer surrounding the ionic head group compresses and the micelle curvature decreases. With sufficient electrolyte, bilayer, lamellar micelles form with a net curvature of zero (Type III microemulsions). With additional electrolyte, the curvature becomes negative and reverse micelles are formed (Type II microemulsions) [12]. Conversely, for a middle-phase microemulsion, increasing surfactant concentration causes the volume of the middle phase to increase until all the oil and water coexists in a Winsor Type IV single phase microemulsion [1].

Non-aqueous phase liquids are trapped in porous media by capillary forces due to high oil–water IFT. While micelles can enhance contaminant ‘‘solubility’’ (solubilization), this process is not nearly as efficient as mobilization, which results from greatly reducing the IFT, as possible with microemulsions, and thus release the trapped oil. This is why mobilization is the only technology evaluated in EOR, and is the preferred environmental technology for light non-aqueous phase liquids (LNAPLs)

such as petroleum hydrocarbons [14-17]. Thus, interfacial properties of the surfactant systems used play an important role in petroleum hydrocarbon remediation.

Biosurfactant research has focused on the properties and behavior of individual biosurfactants (e.g., rhamnolipid) in the aqueous phase [18-20]. The current research has two main objectives: (1) to study the interfacial properties of the rhamnolipid biosurfactant against several hydrocarbons and (2) to determine the efficiency of using mixtures of rhamnolipid biosurfactant with synthetic surfactants to improve the interfacial properties of the surfactant system. Since rhamnolipid proves to be relatively hydrophilic, we hypothesize that mixtures of rhamnolipid biosurfactants with more hydrophobic synthetic surfactants will produce lower IFT, and that the hydrophobicity of the surfactant mixture needs to be tailored to that of the target hydrocarbon in order to achieve ultralow IFTs. By maximizing the effectiveness of biosurfactant-based systems in lowering oil–water IFT, and thus oil recovery, sustainable technologies can be developed using biorenewable materials, an ultimate goal of this research effort.

Materials and Methods

Materials

The rhamnolipid biosurfactant JBR 515 (15 w/v %) was purchased from Jeneil Biosurfactant Co. (Saukville, Wisconsin). JBR 515 was originally received as a blend of 50 w/v% monorhamnolipid ($C_{26}H_{48}O_9$, MW = 504, CMC = 10^{-4} M at neutral pH) and 50 w/v% dirhamnolipid ($C_{32}H_{58}O_{13}$, MW = 650, CMC = 1.5 x 10^{-4} M at neutral

pH) [18-21] with no further alteration. It should be noted that these CMC values were reported at no added salt. JBR 515 has an average molecular weight of 577.

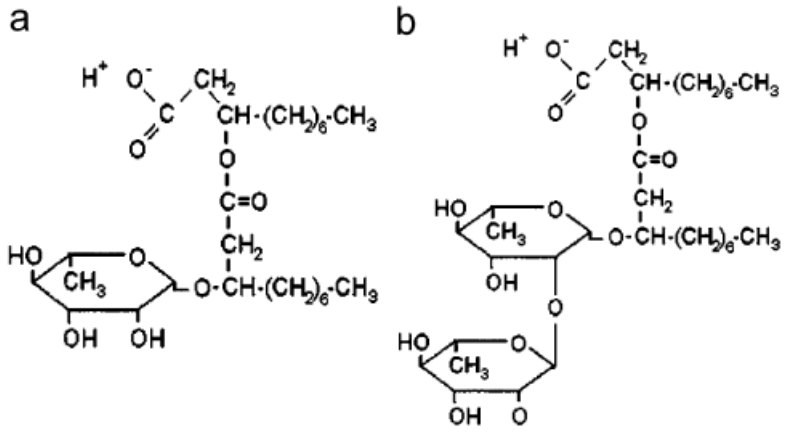


Figure 2.1. Structures of the rhamnolipids: (a) monorhamnolipid (α-L-rhamnopyranosyl-β-hydroxydecanoyl-β-hydroxydecanoate) and (b) dirhamnolipid (2-O-α-L-rhamnopyranosyl-
α-L-rhamnopyranosyl-β-hydroxydecanoyl-β-hydroxydecanoate) (adapted from ref [4] and [18]).

Both rhamnolipids present in JBR 515 are anionic and are produced by Pseudomonas aeruginosa. Rhamnolipid biosurfactants have two head groups and two identical hydrocarbon tails, as seen in Figure 2.1. The carboxylate group gives rhamnolipids their anionic character while the rhamnosyl groups (one and two groups for mono- and di-rhamnolipid, respectively) contribute to the bulky hydrophilic component of their structure. The hydrophobic tails are C8 alkyl chains. JBR 515 has been reported to have an HLB of 22–24 [21]. Rhamnolipids have been reported to be

biologically and environmentally compatible [20]. Throughout this paper we will refer to JBR 515 as rhamnolipid or rhamnolipid biosurfactant.

The synthetic surfactants used were anionic alkyl propoxylated (PO) and alkyl propoxyl ethoxylated (EO) sulfate surfactants. These surfactants have intermediate polarity groups located between conventional hydrophilic (sulfate) and lipophilic (alkyl) groups [22]. The $C_{12,13}$ alcohol PO sulfate surfactant with eight PO groups (C12,13–8PO–SO_4Na, average MW = 713) and the C_{16} polypropylene oxide ether sulfate (C16–10.7PO–SO_4Na, average MW = 1072, and C16–18PO–2EO–SO_4Na, average MW = 1590.7) were donated by Sasol Chemical Co. and Huntsman Chemical Co., respectively. The HLB values of these synthetic surfactants are in the range of 36–40. The CMCs of these synthetic surfactants were as low as the order of 10^{-6}–10^{-4} M [23].

Four hydrocarbons were used in this research: toluene, hexane, decane, and hexadecane. These hydrocarbons were chosen because they represent a range of properties (e.g., solubility, volatility) reflective of environmental contaminants (Table 2.1). Toluene was obtained from J.T. Baker Analyzer Co. with 99.9% purity. Hexane, decane, and hexadecane were purchased from Sigma-Aldrich and each had 99.5% purity. These four hydrocarbons are constituents of petroleum hydrocarbons and represent a wide range of hydrophobicity or equivalent alkane carbon number (EACN), which is routinely used as a guideline for formulating effective microemulsion systems [24, 25]. Since benzene is known to have an EACN of 0, an EACN value of 1 is assigned to toluene [13], while hexane, decane, and hexadecane

by definition have EACN values of 6, 10, and 16, respectively [26]. Since petroleum hydrocarbons have an EACN of 7–8 and motor oil has a value of 19 [12], the four compounds studied represent a wide range of organic contaminants. Sodium chloride was used as the non-amphiphilic electrolyte. All the chemicals were used as purchased without further purification.

Table 2.1. Properties of oils used

Oils	**EACN**	**Density (g/mL)**	**Viscosity (cPs)**	**Aqueous solubility (%)**
Toluene	1	0.868	0.59	0.05
Hexane	6	0.664	0.32	0.014
Decane	10	0.728	0.92	Immiscible
Hexadecane	16	0.776	3.3	Insoluble

Note: All data were measured at 20^{o}C unless otherwise stated and taken from MSDS of the chemicals

Methods

Interfacial measurement. The IFT between the aqueous surfactant solution and the oil phase was measured using glass capillary tubes and a spinning drop tensiometer (Model 500, University of Texas). The capillary tube was 2 mm in diameter and had a volume of 300 μL. An amount of 1–3 μL of hydrocarbon was injected into the tube filled with the surfactant solution. A more detailed description of the method can be found in Childs et al. [27]. Due to the procedure of measuring IFT, volatilization of the oils was negligible. All the measurements were done in triplicate at 25 ± 1 ^{o}C and

repeated if the coefficient of variation was greater than 10%. For dynamic IFT, measurements were made immediately after the components were added to the capillary tube (no pre-equilibration). For equilibrium values of IFT, the aqueous surfactant solution was mixed with the hydrocarbon and left to equilibrate for 2 weeks before the IFT between the excess aqueous phase and the excess oil phase was measured.

Phase behavior. Phase behavior studies were conducted by placing equal volumes of the aqueous and hydrocarbon phases (5 mL of each phase) in 14 mL glass tubes (diameter of 13 mm) with Teflon® screw caps. The surfactant concentration was varied from 0.01 to 12w/w% (1.73×10^{-4}–0.208 M). Most phase behavior studies were conducted at room temperature (23 ± 1 ^{o}C). The sample tubes were gently hand-shaken for 1min once a day for the first 3 days, and then left to equilibrate for 2 weeks [26]. For temperatures other than 23 ± 1 ^{o}C, vials were placed in a water bath (± 1 ^{o}C). The volume of the middle-phase microemulsion was determined by measuring its height in each tube using a ruler with a millimeter scale. The solubilization capacity is indicated by the solubilization parameter (SP), which is defined as the amount of oil (or water) solubilized in the microemulsion per unit mass of surfactant [11]. SP can be calculated by using the volume of the middle phase and the concentration of the surfactant in the middle phase as shown below [13]:

$$\text{SP} = \frac{V_{middle\ phase}\ (mL)}{m_{surfactant}\ (g)} \tag{2.1}$$

where SP is the solubilization parameter (mL oil/g surfactant), $V_{middle\ phase}$ is the volume of oil in the middle phase (mL), and $m_{surfactant}$ is the mass of surfactant in the middle phase (g). In this study, we calculated the SP assuming that all the surfactant entered the middle phase as equilibrium was reached. All phase behavior systems were prepared in triplicate. Deionized water was used in all experiments. All experiments were conducted at neutral pH.

Results and Discussion

Interfacial behavior of rhamnolipid biosurfactants

The interfacial behavior of rhamnolipid was first studied by the dynamic IFT values of the rhamnolipid at 0.01 w/w% as a function of electrolyte concentration (1–20 w/w% depending on each system) for the four hydrocarbons. We chose to use 0.01 w/w% concentration of the rhamnolipid because phase separation occurred with a 0.1 w/w% rhamnolipid concentration at a salinity of 4 w/w%; at 0.01 w/w% rhamnolipid concentration, no phase separation occurred up to 6 w/w% salt. The results showed that the dynamic IFT for toluene (0.025 ± 0.0023 mN/m) was about one order of magnitude lower than the IFTs for hexane, decane, and hexadecane, which were higher than 0.5 mN/m and remained fairly constant regardless of the NaCl concentration in the range of 1 wt% to 6 wt% (Figure A1, Appendix A). Since an ultralow IFT was obtained for toluene and not for the other more hydrophobic (higher EACN) oils, this indicates that the rhamnolipid was hydrophilic, e.g., it preferred the

water phase rather than the oil–water interface for the more hydrophobic oils. Therefore, we selected toluene for subsequent studies with rhamnolipid alone.

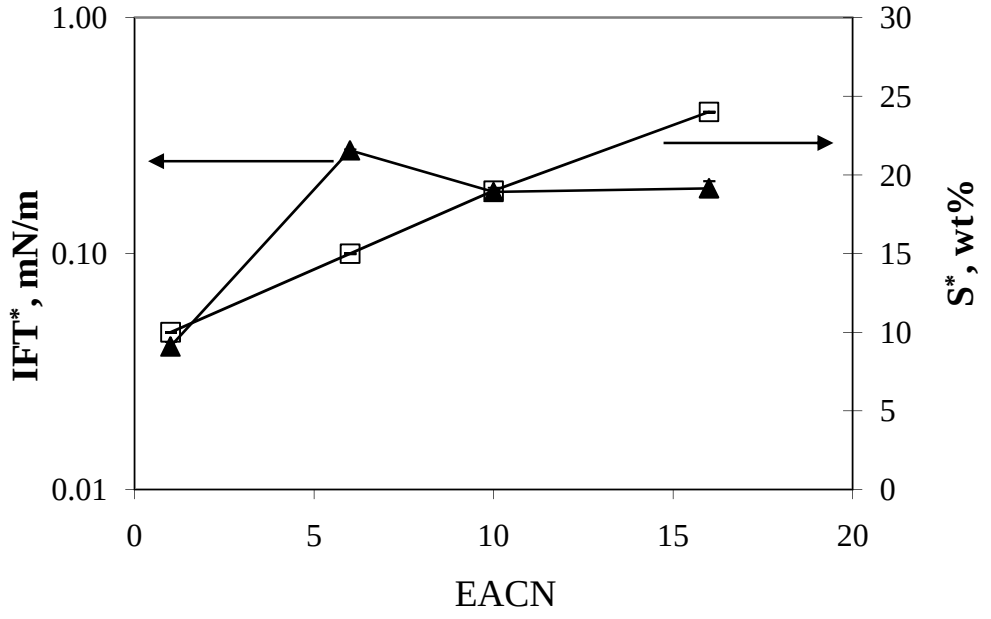


Figure 2.2. Correlation between optimal salinity (S*) (□) and EACN as determined by optimum equilibrium IFT (IFT*) (▲). The rhamnolipid concentration was 0.1w/w% for all oils. Data points for IFTs represent the average from three to five measurements; error bars are included but at times are smaller than the data symbols.

Figure 2.2 shows equilibrium IFT results for the rhamnolipid against the four hydrocarbons. In equilibrium IFT studies, it was possible to use higher salinities up to 20w/w% since the rhamnolipid partitioned from the water to the hydrocarbon phase rather than phase separating as occurred during the dynamic IFT studies. Figure 2.2 shows the correlation between the optimal salinity (S*, the salinity that gave the lowest IFT [25]) for the rhamnolipid versus the EACN of each hydrocarbon. The

salinity range was tested at 1 w/w% intervals. The optimal salinity increased as the EACN increased, which is consistent with the hydrophilic nature of the biosurfactant studied [24]. As the electrolyte (NaCl) was added to the ionic rhamnolipid solution, it reduced the electrical repulsion between the ionic head groups, causing the system net curvature to decrease towards zero where the optimal middle-phase microemulsion is achieved (the lowest IFT and highest SP) [1]. The S* increased with EACN, suggesting that more salt was required to force the ionic surfactant into the hydrocarbon–water interface. The lowest IFT was observed for the lowest optimal salinity—i.e., toluene with an EACN value of 1. This reflects the fact that the rhamnolipid is best matched to the toluene, and thus requires the least salt addition, and generates the lowest IFT. The extremely high values of S* reflect the very hydrophilic nature of this biosurfactant; these values are obviously much higher than desirable in application. As we demonstrate later, mixing these biosurfactants with more hydrophobic surfactants reduces the S*; this is a classical formulation technique for developing a desirable system. At the same time, it should be emphasized that the goal of this work is to evaluate the viability of using biosurfactant mixtures to improve system performance; future work will be necessary to build on these concepts and develop commercially viable systems, both from an economic and an optimum salinity perspective.

Phase behavior of rhamnolipid biosurfactants with toluene

Figure 2.3 summarizes the results of phase study for a series of salt scans with different rhamnolipid concentrations with toluene for two different temperatures (23 ±

1 and 55 ± 1 ^{o}C). The phase diagrams were generated by varying the salt concentration for a series of surfactant concentrations. The boundary of the phase diagram is shown as a line in Figure 2.3; this line connects all the points where a transition in microemulsion type was observed. The boundaries of the phase diagrams were drawn in solid and dashed lines for temperatures of 23 ± 1 and 55 ± 1 ^{o}C, respectively.

Looking at the 23 ± 1 ^{o}C case (the phase diagram represented by the solid boundary) and for a fixed rhamnolipid concentration (e. g., 1 w/w%), the microemulsion transitioned from a Winsor Type I to III to II as the NaCl concentration increased. The IFT decreased to a minimum value of 0.023 ± 0.0012 mN/m as the salinity increased to 15 w/w% within the Type III region. The point at which the IFT between the middle phase and the excess water phase is the same as the IFT between the middle phase and the excess oil phase is called the optimum formulation, and the electrolyte concentration at this condition is called the optimal salinity (S*) [12]. While low IFT ($\leq$ 0.1mN/m) was achieved within the three phase region, higher IFT values were observed in Winsor Type I and II regions (i. e., greater than 1 mN/m). At a fixed electrolyte concentration (e.g., 12 w/w%), the volume of the middle phase increased with increasing rhamnolipid concentration (e.g., the volume of the middle phase increased from 0.40 to 4.5 mL as the rhamnolipid concentration increased from 0.5 to 5 w/w% at 12 w/w% salinity). When the surfactant concentration was high enough, above 10 w/w%, the middle phase incorporated all of the hydrocarbon and water phases into a single microemulsion phase (Winsor Type IV microemulsion). To

our knowledge, this is the first time a complete microemulsion phase diagram including a Winsor Type IV system has been reported for any biosurfactant.

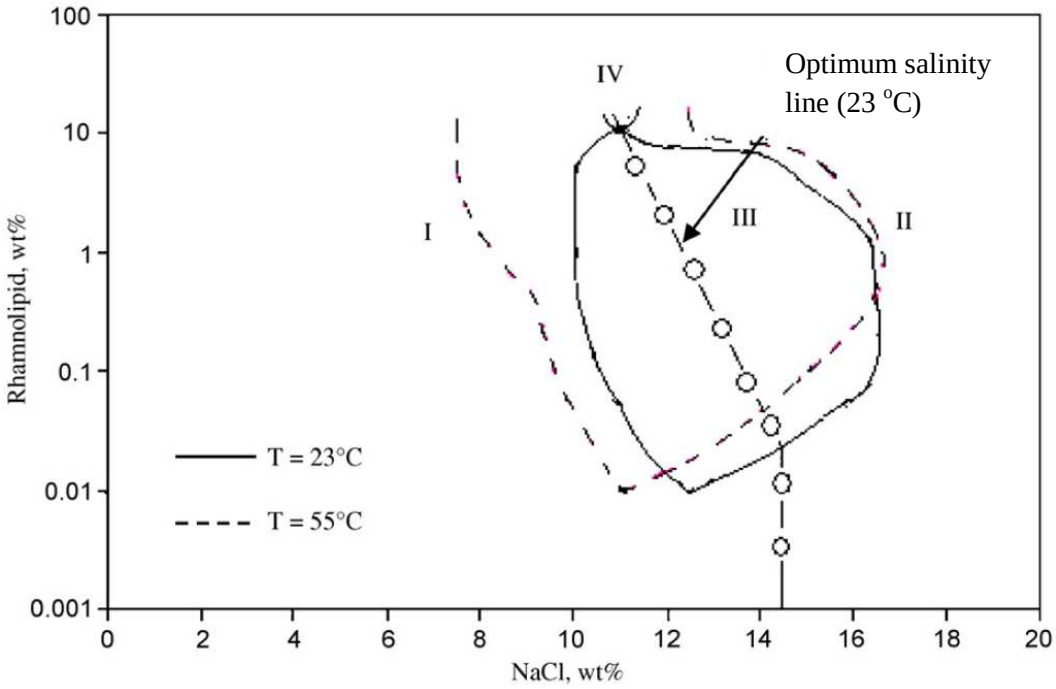


Figure 2.3. Phase diagram of rhamnolipid with toluene (CMC of 0.001 w/w%). The boundary lines (solid for 23 ± 1 °C; dashed for 55 ± 1 °C) connect all the points where a transition for microemulsion type was observed. The line labeled optimum salinity, which cuts through the interior of the phase diagram, corresponds to the optimum salinity at each surfactant concentration, as further studied in Figure 2.4. The phase diagrams were drawn based on averages of triplicate experiments.

At the optimum formulation (S*), the solubilizations of the oil and of the water are equal and SP is at a maximum for a given condition [12]. The results showed that as the surfactant concentration increased, the SP increased at a fixed salt concentration. For a constant salinity of 12 w/w%, as the rhamnolipid concentration

increases from 0.1 to 0.5 to 1.0 w/w%, the SP increased from 5.53 to 6.64 to 7.75 mL/g, respectively. The SP value at 1.0 w/w% surfactant and 12 w/w% NaCl was the highest observed SP value at this salinity, because it was the closest of the surfactant concentrations to the optimum salinity line (see Figure 2.3).

Figure 2.3 also compares the phase behavior of rhamnolipid at two temperatures 23 ± 1 and at 55 ± 1 ^{o}C. Since rhamnolipid is an ionic surfactant, the temperature effect is expected to be very small [1]. Because of this, we chose to study a large temperature range. As seen in Figure 2.3, the two phase diagrams (23 and 55 ± 1 ^{o}C) overlapped with each other over almost the entire range. Hence, even a wide temperature variation did not have a significant impact on the phase behavior of the rhamnolipid. Nonetheless, the shift, while minor, was towards lower salinity. This indicates that the biosurfactant became more hydrophobic at the higher temperature, which demonstrates that the nonionic rhamnosyl group(s) became less soluble at higher temperature, and thus required less salinity to form a middle-phase microemulsion. Nonetheless, we observe that smaller changes in salinity have a larger impact on phase behavior than this large temperature change. This result demonstrates that, even though rhamnolipid biosurfactant possesses both anionic and nonionic characters, the effect of salinity on the anionic character dominates that of temperature on the nonionic character.

Figure 2.4 shows the IFT of rhamnolipid at optimal salinity for toluene as a function of increasing rhamnolipid concentration. Following the optimum salinity line

in Figure 2.3, the CMC was determined at a NaCl concentration of 14.5 w/w% to correspond with this point in the phase diagram.

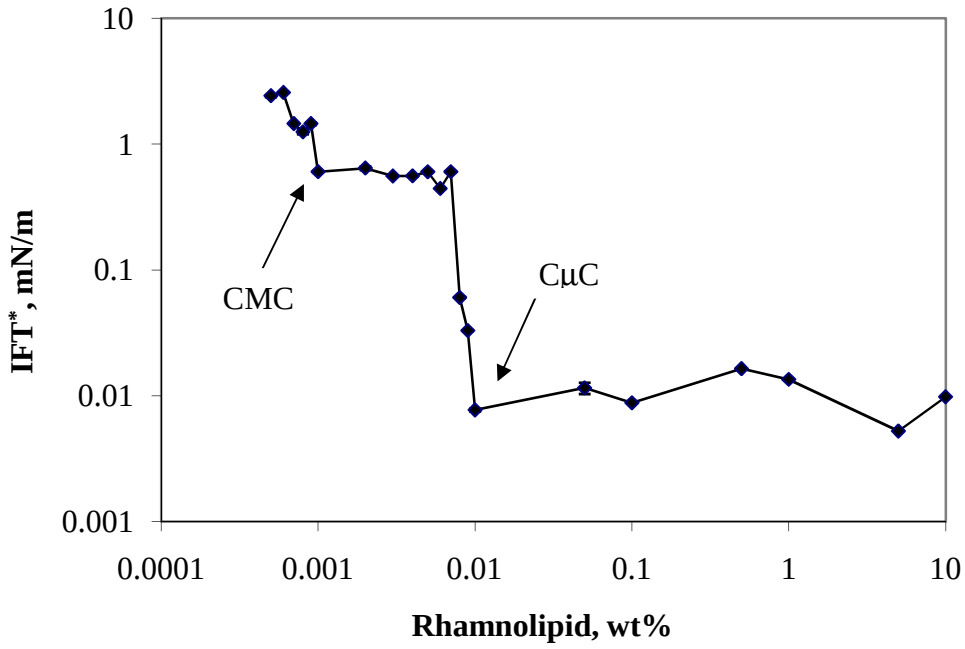


Figure 2.4. Optimum equilibrium IFT for toluene versus rhamnolipid concentration (below the CμC, salinity is constant at 14.5 w/w% as represented by vertical line in Figure 2.3; above the CμC, salinity varies to correspond to optimum salinity in the center of phase boundaries as represented by the slanted line in Figure 2.3). Data points represent the average from triplicate measurements, error bars are included but are at times smaller than the data points.

The concentrations of the rhamnolipid where the first and second sharp reductions occurred in IFT are the CMC and CμC, respectively. The CMC and CμC for the rhamnolipid were 0.001 w/w% (or 1.9×10^{-5} M) and 0.01 w/w% (or 1.9×10^{-4} M) at the salinity level of 14.5 w/w%, respectively. This CMC value is lower than the

reported values mentioned earlier because it was found at a much higher salinity (14.5 w/w%) while reported CMC values were for no added salt. The CMC of the rhamnolipid is lower than the CMC of most conventional synthetic ionic surfactants (i.e., 8×10^{-3} M for sodium dodecyl sulfate) [1]. This lower CMC [4, 10, 18, 19] is due in part to the high salinity level added. However, as discussed above, this high salinity is used to demonstrate the hydrophilic properties of the rhamnolipid biosurfactant; additional work is required to develop a lower salinity system for application purposes. Nonetheless, the low CMC and CμC values are highly desirable, as low rhamnolipid concentration would be required to achieve ultralow IFT.

Mixtures of rhamnolipid and synthetic surfactants

As discussed earlier, the rhamnolipid IFT values for hexane, decane, and hexadecane were an order of magnitude higher than that for toluene. A hypothesis of this work is that, given the hydrophilic nature of rhamnolipid, mixing rhamnolipid with more hydrophobic synthetic surfactants will be able to produce lower IFT values for hydrophobic hydrocarbons by tuning the hydrophilicity and lipophilicity of the surfactant system to the EACN of the hydrocarbon. As an initial test of this hypothesis, we used synthetic surfactants that are more hydrophobic than rhamnolipid. The concentrations of these synthetic surfactants used in the mixtures were above their CMCs. Future work will seek to identify biosurfactants that are more hydrophobic to mix with the rhamnolipid, thus extending the biorenewable nature of the surfactant system.

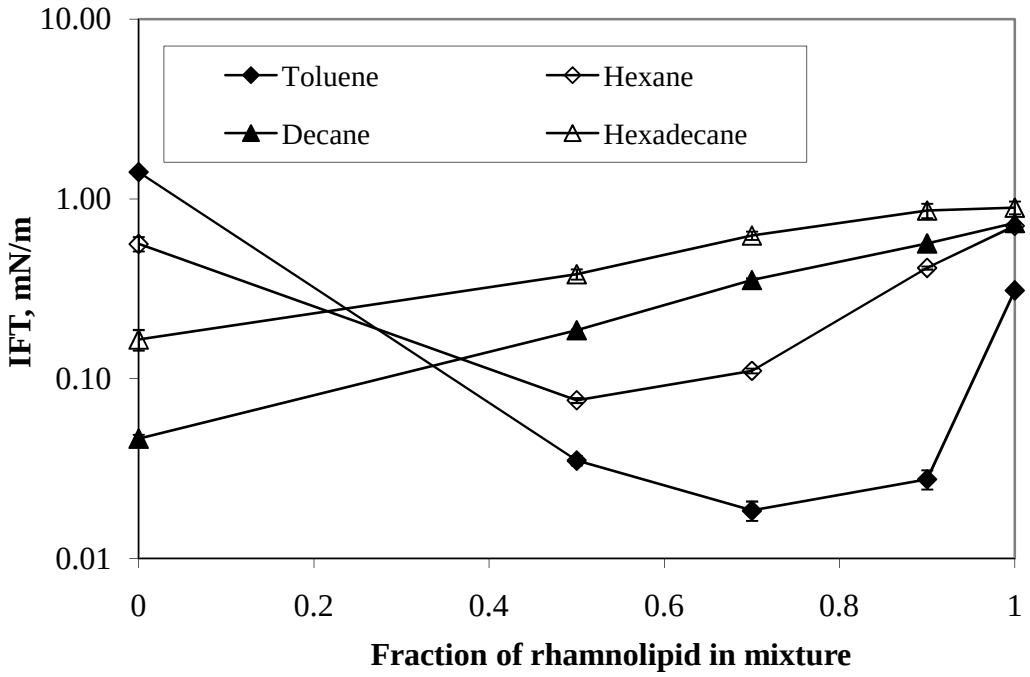


Figure 2.5. IFT of mixtures of rhamnolipid and C12,13–8PO sulfate for toluene (♦), hexane (◊), decane (▲), and hexadecane (Δ) at optimum salinity (S*) for each system. The total surfactant concentration was 0.1 w/w%. The IFT shown in this figure was the optimum IFT for each formulation. Data points represent the average from triplicate measurements, error bars are included but are at times smaller than the data points.

The first synthetic surfactant tested was the alkyl PO sulfate surfactant (C12,13–8PO–SO_4Na or C12,13–8PO). Based on its molecular structure, this surfactant has a hydrophobic characteristic due to the long hydrocarbon chain length (C12,13 versus C8 for rhamnolipid) and the presence of the PO groups which are slightly hydrophobic. We mixed rhamnolipid and C12,13–8PO in different ratios (from 0% to 100% rhamnolipid in the mixture) while maintaining a constant total

surfactant concentration of 0.1 w/w% and varying salt concentration within the range of 3–8 w/w%.

Figure 2.5 summarizes the IFT values at optimal salinity for each surfactant mixture formulation with the four hydrocarbons. When only C12,13–8PO was present (i.e., a value of zero on the x-axis of Figure 2.5), the IFT was lowest for decane followed by hexadecane. The fact that C12,13–8PO produces the lowest IFT for decane demonstrates that C12,13–8PO is hydrophobic, making it a good candidate to mix with the rhamnolipid. When only the rhamnolipid was present (a value on the x-axis of one), the lowest IFT was obtained for toluene, as reported above. However, the addition of a very small amount of C12,13–8PO to the rhamnolipid surfactant (0.09 w/w% of the rhamnolipid and 0.01 w/w% of C12,13–8PO or an x-value of 0.9) reduced the IFT for toluene by over an order of magnitude to less than 0.1 mN/m. Significant IFT reductions for hexane required a higher fraction of C12,13–8PO in the mixture (i.e., an x-axis value less than 0.9). This is reasonable because hexane is more hydrophobic than toluene, thus the surfactant mixture had to be more hydrophobic to be compatible with hexane and the fraction of C12,13–8PO in the mixture had to be higher. For toluene and hexane, synergism was observed—the IFT of the surfactant mixture was lower than the IFT of either surfactant alone. However, synergism was not observed for decane and hexadecane, likely because the rhamnolipid is too hydrophilic for these highly hydrophobic oils. The data in Figure 2.5 thus illustrate the synergism of using surfactant mixtures, but also demonstrate the importance of having the right surfactants to match the properties of the hydrocarbon.

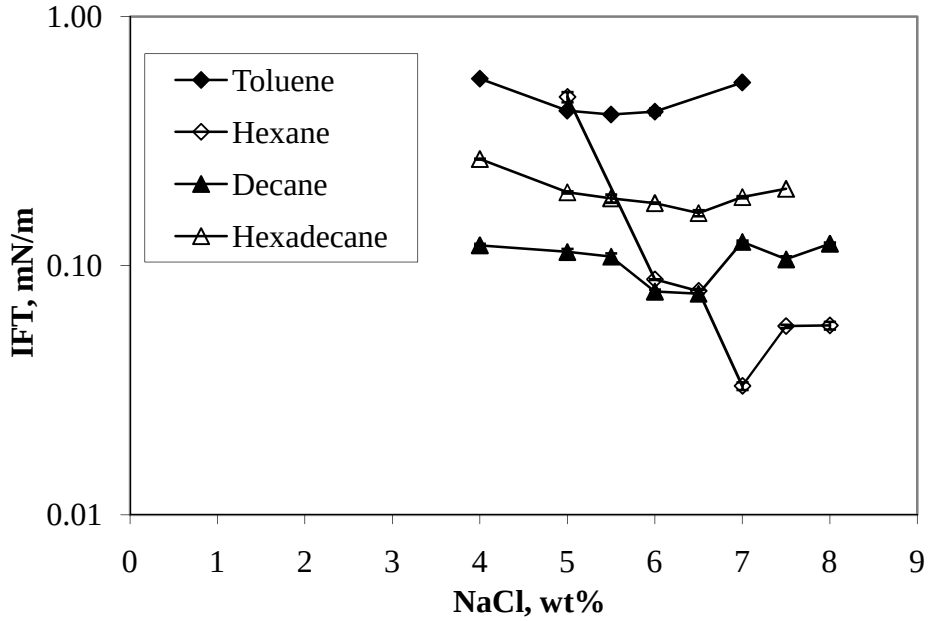


Figure 2.6. IFT of mixtures of rhamnolipid and C16–10.7PO sulfate for toluene (♦), hexane (◊), decane (▲), and hexadecane (Δ). The total surfactant concentration was 0.1 w/w%. The ratio of rhamnolipid to C16–10.7PO sulfate was fixed at 1:1 by weight percent basis (or 2:1 by molar basis). Data points represent the average from triplicate measurements, error bars are included but are at times smaller than the data points.

An alkyl PO sulfate surfactant (C16–10.7PO) sulfate, which is even more hydrophobic than C12,13–8PO, was studied next. The increased carbon chain length and the increased number of PO groups make C16–10.7PO sulfate more hydrophobic than C12,13–8PO. Figure 2.6 shows the IFT of the mixture of rhamnolipid and C16–10.7PO sulfate for the four hydrocarbons. A preliminary IFT test was done by varying surfactant ratio in the mixture and salt for each surfactant ratio. It was found from this test that the ratio of rhamnolipid to C16–10.7PO of 1:1 had the highest rhamnolipid

concentration in the mixture and generated the lowest IFT. Therefore, the ratio of rhamnolipid to C16–10.7PO was kept constant at 1:1 by weight percent basis (1:2 by molar basis) and salinity was varied. A strong synergism was observed for hexane, which is a medium carbon chain length hydrocarbon or medium hydrophobic hydrocarbon. The rhamnolipid and C16–10.7PO mixture produced a lower IFT for hexane than previously shown in Figure 2.5 for the rhamnolipid and C12,13–8PO mixture at the same mixing ratio, reducing the IFT (0.073 ± 0.0032 mN/m from Figure 2.5 versus 0.033 ± 0.0012 mN/m in Figure 2.6). The IFT values for decane and hexadecane decreased only slightly for the rhamnolipid and C16–10.7PO mixtures (Figure 2.6). The IFTs against these latter two hydrocarbons were not in the ultralow IFT range. On the other hand, the IFT for toluene increased significantly from 0.035 ± 0.0022 mN/m for the rhamnolipid and C12,13–8PO system (Figure 2.5) to 0.41 ± 0.0057 mN/m for the rhamnolipid and C16–10.7PO system (Figure 2.6). This is expected since C16-10.7PO sulfate is more hydrophobic than C12,13–8PO sulfate and is thus more effective in lowering IFT with more hydrophobic hydrocarbons. The results indicated that C16–10.7PO sulfate was too hydrophobic for toluene (low EACN oil) and not hydrophobic enough for decane and hexadecane (high EACN oils). An even more hydrophobic surfactant is needed to achieve ultralow IFT for decane and hexadecane.

A more hydrophobic surfactant, alkyl polypropylene oxide ether sulfates C16–18PO–2EO–SO4Na, was studied next [22]. This surfactant is more hydrophobic than C16–10.7PO sulfate due to the greater number of PO groups (18PO). While EO

groups are hydrophilic, the presence of only two EO groups was not expected to have much effect on IFT since the surfactant contained a larger number of PO groups.

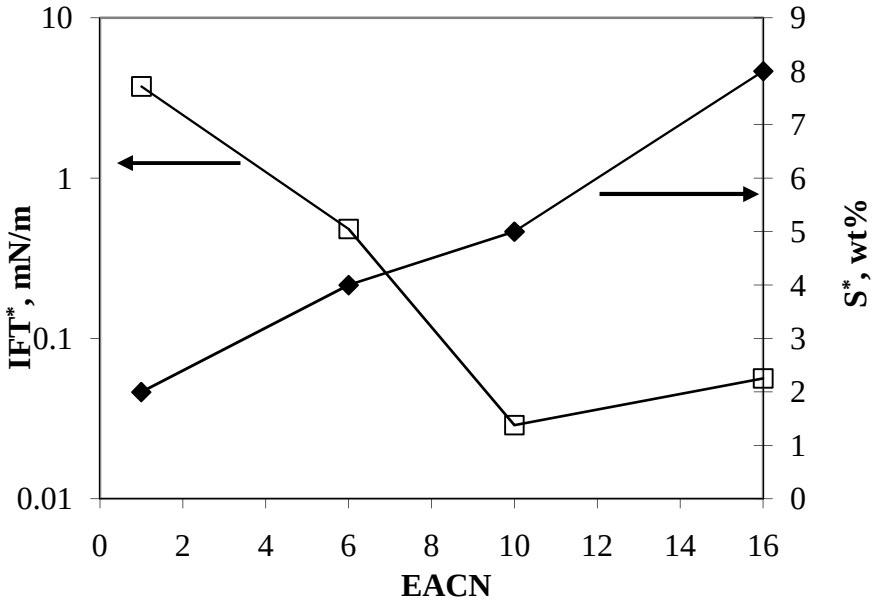


Figure 2.7. Optimum IFT (m) and optimum salinity (S*) (&) of a mixture of rhamnolipid and C16–18PO–2EO sulfate versus EACN (EACN values of 1 for toluene, 6 for hexane, 10 for decane, and 16 for hexadecane). The total surfactant concentration was 0.1 w/w%. The ratio of rhamnolipid to C16–18PO–2EO sulfate was fixed at 3:7 by weight basis (or 1:1 by molar basis). Data points represent the average from triplicate measurements, error bars are included but are at
times smaller than the data points.

Figure 2.7 shows the optimum IFT and the optimum salinity of the mixture of rhamnolipid and C16–18PO–2EO sulfate surfactants for all four hydrocarbons at a fixed ratio of rhamnolipid to C16–18PPO–2EO sulfate of 3:7 by weight basis or 1:1

by molar basis. We observed a similar trend between EACN and optimum salinity as shown in Figure 2.2. The optimum salinity increased as the EACN increased. Also, the S* for hexane of the rhamnolipid/C16–18PO–2EO sulfate mixture (4 w/w%) was significantly lower than that for the rhamnolipid alone (15 w/w%). This is reasonable because the surfactant mixture is much more hydrophobic than the rhamnolipid alone. This mixture effect demonstrates the formulation technique mentioned above for producing a more desirable surfactant system (in this case reducing S*). Future work can extend this work to produce even lower values of S*. The IFT generated by the rhamnolipid/ C16–18PO–2EO sulfate mixture decreased with increasing EACN. The IFTs for decane and hexadecane were very low, in the ultralow IFT range (< 0.1 mN/m). Thus C16–18PO–2EO sulfate was hydrophobic enough to provide an appropriate hydrophilic–lipophilic balance to the surfactant mixture against decane and hexadecane. However, C16–18PO–2EO sulfate was too hydrophobic for hexane and toluene since the IFTs of the mixture for toluene and hexane were higher than all of the other surfactant mixtures.

Table 2.2 summarizes the best formulations achieved for each hydrocarbon. It should be noted that the molar fraction of rhamnolipid exceeds 0.5 for all of these formulations. In other words, rhamnolipid is always the dominant surfactant in the mixture. Another important point is that formulating surfactant mixtures to match the hydrophobic properties of the hydrocarbons resulted in ultralow IFT (< 0.1mN/m) in all cases, illustrating the importance of tailoring the surfactant system to the oil. For hydrocarbon mixtures, the best surfactant formulation can be identified using our

results as a guide. For example, if an oil spill has an EACN value of 6.2, then the best formulation would be near that developed for hexane in this work; formulation studies would be needed to verify and modify this formulation as necessary. Finally, our work shows that while rhamnolipid works best for relatively hydrophilic oils, when mixed with more hydrophobic surfactants it also works well for higher EACN oils.

Table 2.2. Optimum formulations of surfactant mixtures for different hydrocarbons

Biosurfactants	**Synthetic Surfactants**	**Oils**	**S* (w/w%)**	**Opt. IFT (mN/m)**
Rhamnolipid (0.08 w/w%)	C12,13-8PO sulfate (0.02 w/w%)	Toluene	4	0.032 ± 2.02E-03
Rhamnolipid (0.05 w/w%)	C16-10.7PO sulfate (0.05 w/w%)	Hexane	6	0.069 ± 2.46E-04
Rhamnolipid (0.03 w/w%)	C16-18PO-2EO sulfate (0.07 w/w%)	Decane	5	0.029 ± 4.52E-04
Rhamnolipid (0.03 w/w%)	C16-18PO-2EO sulfate (0.07 w/w%)	Hexadecane	8	0.056 ± 1.03E-03

Conclusions

This work described the interfacial properties of rhamnolipid biosurfactant against several LNAPLs. Based on these properties, we were able to formulate optimum mixtures with synthetic surfactants that produced ultralow IFTs for toluene, hexane, decane, and hexadecane. The results showed that rhamnolipid biosurfactant

was quite hydrophilic relative to the hydrocarbons tested and that mixing rhamnolipids with more hydrophobic synthetic surfactants enhanced the interfacial activity of the rhamnolipid against these hydrocarbons. We achieved IFT values less than 0.1mN/m for all of the hydrocarbons by using tailored mixtures of rhamnolipid with synthetic surfactants. Future work will identify biosurfactants that are more hydrophobic to mix with the rhamnolipid, thus further reducing the optimum salinity and extending the biorenewable nature of the surfactant system. Future work should also assess the economics of these biosurfactant mixtures and utilize optimum surfactant formulations for each hydrocarbon in column studies to investigate the hydrocarbon removal efficiency in continuous flow systems.

Acknowledgements

Research support from the Integrated Petroleum Environmental Consortium (IPEC) is acknowledged. Gratitude is also expressed to Sasol and Huntsman for supplying synthetic surfactant samples and to Ashley Edelen, an undergraduate student at the University of Oklahoma for performing part of the experiments. Gratitude is also expressed to the industrial sponsors of Oklahoma University's Institute for Applied Surfactant Research (IASR) (www.cbme.ou.edu/iasr/).

References

1. Rosen, M.J., 1989. Surfactants and Interfacial Phenomena, second ed. Wiley, New York.

2. Desai, J.D., Banat, I.M., 1997. Microbial production of surfactants and their commercial potential. Microbiol. Mol. Biol. Rev. 61 (1), 47–64.
3. Georgiou, G., Lin, S.C., Sharma, M.M., 1992. Surface-active compounds from microorganisms. Bio/Technology 10, 60–65.
4. Urum, K., Pekdemir, T., 2004. Evaluation of biosurfactants for crude oil contaminated soil washing. Chemosphere 57, 1139–1150.
5. Youssef, N.H., Nguyen, T.T., Sabatini, D.A., McInerney, M.J., 2007. Basis for formulating biosurfactant mixtures to achieve ultra low interfacial tension values against hydrocarbons. J. Ind. Microbiol. Biotechnol. 34 (7), 497–507.
6. Lin, S.C., Minton, M.A., Sharma, M.M., Georgiou, G., 1994. Structural and immunological characterization of a biosurfactant produced by Bacillus lichenisformis JF-2. Appl. Environ. Microbiol. 60 (1), 31–38.
7. Bognolo, G., 1999. Biosurfactants as emulsifying agents for hydrocarbons. Colloids Surf. A: Physicochem. Eng. Aspects 152 (1–2), 41–52.
8. Maier, R.M., Soberon-Chavez, G., 2000. Pseudomonas aeruginosa rhamnolipids: biosynthesis and potential applications. Appl. Microbiol. Biotechnol. 54 (5), 625–633.
9. Mulligan, C.N., Gibbs, B.F., 1993. Factors influencing the economics of biosurfactants. In: Kosaric, N. (Ed.), Biosurfactants: Production, Properties, Applications. Marcel Dekker, Inc., New York, NY, pp. 329–371.
10. McCray, J.E., Bai, G., Maier, R.M., Brusseau, M.L., 2001. Biosurfactant-enhanced solubilization of NAPL mixtures. J. Contam. Hydrol. 48 (1–2), 45–68.

11. Acosta, E., Tran, S., Uchiyama, H., Sabatini, D.A., Harwell, J.H., 2002. Formulating chlorinated hydrocarbon microemulsions using linker molecules. Environ. Sci. Technol. 36, 4618–4624.
12. Acosta, E., Do, P.M., Harwell, J.H., Sabatini, D.A., 2003. Linker modified microemulsions for a variety of oils and surfactants. J. Surfactants Deterg. 6 (4), 353–363.
13. Bourrel, M., Schechter, R.S., 1988. Microemulsions and related systems: formulation, solvency, and physical properties. Surfactant Sci. Ser. 30, 229–302.
14. Sabatini, D.A., Knox, R.C., Harwell, J.H. (Eds.), 1995. Surfactant Enhanced Subsurface Remediation: Emerging Technologies. ACS Symposium Series 594. American Chemical Society, Washington, DC, 312pp.
15. Sabatini, D.A., Knox, R.C., Harwell, J.H., Wu, B., 2000. Integrated design of surfactant enhanced DNAPL remediation: effective supersolubilization and gradient systems. J. Contam. Hydrol. 45 (1), 99–121.
16. Wu, B., Cheng, H., Childs, J., Sabatini, D.A., 2001. Surfactant enhanced removal of hydrophobic oils from source zones. In: Smith, J.A., Burns, S.E. (Eds.), Physicochemical Groundwater Remediation. Kluwer Publishing, New York, NY, pp. 245–269.
17. Childs, J.D., Acosta, E., Scamehorn, J.F., Sabatini, D.A., 2005. Surfactant-enhanced treatment of oil-based drill cuttings. J. Energy Resour. Technol. 127 (2), 153–162.

18. Helvaci, Ş. Ş., Pecker, S., Özdemir, G., 2004. Effect of electrolytes on the surface behavior of rhamnolipids R1 and R2. Colloids Surf. B: Biointerfaces 35, 225–233.
19. Özdemir, G., Malayoglu, U., 2004. Wetting characteristics of aqueous rhamnolipids solutions. Colloids Surf. B: Biointerfaces 39, 1–7.
20. Özdemir, G., Peker, S., Helvaci, Ş. Ş., 2004. Effect of pH on the surface and interfacial behavior of rhamnolipids R1 and R2. Colloids Surf. A: Physicochem. Eng. Aspects 234, 135–143.
21. Xie, Y., Li, Y., Ye, R., 2005. Effect of alcohols on the phase behavior of microemulsions formed by a biosurfactant—rhamnolipid. J. Dispersion Sci. Technol. 26, 455–461.
22. Minãna-Perez, M., Graciaa, A., Lachaise, J., Salager, J.L., 1995. Solubilization of polar oils with extended surfactants. Colloids Surf. A: Physicochem. Eng. Aspects 100, 217–224.
23. Witthayapanyanon, A., Acosta, E.J., Harwell, J.H., Sabatini, D.A., 2006. Formulation of ultralow interfacial tension systems using extended surfactants. J. Surfactants Deterg. 9, 331–339.
24. Salager, J.L., Morgan, J.C., Schechter, R.S., Wade,W.H., Vasquez, E., 1979a. Optimum formulation of surfactant/water/oil systems for minimum interfacial tension or phase behavior. Soc. Petrol. Eng. J. 19, 107–115.

25. Salager, J.L., Bourrel, M., Schechter, R.S., Wade, W.H., 1979b. Mixing rules for optimum phase—behavior formulations of surfactant/oil/water systems. Soc. Petrol. Eng. J. 19, 271–278.

26. Acosta, E.J., Nguyen, T., Witthayapanyanon, A., Harwell, J.H., Sabatini, D.A., 2005. Linker-based bio-compatible microemulsions. Environ. Sci. Technol. 39, 1275–1282.

27. Childs, J.D., Acosta, E., Knox, R., Harwell, J.H., Sabatini, D.A., 2004. Improving the extraction of tetrachloroethylene from soil columns using surfactant gradient systems. J. Contam. Hydrol. 71, 27–45.

CHAPTER 3

Formulating Alcohol-Free Microemulsions Using Rhamnolipid Biosurfactant and Rhamnolipid Mixtures[2]

Abstract

This research focused on developing alcohol-free biosurfactant-based microemulsions. Rhamnolipid-based mixtures were found to have doubled the solubilization parameter as compared to sodium bis(2-ethyl) dihexyl sulfosuccinate/sodium dihexyl sulfosuccinate/sodium mono- and dimethyl naphthalene sulfonate at the same total molar concentration. For the first time, a phase diagram was developed for surfactant mixtures containing soy methyl ester ethoxylate, rhamnolipid and oleyl alcohol with limonene oil. This phase diagram can be used as a guideline for selecting a surfactant system and surfactant ratio to formulate microemulsions with a given oil. In addition, the alcohol-free biosurfactant-based microemulsions required reasonable salinity values for limonene, making it viable in a variety of applications.

Keywords: Biorenewable surfactant, biosurfactant, interfacial tension, linker, microemulsion, solubilization, characteristic curvature

[2] This chapter or portions thereof has been published previously in *Journal of Surfactants and Detergents* under the title "Formulating Alcohol-Free Microemulsions Using Rhamnolipid Biosurfactant and Rhamnolipid Mixture" Journal of Surfactants and Detergents, 2009, 12, 109-115. This current version has been formatted for this dissertation.

Introduction

Biosurfactants are produced from microorganisms which have diverse structures including glycolipids, phospholipids, polysaccharide-lipid complexes, lipopeptides and hydroxylated and cross-linked fatty acids [1, 2]. The rhamnolipid biosurfactant studied in this research belongs to the glycolipid species, which are composed of carbohydrate heads and lipid tails as shown in Figure 3.1 [3]. The glycolipid biosurfactants have been evaluated for use in many applications such as environmental bioremediation, removal of heavy metals from contaminated oil, biomedical applications [4–6], cosmetics and personal care products [7], and in the perfume and fragrance industry [8].

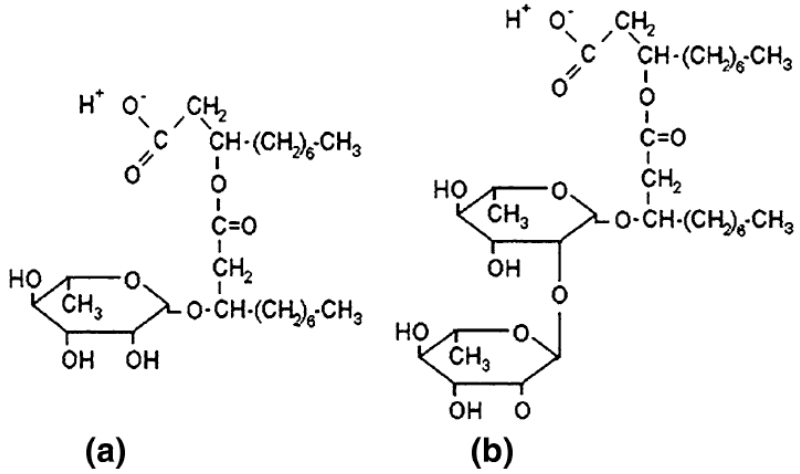


Figure 3.1. Molecular structures of the rhamnolipids: (a) monorhamnolipid, (b) dirhamnolipid (adapted from ref. [3]).

In terms of molecular structure, rhamnolipid has two heads and two tails. The two heads, rhamnosyl (sugar) and carboxylic acid, are both very hydrophilic. In

addition, the two short tails of C8 alkyl chains provide only limited interaction with the oil phase. As a result, rhamnolipid is fairly hydrophilic, and thus promotes interactions between the aqueous phase and the surfactant layer and forms aggregates in the water phase (Winsor Type I). The hydrophilic-lipophilic balance of rhamnolipid was reported as 22–24 [9]. Rhamnolipid biosurfactants have been reported to be biologically and environmentally compatible [10].

Winsor Types I–IV microemulsions [11, 12] have been used for a wide range of applications [12–14]. However, only limited studies have evaluated biosurfactant-based microemulsions, with the addition of alcohols being necessary to form microemulsions [9, 15]. In our previous study, we were able to formulate alcohol-free microemulsions with rhamnolipid. However, synthetic surfactants were used to adjust the hydrophilic/lipophilic balance of the surfactant system to enhance the microemulsion formation [16]. The goal of this research is to formulate alcohol-free biosurfactant-based microemulsions for oils of intermediate hydrophobicity. The primary objective of this research is to illustrate that rhamnolipid biosurfactant can be used in mixtures to lower interfacial tension (IFT) and increase solubilization for representative oils of interest. The secondary objective of this work is to compare the effectiveness of rhamnolipid biosurfactant and synthetic surfactants in enhancing microemulsion formation and solubilization. The final objective of this work is to study the role of rhamnolipid biosurfactant in microemulsion formation (i.e., cosurfactant or hydrophilic linker). Sabatini et al. [17] discussed that hydrophilic linkers are amphiphilic molecules that have between six and nine carbons in their tail

per head group. With the structures discussed earlier, the question arises: will rhamnolipid play a role as a cosurfactant, which coadsorbs with the surfactant at the oil/water interface, or a hydrophilic linker, which enhances the interaction between the surfactant and the water phases [18]. The final objective of this work is to answer these two questions based on the optimum salinity, the interfacial tension, the synergism the rhamnolipid with lipophilic linker and the characteristic curvature of the rhamnolipid.

To interpret the microemulsion formulations, we will use the optimum solubilization parameter (SP*). The SP* is defined as the solubilization parameter at the middle phase microemulsion that solubilizes equal amounts of oil and water [12].

Materials and Methods

Materials

The rhamnolipid biosurfactant (Figure 3.1) JBR 515 (15 w/v%) was purchased from Jeneil Biosurfactant Co. (Saukville, WI, USA). JBR 515 was originally received as a blend of 50 wt% monorhamnolipid ($C_{26}H_{48}O_9$, MW= 504, CMC = 10^{-4} M at neutral pH) and 50 wt% dirhamnolipid ($C_{32}H_{58}O_{13}$, MW= 650, CMC = 1.5 9 10^{-4} M at neutral pH) [3, 9, 10, 19] which gives the JBR 515 an average molecular weight of 577. The CMC values reported above were with no added salt. Both mono- and dirhamnolipids present in JBR 515 are produced by Pseudomonas aeruginosa. Throughout this paper we will refer to JBR 515 as rhamnolipid (JBR) or rhamnolipid biosurfactant.

Biorenewable surfactants are made from renewable feed stocks such as soya plants, rendering them readily biodegradable with low toxicity: methyl ester ethoxylate surfactant with three ethoxylated groups (SMEE3EO). Thus, the fatty acid (R) composition is dominantly C18 alkyl chain (69–93%) with about 24% oleic acid (C18:1), 54% linoleic acid (C18:2) and 7% linolenic acid (C18:3) of total fatty acid composition. This surfactant was synthesized and provided by Huntsman Chemical Co. (Woodlands, TX, USA) (99–100 wt% purity).

Synthetic surfactants used are sodium dihexyl sulfosuccinate (SDHS) and sodium bis(2-ethyl) dihexyl sulfosuccinate (SBDHS). SDHS is a Fluka brand with 80% solution in water. SBDHS was purchased in powder form (~ 100%) from Fisher Scientific. Oleyl alcohol (OA, 85%) purchased from Sigma-Aldrich was used as the lipophilic linker.

The two oils studied in this work were limonene and No. 2 diesel, which represent oils of intermediate hydrophobicity or equivalent alkane carbon number (EACN, 5.7 and 12–14 for limonene and diesel, respectively [20, 21]) and are of interest in formulations used for hard surface cleaners, environmental remediation and biodiesel applications [22–26]. Limonene (98+ %) was purchased from Sigma-Aldrich. No. 2 diesel (86.23% carbon, 13.14% hydrogen, 0.034% sulfur, 31.0% aromatic, 64.1% paraffin and 4.9% olefin [27]) was purchased from a local gas station as a commercial grade. Benzene (98+ %) was purchased from Sigma-Aldrich. Sodium chloride was used as the electrolyte. All chemicals were used without any further purification.

Methods

Phase study. Phase behavior studies were conducted by placing equal volumes of the aqueous and oil phases in 14-mL glass tubes with PTFE screw caps using salinity scan using standard procedures [13]. The sample tubes were handshaken for 1 min once a day for the first 3 days, and then left to equilibrate at a desired temperature for 2 weeks before any further measurement [13]. The volume of the middle phase microemulsion was determined by measuring its height in each tube. The solubilization capacity was quantified using the solubilization parameter (SP), which is calculated using Equation 3.1 below [12]:

$$\text{SP} = \frac{V_O\ (mL)}{m_S\ (g)} \tag{3.1}$$

where SP is the solubilization parameter (mL oil/g surfactant), V_O is the volume of oil in the middle phase (mL) and m_S is the mass of surfactant in the middle phase (g). In the SP calculation, if the biosurfactant is identified as a cosurfactant, it was taken into account in the denominator with the mass of the surfactant in Equation 3.1; if the biosurfactant is identified as a linker, it is not included in the calculation.

The partitioning of the rhamnolipid into the middle phase was quantified by subtracting the mass of these molecules in the excess water by the total initial mass added. JBR concentration was analyzed by UV 2100 Spectrometer (UNICO) at the wavelength 272 nm. It should be noted that JBR is the only component that has UV absorbance at this wavelength.

Interfacial tension. The interfacial tension between the aqueous and the oil phases was measured using glass capillary tubes and a spinning drop tensiometer (Model 500 purchased from the University of Texas) according to standard methods [28].

Results and Discussions

Formulating Microemulsions with Rhamnolipid.

In our previous work [16], we studied the phase behavior of rhamnolipid with toluene. We found that rhamnolipid was very hydrophilic relative to toluene, which is a very hydrophilic oil. In this work, our goal is to formulate microemulsions with higher EACN oils; thus, rhamnolipid will need to be mixed with more hydrophobic surfactants. Figure 3.2 plots the interfacial tension between the excess oil and excess water of the middle phase microemulsion formulations as a function of salinity for limonene and diesel, first using mixtures of SBDHS and rhamnolipid only and then with the addition of OA as a lipophilic linker. First of all, it should be noted that no microemulsion was observed for either limonene or diesel with SDBHS alone at either 0.05 or 0.1 M. However, a 0.05-M equal-molar mixture of SDBHS and rhamnolipid was able to produce Types I, III and II microemulsions and produce ultralow interfacial tension for both oils (\0.1 mN/m). This illustrates that rhamnolipid acted synergistically with SDBHS to form microemulsions with limonene and diesel (EACN values of ~ 6 and 12–14, respectively).

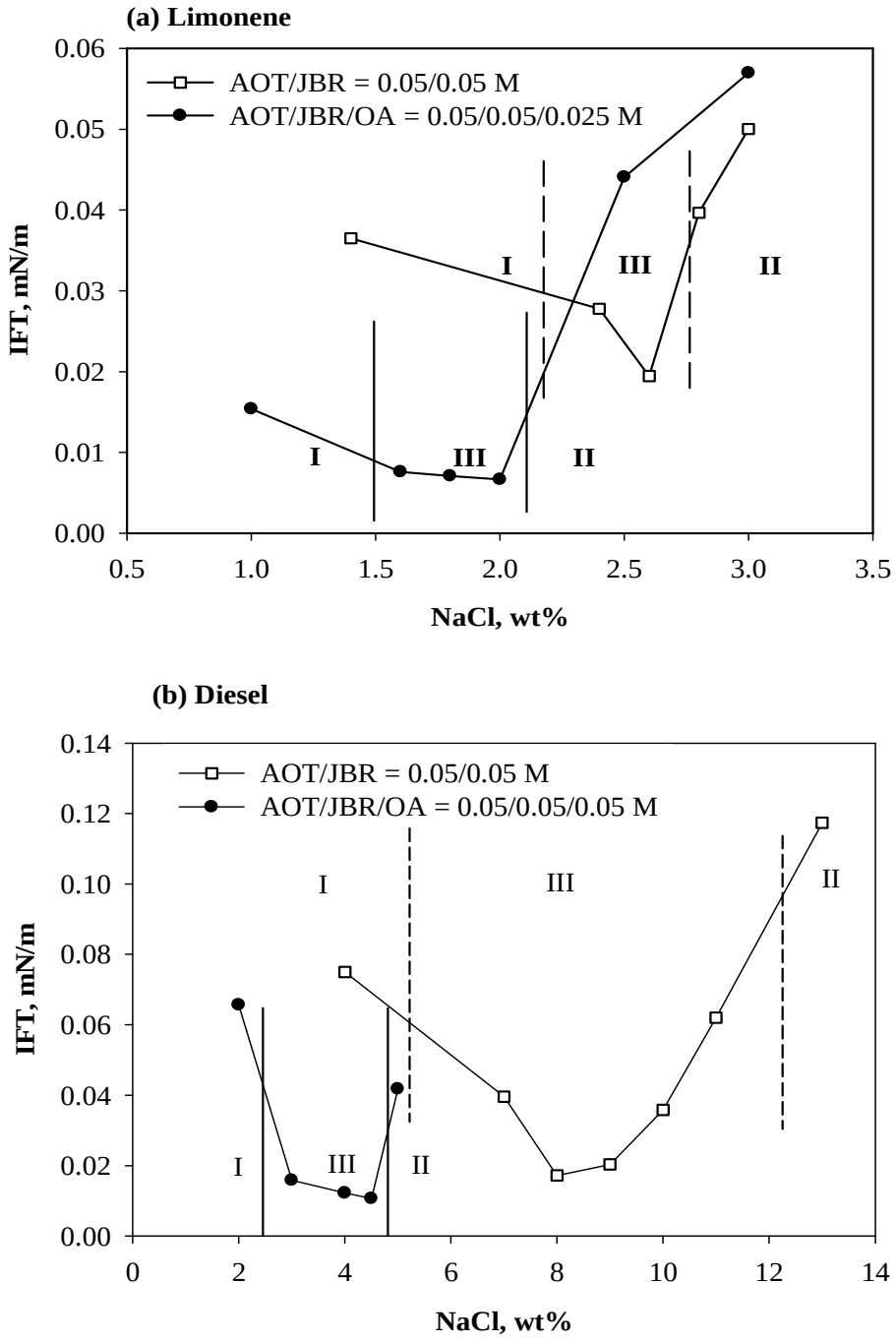


Figure 3.2. Microemulsion formulations (Winsor Types I, II and III) with (a) limonene and (b) diesel using two surfactant mixtures containing rhamnolipid: SBDHS/JBR (open squares) and SBDHS/JBR/OA (filled circles) (at 23 ± 1 ^{o}C).

We also want to assess the role of rhamnolipid in microemulsion (e.g., does it act as a cosurfactant or a hydrophilic linker). Acosta et al. [18] observed that adding hydrophilic linker to a surfactant system was expected to have little impact on solubilization capacity while adding a cosurfactant was expected to increase the solubilization capacity. Adding rhamnolipid to SDBHS obviously lowered the interfacial tension, which also increased the solubilization capacity of the surfactant system, allowing microemulsion formation where SDBHS alone could not.

Table 3.1. Solubilization parameters and fraction of JBR in the middle phase microemulsion at optimum formulations of rhamnolipid microemulsions (at 23 ± 1 ^{o}C).

Formulation	S^* **(% NaCl)**	**SP* (mL oil/g surf)**	**IFT$^*_{o/w}$ (mN/m)**	Φ **(% JBR)**
AOT/JBR-limonene	2.8	9.5	1.9E-02±9E-4	54
AOT/JBR/OA-limonene	1.8	11.2	6.7E-03±4E-4	67
AOT/JBR-diesel	9.5	8.9	2.8E-02±5E-4	19
AOT/JBR/OA-diesel	4.25	14.4	1.1E-02±8E-4	23

S^* optimum salinity, SP* optimum solubilization parameter, IFT$^*_{o/w}$ excess oil/water interfacial tension at optimum formulation, Φ fraction of JBR in the optimum middle phase microemulsion

In our work, OA was used as the lipophilic linker. Acosta et al. [29] found that an equimolar concentration of hydrophilic and lipophilic linkers showed the most effective solubilization enhancement. In this work, we first started at 0.05 M of both

rhamnolipid and OA for limonene and diesel. However, 0.05 M of OA seemed to work best with diesel microemulsions but seemed to be too hydrophobic for limonene microemulsions. OA concentration was thus reduced by half to 0.025 M for limonene microemulsions.

Table 3.1 summarizes the optimum salinity (S*), optimum solubilization parameter (SP*), optimum interfacial tension and fraction of rhamnolipid in each of the optimum middle phase microemulsion systems shown in Figure 3.2. It can be seen that the optimum salinity decreases with the addition of OA due to its lipophilicity; this is true for both limonene and diesel microemulsions. It is also observed that for the more hydrophobic or higher EACN oil (diesel), the optimum salinity is higher. This result is consistent with Acosta et al. [20] and followed the relationship proposed by Salager et al. [30, 31] that relates different variables in microemulsion formulations.

As also seen in Table 3.1, the SP* values increase with the addition of OA in both limonene and diesel microemulsions. This increase in SP* with OA indicates that rhamnolipid can either be a hydrophilic linker or a cosurfactant [18]. However, without the lipophilic linker OA in the formulation, the fraction of rhamnolipid in the middle phase is 54 and 19% (by weight) for limonene and diesel microemulsions, respectively. As OA was added, the partition of rhamnolipid in the middle phase increases to 67% (24% increase) for limonene and 23% (21% increase) for diesel. Acosta et al. [18] showed that the hydrophilic linker SMDNS fraction in the middle phase microemulsion increased by 50% when lipophilic linker OA was added to their

formulation. Our results, therefore, indicate that the rhamnolipid biosurfactant acts as a hydrophilic cosurfactant rather than a hydrophilic linker.

The Characteristic Curvature of Rhamnolipid Biosurfactant

The surfactant characteristic curvature (Cc) was proposed by Acosta et al. [32] as the dimensionless net curvature of the surfactant that reflects the tendency of the surfactant to form normal micelles, reverse micelles or intermediate aggregates. A negative value of Cc corresponds to a hydrophilic surfactant and tends to form O/W microemulsions (normal micelles) while a positive value of Cc corresponds to a hydrophobic surfactant and tends to form W/O microemulsions (reverse micelles). The characteristic curvature was also discussed in other articles as the r parameter [33–35].

In this study, we used the simplified model developed by Acosta et al. [32] based on the hydrophilic–lipophilic deviation (HLD) equation shown below to estimate the Cc value of the rhamnolipid:

$$\mathrm{HLD} = \ln(S) - K \times N_{C,O} + \mathrm{Cc} \tag{3.2}$$

where S is the salinity of the aqueous phase (g/100 mL or wt.%), K is an empirical constant depending on the type of surfactant head group, $N_{C,O}$ is the number of carbon atoms in the molecule of the oil (or EACN of the oil). This simplified Equation 3.2 assumes there is no alcohol used in this study and the experiments are done at the reference temperature. At optimum formulation, HLD = 0 and S is denoted as S^*, optimum salinity [32, 34, 35]. Based on this concept, Acosta et al. [32] developed the equation to estimate the Cc value of a target surfactant in mixtures with a reference surfactant with a known Cc value:

$$\ln (S^*/S_1^*) = X_2 [(Cc_1 - Cc_2) + (K_2 - K_1) N_{C,O}] \quad (3.3)$$

where S^* is the optimum salinity for the surfactant mixture, S_1^* is the optimum salinity for the reference surfactant, X_2 is the molar fraction of the target surfactant, and 1 and 2 denotes for the reference and target surfactants, respectively. When the oil used is benzene, which has the $N_{C,O}$ value of 0, Equation 3.3 can be simplified as:

$$\ln (S^*/S_1^*) = X_2 (Cc_1 - Cc_2) \quad (3.4)$$

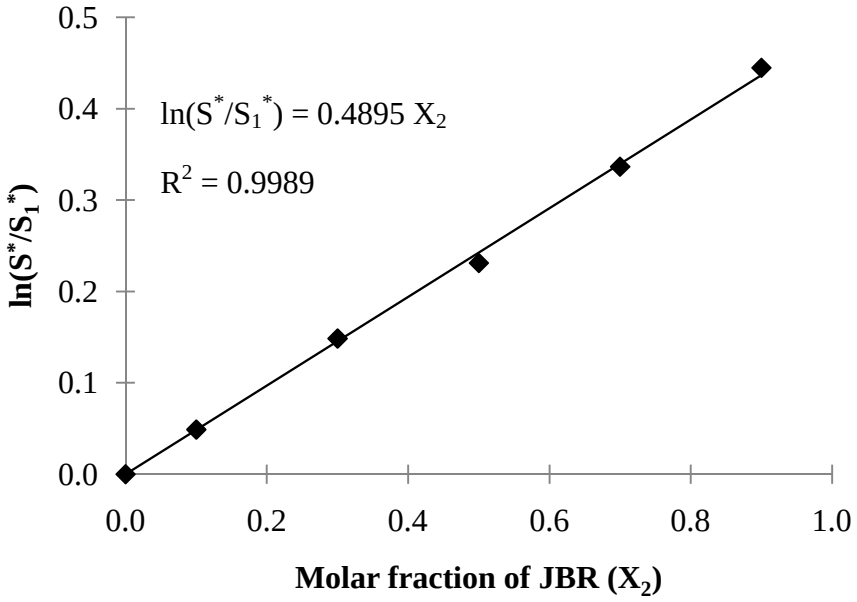


Figure 3.3. Shift in optimum electrolyte concentration [ln (S^*/S_1^*)] for SDHS-JBR-benzene at 23 ± 1 ^oC microemulsions as a function of the fraction of JBR in the system.

A plot of ln (S^*/S_1^*) versus X_2 will provide the value of $(Cc_1 - Cc_2)$ as the slope and the value Cc_2 can thus be calculated with the known value of Cc_1. The Cc value of

SDHS was calculated to be -0.92 [32] and is used as the reference surfactant in our work. Figure 3.3 plots ln (S^*/S_1^*) versus X_2 (molar fraction of JBR in the mixture) for formulation of SDHS–JBR mixture with benzene. As predicted by Equation 3.4, ln (S^*/S_1^*) correlates linearly with the molar fraction of JBR with a high correlation factor (R^2 = 0.99). The slope gives a value of Cc_1 - Cc_2 = 0.49 and, with Cc_1 = -0.92 from above, Cc_2 = -1.41. The negative value of Cc_2 indicates that the rhamnolipid is a hydrophilic surfactant, and the magnitude of Cc_2 indicates that rhamnolipid is more hydrophilic than SDHS due to the more negative value of Cc. Knowing the Cc value of the rhamnolipid, one can compare the hydrophilicity of the rhamnolipid with conventional hydrophilic surfactants such as sodium dodecyl sulfate (Cc = -2.34), sodium octanoate (Cc = -2.11) and sodium dodecyl benzene sulfonate (Cc = -0.91) [32]. This can serve as a helpful guideline when rhamnolipid biosurfactant is considered to replace conventional surfactants in microemulsion formulation. It should also be noted that the Cc value of the rhamnolipid is much less negative as compared to that of the hydrophilic linker SMDNS, which was found to have a Cc value of -3.5 [32]. This finding is consistent with the result discussed in the earlier section that rhamnolipid behaves as a cosurfactant rather than a hydrophilic linker in microemulsion formation.

Phase Diagram of Rhamnolipid Surfactant Mixture

Having characterized the hydrophilicity of rhamnolipid (JBR), we replaced the conventional surfactant SBDHS by the biorenewable surfactant soy methyl ester ethoxylate (with three EO groups; SMEE3EO). Figure 3.4 represents the phase

diagram of systems containing SMEE3EO/JBR/ OA at fixed ratio of 4/1.75/2.5 (by wt.%) with limonene.

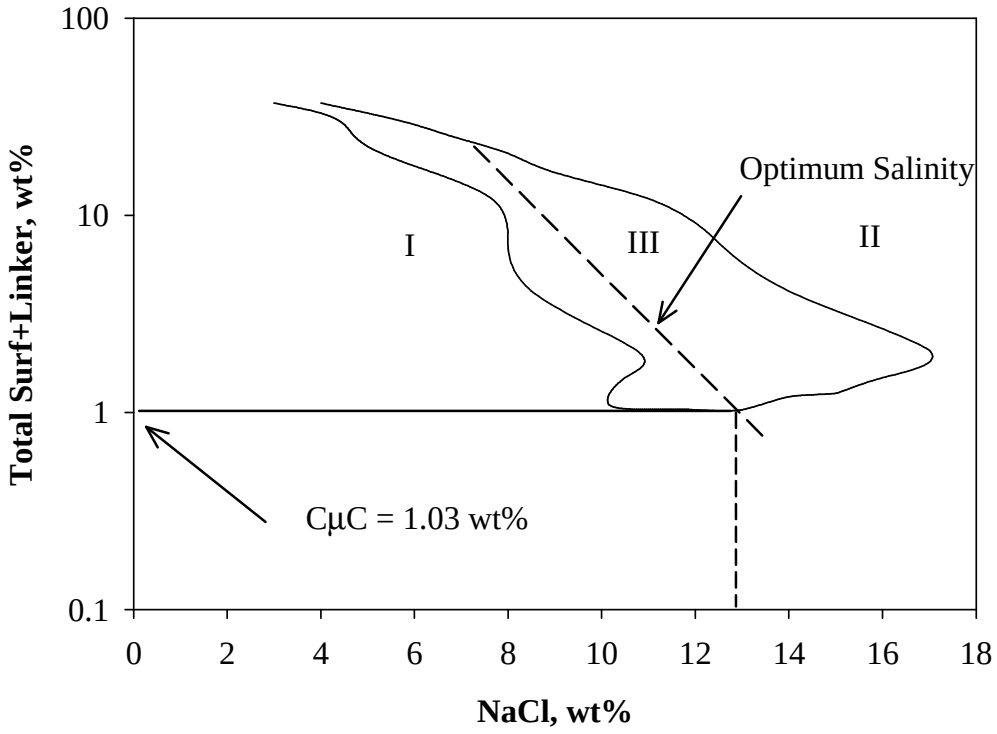


Figure 3.4. Phase diagram of formulation (Winsor Types I, II and III) composed of SMEE3EO, JBR and OA with limonene at fixed ratio of SMEE3EO/JBR/OA = 4/1.75/2.5 by wt.%. The phase boundary connects all the points where a transition for microemulsion type was observed. The line labeled optimum salinity, which cuts through the interior of the phase diagram, corresponds to the optimum salinity at each surfactant concentration, as further studied in Figure 3.5 (at 23 ± 1 ^{o}C).

The phase diagram plots the total surfactant and lipophilic linker concentration on the y-axis as a function of salinity on the x-axis. At a given total surfactant and

linker concentration (e.g., at 5 wt.%), as the salinity increases, the microemulsion transitions from Winsor Types I to III to II. Along the body of the phase diagram represented by the dashed line, as the total surfactant and linker concentration increases, the volume of the middle phase microemulsion increases. At high total surfactant and linker concentrations (above 10 wt.%), the salinity range of middle phase microemulsions gets smaller, approaching Winsor Type IV microemulsion. To our knowledge, only one study has reported a Type IV microemulsion for a biosurfactant [16].

In contrast to the SMEE3EO/JBR/OA systems, surfactant systems composed only of SMEE3EO and OA without rhamnolipid (JBR) produced either liquid crystal or Type II microemulsion for both limonene and diesel because the system was too hydrophobic for both oils. To such a system, the addition of a hydrophilic component such as rhamnolipid is needed to adjust the hydrophilicity/lipophilicity of the surfactant system. On the other hand, when the surfactant system contained only SMEE3EO and rhamnolipid, only Type I microemulsions were formed over a wide range of salinity (up to 9 wt.%) due to the very hydrophilic nature of the surfactant system. In this case, the lipophilic OA was needed to increase the lipophilicity of the surfactant system. Figure 3.4 plots the phase boundaries based on varying the total concentration of surfactants and lipophilic linker and varying the salinity. The phase diagram slants to the left at higher surfactant concentration, indicating that with increasing surfactant/linker concentration the surfactant membrane becomes more lipophilic, requiring less salinity to concentrate the surfactant at the interface; this is

most often due to preferential partitioning of hydrophilic components into the water phase at elevated concentrations, leaving behind a more lipophilic surfactant membrane [12].

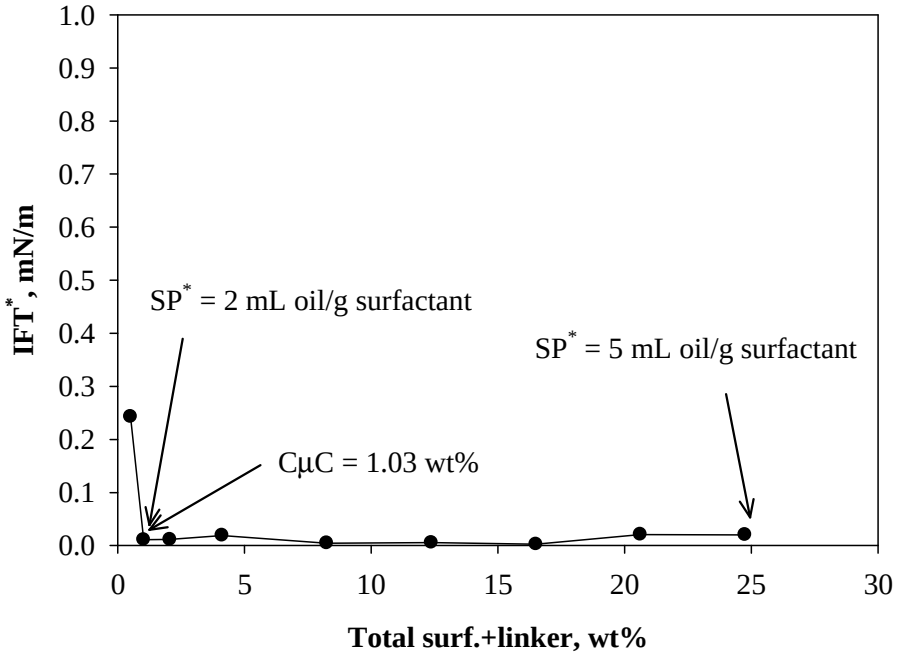


Figure 3.5. Interfacial tensions at optimum formulations of surfactant-limonene microemulsions from Figure 3.4 (below CμC, salinity is constant at 13 wt.% as presented by the vertical dashed line in Figure 3.4; above the CμC, salinity varies to correspond to optimum salinity in the center of the phase boundaries as represented by the slanted dashed line in Figure 3.4) (at 23 ± 1 ^{o}C).

Figure 3.5 reports IFT values with increasing surfactant/linker concentration along the dashed line in Figure 3.4; the minimum IFT occurs at the critical microemulsion concentration (CμC)—above this concentration, the IFT is relatively constant. The CμC is the lowest surfactant concentration where the middle phase

(Type III) microemulsion occurs, as noted on Figure 3.4. The results from the phase diagram in Figure 3.4 can be used as a guideline in manipulating the surfactant/linker ratio in the formulation. For example, in order to formulate microemulsions for diesel, using this surfactant/linker system, a higher ratio of OA and lower ratio of JBR will be required to produce a more hydrophobic formulation. On the other hand, the studied surfactant/linker ratio may still be able to form microemulsions with toluene. These formulations in Figure 3.4 generated ultralow interfacial tensions (less than 0.1 mN/m as seen in Figure 3.5). In addition, we observed a slight increase in optimum solubilization parameter as total surfactant/linker concentration increases, ranging from 2 to 5 mL oil/g surfactant (see values reported at select points on Figure 3.5).

It should be noted that the rhamnolipid biosurfactant used in this study has the fatty acid tails of C8 chain length. However, there are rhamnolipid biosurfactants made from different sources that have the chain length ranging from C8 to C14. The rhamnolipid with longer tails is more hydrophobic. Thus the rhamnolipid biosurfactant used here is the least hydrophobic type since its tail length is the shortest within the typical range. Longer tail rhamnolipid biosurfactants will modify the surfactant system to be more hydrophobic. As a result, they will either achieve the optimum formulation at lower salinity for studied oils (limonene and diesel) or be easier to formulate microemulsions with oils that are more hydrophobic than the studied oils.

Acknowledgments

Research support from the Oklahoma Center for the Advancement of Science and Technology (OCAST) is acknowledged. Gratitude is also expressed to George Smith from Huntsman for supplying the methyl ester ethoxylate surfactant. Gratitude is also expressed to the industrial sponsor of Oklahoma University's Institute for Applied Surfactant Research (IASR) (www.cbme.ou.edu/iasr/) and to the Sun Oil Company endowed Chair (DAS) at the University of Oklahoma.

References

1. Lin SC, Minton MA, Sharma MM, Georgiou G (1994) Structural and immunological characterization of a biosurfactant produced by Bacillus lichenisformis JF-2. Appl Environ Microbiol 60(1):31–38.
2. Urum K, Pekdemir T (2004) Evaluation of biosurfactants for crude oil contaminated soil washing. Chemosphere 57:1139–1150.
3. Helvaci ŞŞ, Pecker S, Özdemir G (2004) Effect of electrolytes on the surface behavior of rhamnolipids R1 and R2. Colloids Surf B Biointerfaces 35:225–233.
4. Kitamoto D, Isoda H, Nakahara T (2002) Functions and potential applications of glycolipid biosurfactants—from energy-saving materials to gene delivery carries. J Biosci Bioeng 94(3):187–201.
5. Miller RM (1995) Biosurfactant-facilitated remediation of metal contaminated soils. Environ Health Perspect 103(Suppl 1):59–62.

6. Herman DC, Lenhard RJ, Miller RM (1997) Formation and removal of hydrocarbon residual in porous media: effects of attached bacteria and biosurfactants. Environ Sci Technol 31:1290–1294.
7. Mager H, Röthlisberger R, Wzgner F (1987) Use of sophoroselipid lactone for the treatment of dandruffs and body odour. European Patent 0,209,783.
8. Inoue S, Miyamoto N (1980) Process for producing a hydroxyfatty acid ester. US Patent 4,201,844.
9. Xie Y, Li Y, Ye R (2005) Effect of alcohols on the phase behavior of microemulsions formed by a biosurfactant—rhamnolipid. J Dispers Sci Technol 26:455–461.
10. Özdemir G, Peker S, Helvaci ŞŞ (2004) Effect of pH on the surface and interfacial behavior of rhamnolipids R1 and R2. Colloids Surf A Physicochem Eng Asp 234:135–143.
11. Rosen MJ (1989) Surfactants and interfacial phenomena. Wiley, New York.
12. Bourrel M, Schechter RS (1988) Microemulsions and related systems: formulation, solvency, and physical properties, surfactant science series 30. Marcel Dekker, New York.
13. Acosta EJ, Nguyen T, Witthayapanyanon A, Harwell JH, Sabatini DA (2005) Linker-based bio-compatible microemulsions. Environ Sci Technol 39:1275–1282.
14. Komesvarakul N, Sanders MD, Szekeres E, Acosta EJ, Faller JF, Mentlik T, Fisher LB, Nicoll G, Sabatini DA, Scamehorn JF (2006) Microemulsions of

triglyceride-based oils: the effect of co-oil and salinity on the phase diagrams. J Cosmet Sci 55:309–325.

15. Xie Y, Ye R, Liu H (2007) Microstructure studies on biosurfactant-rhamnolipid/n-butanol/water/n-heptane microemulsion system. Colloids Surf A Physicochem Eng Asp 292:189–195.
16. Nguyen TT, Youssef NH, McInerney MJ, Sabatini DA (2008) Rhamnolipid biosurfactant mixtures for environmental remediation. Water Res 42:1735–1743.
17. Sabatini DA, Acosta E, Harwell JH (2003) Linker molecules in surfactant mixtures. Curr Opin Colloid Interface Sci 8:316–326.
18. Acosta E, Uchiyama H, Sabatini DA, Harwell JH (2002) The role of hydrophilic linkers. J Surfactants Deterg 5(2):151–157.
19. Özdemir G, Malayoglu U (2004) Wetting characteristics of aqueous rhamnolipids solutions. Colloids Surf B Biointerfaces 39:1–7.
20. Acosta E, Szekeres E, Sabatini DA, Harwell JH (2003) Net average curvature model for solubilization and supersolubilization of surfactant microemulsions. Langmuir 19:186–195.
21. Wu B, Cheng H, Childs JD, Sabatini DA (2002) Surfactant enhanced removal of hydrophobic oils from source zones. In: Physicochemical groundwater remediation. Kluwer, New York, pp 245–269.
22. Matta GB (1985) D-Limonene based aqueous cleaning products. US Patent 4,511,488.

23. Erilli R, Lysy R, Durbut P, Broze G (1995) Hard surface cleaner. US Patent 5,393,468.
24. Whang LM, Liu PWG, Ma CC, Cheng SS (2008) Application of biosurfactants, rhamnolipid, and surfactin, for enhanced biodegradation of diesel-contaminated water and soil. J Hazard Mater 151:155–163.
25. Lif A, Holmberg K (2006) Water-in-diesel emulsions and related systems. Adv Colloid Interface Sci 123–126:231–239.
26. Castro Dantas TN, Silva AC, Neto AAD (2001) New microemulsion systems using diesel and vegetable oils. Fuel 80:75–81.
27. Tat ME, Gerpen JHV (2000) The specific gravity of biodiesel and its blends with diesel fuel. J Am Oil Chem Soc 77(2):115–119.
28. Childs JD, Acosta E, Knox R, Harwell JH, Sabatini DA (2004) Improving the extraction of tetrachloroethylene from soil columns using surfactant gradient systems. J Contam Hydrol 71:27–45.
29. Acosta E, Uchiyama H, Tran S, Sabatini DA, Harwell JH (2002) Formulating chlorinated hydrocarbon microemulsions using linker molecules. Environ Sci Technol 36:4618–4624.
30. Salager JL, Morgan JC, Schechter RS, Wade WH, Vasquez E (1979) Optimum formulation of surfactant/water/oil systems for minimum interfacial tension or phase behavior. Soc Petrol Eng J 19:107–115.

31. Salager JL, Bourrel M, Schechter RS, Wade WH (1979) Mixing rules for optimum phase-behavior formulations of surfactant/oil/water systems. Soc Petrol Eng J 19:271–278.
32. Acosta EJ, Yuan JS, Bhakta AS (2008) The characteristic curvature of ionic surfactants. J Surfactants Deterg 11:145–158.
33. Salager JL (1999) Ionic microemulsions. In: Kumar P, Mittal KL (eds) Handbook of microemulsion science and technology. Marcel Dekker, New York, pp 247–280.
34. Salager JL (1999) Microemulsions. In: Broze G (ed) Handbook of detergents—part a: properties. Marcel Dekker, New York, pp 253–302.
35. Witthayapanyanon A, Harwell JH, Sabatini DA (2008) Hydrophilic–lipophilic deviation (HLD) method for characterizing conventional and extended surfactants. J Colloid Interface Sci 325:259–266.

CHAPTER 4

Biodiesel production via peanut oil extraction using diesel-based reverse micellar microemulsions[3]

Abstract

Vegetable oils have been studied as a feasible substitute for diesel fuel, and short term tests using neat vegetable oils showed promise with results comparable to those of diesel fuel. However, after long-term usage of vegetable oils, engine durability problems such as ring sticking, injector coking, flow, and atomization arise due to the high oil viscosity, drying with time and thickening in cold conditions. Vegetable oil/diesel blending as biodiesel fuel has been shown to be one technique to reduce vegetable oil viscosity. The goal of this research is to demonstrate the feasibility of producing this biodiesel fuel via vegetable oil extraction using diesel-based reverse micellar microemulsions as extraction solvent. In this extraction technique, peanut oil is directly extracted into the oil phase of the microemulsion based on the "likes dissolve likes" principle and the product of the extraction process is peanut oil/diesel blend. The results show that diesel-based reverse micellar microemulsion system extract oil from peanuts more effectively than both diesel and hexane alone under the same extraction condition. An extraction efficiency of 95 % was achieved at room temperature and short extraction time of 10 minutes in just a single extraction step.

[3] This chapter or portions thereof has been submitted to *Fuel* under the title "Biodiesel Production via Peanut Oil Extraction Using Diesel-Based Reverse Micellar Microemulsions", September 2009. This current version has been formatted for this dissertation.

The extracted peanut oil/diesel blend was tested for peanut oil fraction, viscosity, cloud point and pour point, which all meet the requirements for biodiesel.

Keywords: vegetable oil extraction, reverse micellar microemulsion, biodiesel

Introduction

Concerns over current energy shortages and environmental restrictions have raised interest in the development and use of non-petroleum-based renewable fuels. Vegetable oils are one option being considered for use as renewable fuels as they have been shown to have a performance comparable to that of diesel fuel [1-4]. However, long-term usage of vegetable oils in diesel engines causes engine durability problems such as flow, injector coking and ring sticking [5]. These problems are mainly due to the high viscosity of vegetable oils [6-8]. Several methods have been evaluated for reducing the viscosity of vegetable oils including: a dilution technique in which vegetable oils are blended in small portion with diesel; a microemulsion technique in which microemulsions with vegetable oils or blends of vegetable oil and diesel are formed with or without additives such as methanol, ethanol, or butanol; and a biodiesel technique, in which vegetable oils are cracked and converted into their esters or biodiesels [6, 7, 9]. In this research, we focus on the extraction of peanut oil using reverse micellar microemulsions of diesel to produce a blend of peanut oil and diesel as a dilution technique to reduce the viscosity of the extracted peanut oil for biodiesel application.

Solvent extraction of oilseeds has been the most popular process for the separation of oil and meal products in vegetable oilseeds [10-12]. Other methods of extracting oil from oilseeds include mechanical pressing [13], aqueous extraction [14-17], enzymatic aqueous extraction [18] and reverse micellar extraction [19]. Among these methods, which are often used to extract oil for cooking purposes, solvent extraction using hexane has been the most popular method that gives high oil extraction efficiency [10, 11]. In this research, we used reverse micellar microemulsions of diesel as the extraction solvent to extract oil from peanut seeds into the oil phase of the microemulsion to produce blends of peanut oil and diesel.

Several research groups have studied the simultaneous extraction of vegetable oil and proteins by using reverse micelles, but their work focused primarily on the extraction of proteins [19, 20]. In their work, the oil extraction mechanism was based on the solubilization of vegetable oil in the reverse micellar microemulsion of isooctane and of protein in the water pool of the reverse micelles. However, in our work, the extraction product was not edible oil [19, 21], but instead was a blend of vegetable oil and diesel that can be used as biodiesel fuel.

A number of researches have studied the feasibility of using vegetable oil/diesel blends or their W/O microemulsions as diesel fuels [6, 7, 9, 22]. In these studies, it has been shown that vegetable oil/diesel blends with a ratio of up to 20% of vegetable oil or W/O microemulsions with a ratio of vegetable oil/diesel of up to 40% of vegetable oil can be used in diesel engines without modification. Therefore, based

on these findings, we aim to produce blends of vegetable oil and diesel or their W/O microemulsions via the extraction process.

The proposed mechanism of vegetable oil extraction using reverse micellar microemulsions is based on the “like dissolves like” principle, which is similar to that of solvent extraction technology. This principle means that a polar solute is more soluble in a polar solvent while a non-polar solute is more soluble in a non-polar solvent [11]. Reverse micellar microemulsions have oil as the continuous phase and water as the inner core of the micelles. As a result, vegetable oil is extracted directly into the oil continuous phase and/or into the hydrophobic region of the reverse micelles while the polar protein is simultaneously extracted into the water pools of the reverse micelles [19]. A notable advantage of this method is reduced emulsion formation and thus fewer refining steps compared to those in edible oil extraction.

Microemulsions are thermodynamically stable emulsions that contain water and oil domains separated by surfactant films [23]. Microemulsions can exist in four forms as the well known Winsor-Type microemulsions. Winsor Type I (oil-in-water or O/W) microemulsions solubilize oil into spherical, normal micelles within the continuous water phase while Type II (water-in-oil or W/O) microemulsions solubilize water in reverse micelles which occur in the oil phase. Type III (middle phase) microemulsions exhibit three phases, excess oil and water phases in equilibrium with a bicontinuous phase when lamellar micelles are formed in the system [24]. In a middle phase microemulsion, increasing surfactant concentration causes the volume of the middle phase to increase until all the oil and water coexists in a Type IV single phase

microemulsion [23]. This study will use Type II water-in-oil (W/O) microemulsions as the extraction solvent to extract vegetable oil to produce a blend of vegetable oil and diesel.

The overall goal of this research is to extract oil from peanuts using W/O microemulsions of diesel to produce blends of vegetable oil and diesel for biodiesel application. We hypothesize that the extraction of oilseeds using reverse micellar microemulsions is based on the "like dissolve like" principle and thus will extract vegetable oil directly into the oil phase of the microemulsion because oil is the continuous phase of W/O (reverse micelle) microemulsions. Thus, there are four objectives: (1) to formulate diesel-based W/O microemulsions; (2) to compare the oil extraction efficiency using diesel as the solvent versus formulated diesel-based W/O microemulsions; (3) to study the effects of various extraction parameters such as solid-to-solvent ratio, extraction time, extraction shaking speed and extraction temperature on the oil extraction efficiency; and (4) to analyze the quality of the extracted oil blends as biodiesel including the viscosity, the fraction of peanut oil and diesel, the free fatty acid and the cloud and pour point of the fuel.

Materials and Methods

Materials

Biosurfactants used in this research are rhamnolipid and sophorolipid. Rhamnolipid (JBR) biosurfactant was purchased from Jeneil Biosurfactant Co. (Saukville, Wisconsin) with 15 wt% active and an average molecular weight of 577.

Rhamnolipid biosurfactant was originally a blend of 50 wt% monorhamnolipid (MW=504) and 50 wt% dirhamnolipid (MW=650) as shown in Figures 4.1a and 4.1b [25]. Sophorolipid (SPL) biosurfactant was synthesized and donated by the United States Department of Agriculture (USDA) with highly purity (~ 100 wt% active) and specific molecular structure as shown in Figure 4.1c [26]. In addition, soy bean lecithin, sodium bis(2-ethyl) dihexyl sulfosuccinate (SBDHS) (Fisher Scientific), and oleyl alcohol (Sigma Aldrich) were also used as shown in Table 4.1.

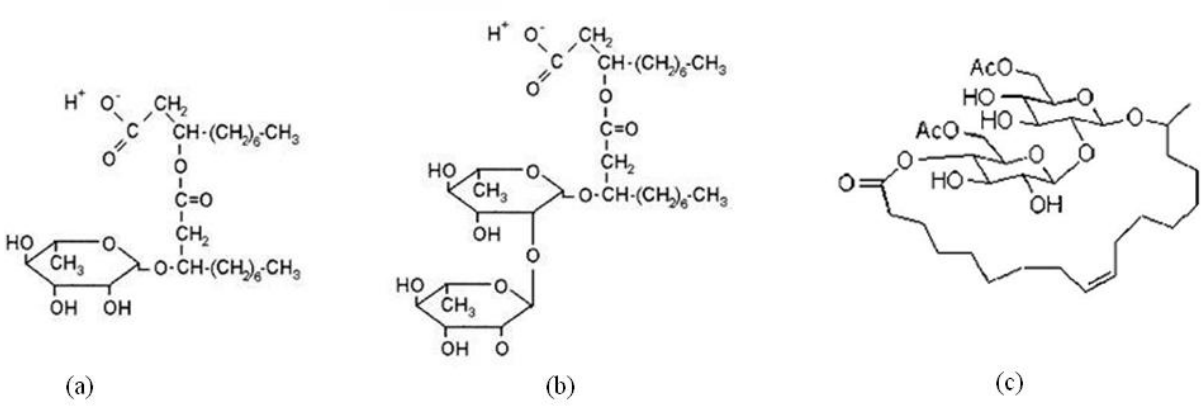


Figure 4.1. Structures of the rhamnolipids: (a) monorhamnolipid, (b) dirhamnolipid (adapted from ref. [25]) and (c) Sophorolipid (Ac = Acetyl) (adapted from ref. [26]).

In this study, peanuts were used as the oil seed to investigate the oil recovery efficiency of diesel-based reverse micellar microemulsion extraction. Peanuts were purchased from America's Best Nuts Co. (Rocky Mountain, North Carolina) as blanched. Peanut oil was purchased from Sigma-Aldrich, and diesel oil was commercial No. 2 diesel purchased from a local gas station. The composition of No. 2

diesel fuel commonly contains 86.23% carbon, 13.14% hydrogen, 0.034% sulfur, 31.0% aromatic, 64.1% paraffin and 4.9% olefin [27]. All chemicals were used without any further purification.

Table 4.1. Surfactants used in this work.

Surfactants	**Mol. Wt.**
Rhamnolipid (JBR)	577
Sophorolipid (SPL)	688
Lecithin	770
Sodium bis(2-ethyl) dihexyl sulfosuccinate (SBDHS)	445
Oleyl alcohol (OA)	268

Methods

Phase study. Phase behavior studies were conducted by placing equal volumes of the aqueous and diesel phases (5 mL of each phase) in 14 mL glass tubes (diameter of 13 mm) with Teflon® screw caps. For a given surfactant concentration and linker concentration, the salt concentration was varied to delineate the transition between the different microemulsion types, which were identified visually and by passing a laser light through the phases. The sample tubes were hand-shaken for one minute, once a day for the first three days, and then left to equilibrate at room temperature for two weeks [28].

Vegetable oil extraction. The moisture content of peanuts was determined by measuring the difference in weight of 3.0 grams of ground peanuts before and after

drying in the oven until the weight remains constant. The moisture content was found to be 5.3 %, which is consistent with results from other studies [15, 21]. Since the desired moisture content for solvent extraction of oil was reported to be 2-6% [29], in this study, we kept the moisture content of peanuts the same at its initial value in all experiments since the moisture content of peanuts used was measured to be 5.3 %.

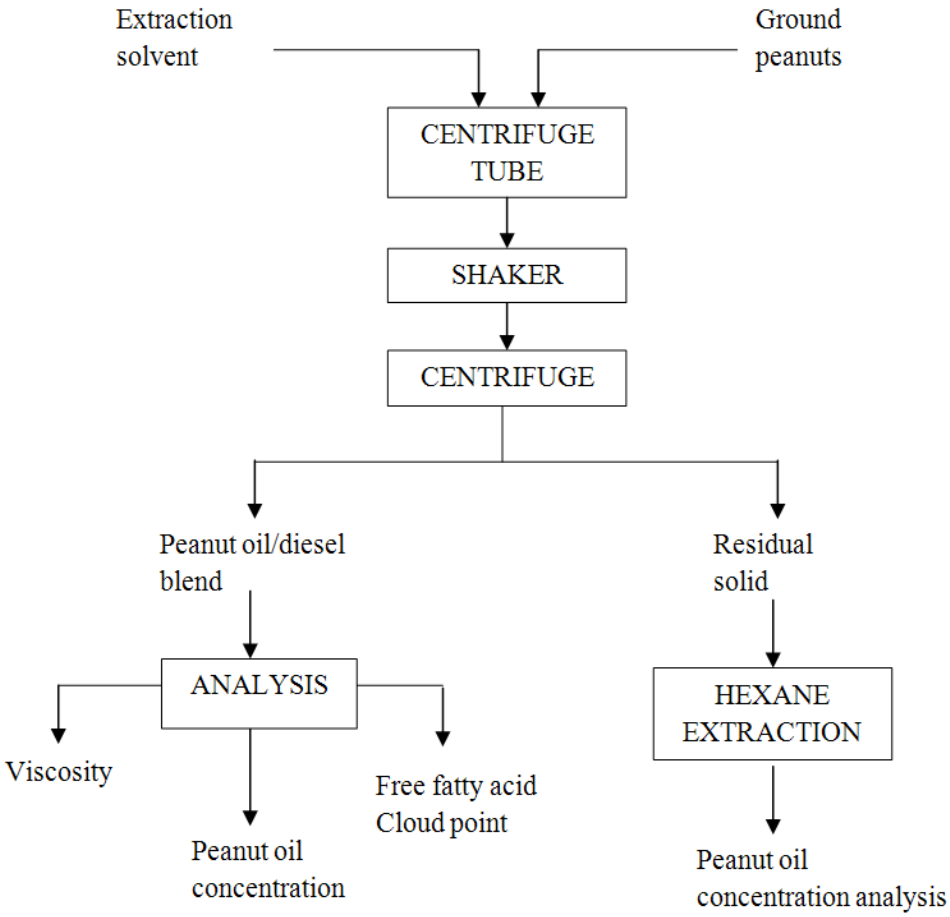


Figure 4.2. Schematic diagram of the extraction process.

The extraction process includes three steps: seed grinding, solid/solvent dispersion, and solid/liquid separation. The extraction was carried out by dispersing

the ground seeds into the W/O microemulsion and then agitating the dispersion to enhance the extraction of the oil, as shown in Figure 4.2. The formulated diesel-based W/O microemulsions were used as the extraction solvent. Each extraction experiment was carried out in single batch basis except for the study of multi step extraction. All extraction experiments were done in triplicates.

Seed grinding. Grinding ruptures the seed cells to help release their constituents in order to increase the oil extraction efficiency. Grinding was done using a mechanical grinder. Since the oil extraction mechanism is strongly dependent on "like dissolves like" principle, essentially no diffusion takes place through the cell walls. The total amount of oil available for extraction is therefore dependent on the amount of surface area. Small particles will provide a higher surface area to volume ratio and more oil will be located at the surface instead of inside of the particles [30]. Thus, grinding is a critical step in the oil extraction. This study used seed size of 0.5 – 0.84 mm, which is categorized as medium size [21, 31].

Solid/solvent dispersion. A certain amount of ground peanuts was dispersed in a certain volume of W/O microemulsion of diesel for a period of time by mechanical shaking. In all experiments, 3.0 grams of ground peanuts was used and the volume of W/O microemulsions was adjusted according to the studied solid-to-solvent ratio. Extraction parameters such as solvent types, solid-to-solvent ratio, extraction time, shaking speed and extraction temperature were varied one at a time to determine their effects on the oil extraction yield.

Solid/liquid separation. The extracted oil blend and the solid phase after the dispersion were separated by centrifugation at 4000 rpm for 30 minutes to ensure complete separation [21]. The oil phase was transferred into a separate container for further analysis. The residual solid was extracted with 20 mL hexane, followed by evaporation of hexane to obtain residual oil.

Analysis of extracted oil blends

Peanut oil extraction efficiency. Both the extracted oil blends and the residual oil were analyzed by HPLC with evaporative light scattering detector (ELSD) using Alltech Altima HP C18 5u column with the length of 250 mm and inside diameter of 4.6 mm. A mixture of 20% dichloromethane and 80% methanol was used as the analyzing solvent. Both the extracted oil blend and the residual oil blend were analyzed to determine the extraction efficiency of the extraction based on Equation 4.1. A mass balance was also done to check the validity of the analyzed results. The oil extraction efficiency was calculated by Equation 4.1 below [30]:

$$\% \text{ oil extraction} = \frac{\text{Weight of extracted peanut oil}}{\text{Weight of total oil in raw peanuts}} \times 100\% \qquad (4.1)$$

Viscosity measurement. Kinematic viscosity, one of the fuel properties, was determined from measured dynamic viscosity. The dynamic viscosity with the unit of centipoises (cP) of the extracted oil blend was measured using the Brookfield Programmable DV-III + Rheometer with spindle number 18 for low viscosity measurement. A volume of 6.7 mL of sample was placed in the chamber for

measurement. The temperature was controlled at 25 and 40 ^{o}C. The kinematic viscosity with the unit of centistokes (cSt) was calculated from the dynamic viscosity by Equation 4.2:

$$\text{Kinematic viscosity (cSt)} = \frac{\text{Dynamic viscosity (cSt)}}{\text{Solution density (g/mL)}} \qquad (4.2)$$

Cloud point and pour point tests. The two fuel properties, cloud point and pour point, were also determined. The cloud point is the temperature at which the fuel begins to thicken and become cloudy. The pour point is the temperature at which the fuel begins to thicken and no longer pour. The cloud point and the pour point are important properties of fuels since at the cloud point, some engines fail to run and at the pour point, all engines fail [32]. Thus, cloud and pour points of the extracted oil blend was determined by observing it to thicken and become cloudy at cold temperature as they are cold properties of fuels [33].

Results and Discussion

Formulation of diesel-based microemulsions

The formulation of diesel-based microemulsions was done via phase behavior studies by varying surfactant concentration and salinity as shown in Figure 4.3. Salinity was scanned for each surfactant concentration. As the salinity increases, the microemulsion transitions from Type I (water-in-oil) to Type III (bicontinuous) to Type II (oil-in-water).

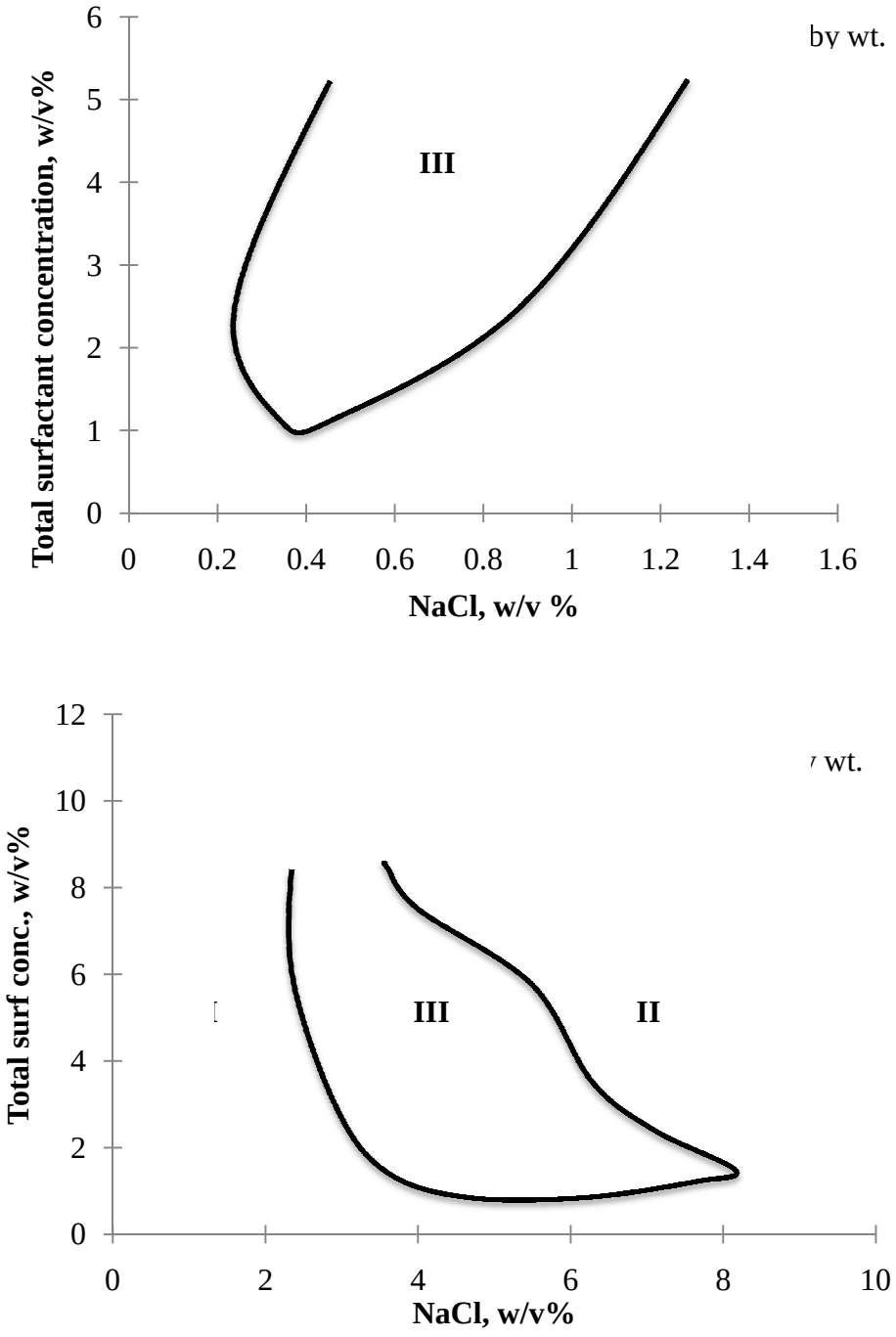


Figure 4.3. Partial fish phase diagrams with diesel of two surfactant systems: (a) Lecithin/SPL/JBR = 1/1/0.628 by wt. and (b) SBDHS/JBR/OA = 1.11/1.44/0.67 by wt.

Two surfactant systems were used to formulate microemulsions with diesel: Lecithin/SPL/JBR at ratio of 1/1/0.63 w/v% (Figure 4.3a) and SBDHS/JBR/OA at ratio of 1.1/1.4/0.67 w/v% (Figure 4.3b). The two surfactant systems show different phase behavior with diesel. For the Lecithin/SPL/JBR system (Figure 4.3a), the Type III middle phase microemulsion region (range of salinity or salinity window) gets wider as the total surfactant concentration increases. However, with further increases in surfactant concentration, the salinity window narrows as the system approaches Type IV.

For the system of SBDHS/JBR/OA, the phase diagram slants in the opposite direction as compared to the system of Lecithin/SPL/JBR. These phase behaviors indicate that the two surfactant systems have very different hydrophilicity-hydrophobicity characteristics. Thus, their W/O microemulsions with diesel were chosen as the extraction solvent to study the effect of extraction solvents on the oil extraction efficiency.

Effects of operating parameters on oil extraction efficiency

Solvent-based vegetable oil extraction involves the transfer of the oil from the solid oilseeds to the liquid solvent. The extraction depends on the nature of the solvent and oil, the contacting time between the oilseed particles and the solvent, the shaking speed, the extraction temperature and the solid-to-solvent ratio [29, 31]. Sufficient contact time is required for the solvent and the solid to equilibrate to ensure the most efficient extraction of the oil. Temperature affects the rate at which the solvent and the

solid obtain equilibrium; and this rate increases as the extraction temperature increases. A faster rate will make the process more feasible and economical. However, the extraction temperature should be below the initial boiling point of the solvent due to the safety hazard of rapid vaporization and pressurization of the extraction process [29]. Therefore, these five factors affecting the extraction process were investigated in this study.

Effect of extraction solvent

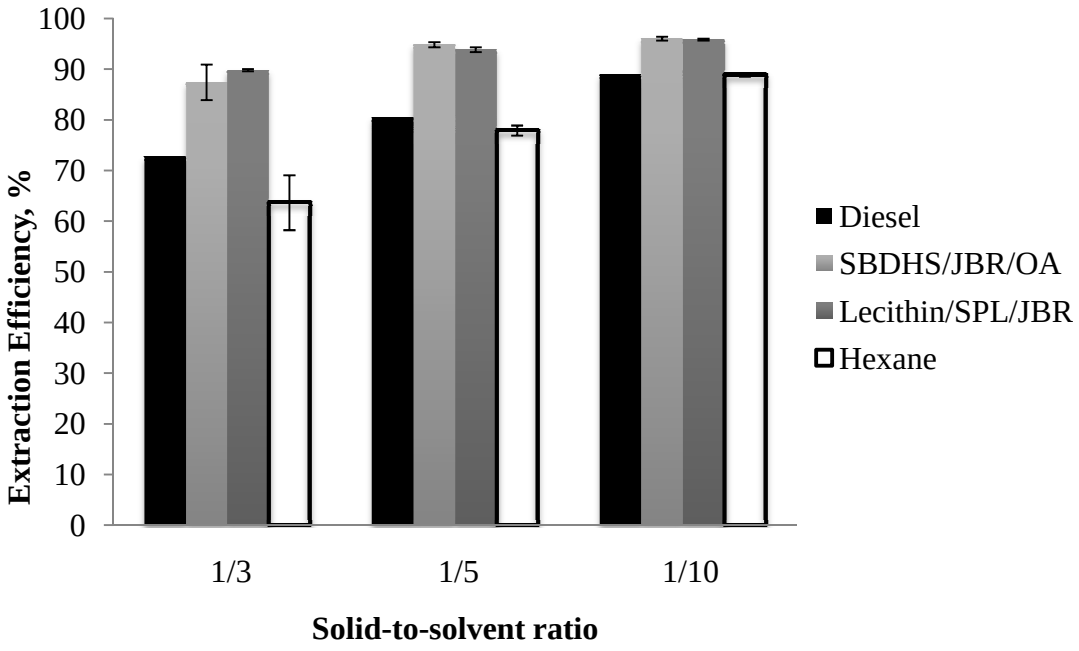


Figure 4.4. Effect of extraction solvent on oil extraction efficiency at 60 minute extraction time and 200 rpm shaking speed.

The oil extraction efficiency was compared for three types of solvents: diesel, diesel-based W/O microemulsion of Lecithin/SPL/JBR (0.5/0.5/0.31 w/v%, NaCl 2.5

w/v%) surfactant system and diesel-based W/O microemulsion of SBDHS/JBR/OA (0.56/0.72/0.34 w/v%, NaCl 9 w/v%) surfactant system. The efficiency of these three solvents was compared with the conventional extracting solvent hexane.

As seen in Figure 4.4, at the same extraction condition of 60 minutes of extraction and a shaking speed of 200 rpm, we obtained higher oil extraction efficiency with diesel-based reverse micellar (RM) microemulsions than with either hexane or diesel only at all solid to solvent ratios. For example, at the solid-to-solvent ratio of 1/10, the oil extraction efficiency produced with the RM microemulsions is about 96 % while that produced by diesel and hexane is about 89 %. This could be due to the presence of surfactants in reverse micellar microemulsions, which increases the polarity of the solvent, thereby increasing the extraction of more polar portions of vegetable oil. The oil extraction efficiency produced from diesel-based reverse micellar microemulsions of two different surfactant systems are statistically the same at all solid-to solvent ratios. Therefore, in further study, the diesel-based reverse micellar microemulsion of SBDHS/JBR/OA surfactant system was used to study different effects on the extraction yield.

Effect of solid-to-solvent ratio

The effect of solid-to-solvent ratio on the oil extraction efficiency is shown in Figure 4.5. The ratio was varied from 1:2 to 1:15 (w/v). The extraction time was 40 minutes at the shaking speed of 200 rpm. As the solid-to-solvent ratio increases from 1:2 to 1:5, the extraction efficiency increases from 79.5 ± 3.3 % to 94.1 ± 0.9 %. However, ratios above 1:5 have no significant effect on the oil extraction efficiency

since only sufficient amount of solvent is required to dissolve all the oil in the seeds. Therefore, in the following study, we used a solid-to-solvent ratio of 1:5 (w/v).

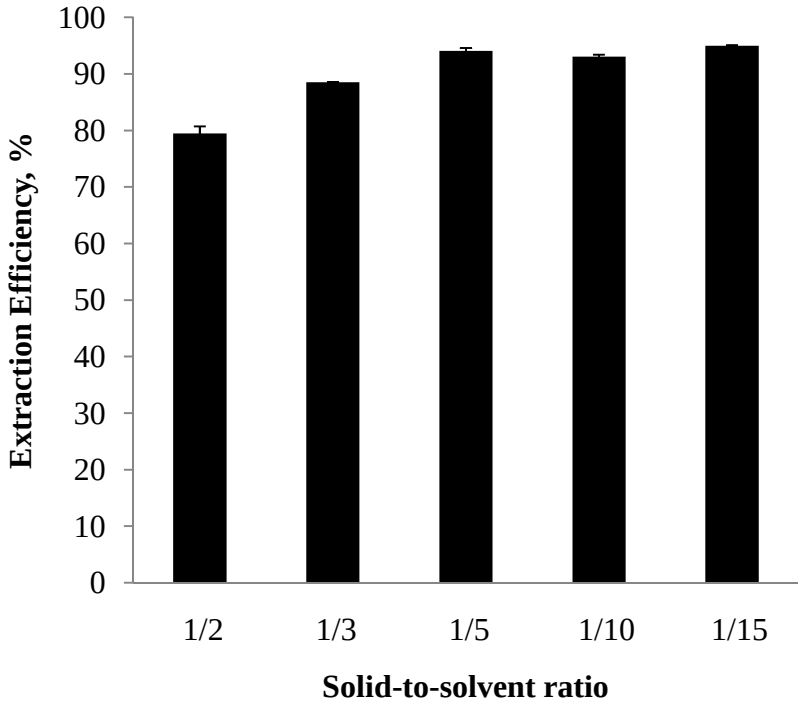


Figure 4.5. Effect of solid-to-solvent ratio on oil extraction efficiency at 40 minute extraction time and 200 rpm shaking speed using formulation of AOT/JBR/OA = 0.0125/0.0125/0.0125 M diesel-based reverse micellar microemulsion.

Effect of extraction time

In the study of the effect of extraction time on the amount of oil extracted, the extraction was carried out for various amounts of time from 5 to 60 minutes (Figure 4.6). The extraction was done at a solid-to-solvent ratio of 1:5 and shaking speed of 200 rpm. After 10 minutes of extraction, 91.6 ± 2.5 % oil was extracted. For a longer time of 40 minutes, the oil extraction efficiency increases to 94.1 ± 0.9 %. With this

extraction technology, high oil extraction was obtained at much shorter time than with other extraction methods such as aqueous extraction [34] and enzyme-assisted aqueous extraction [35] which require times of 18 – 25 hours.

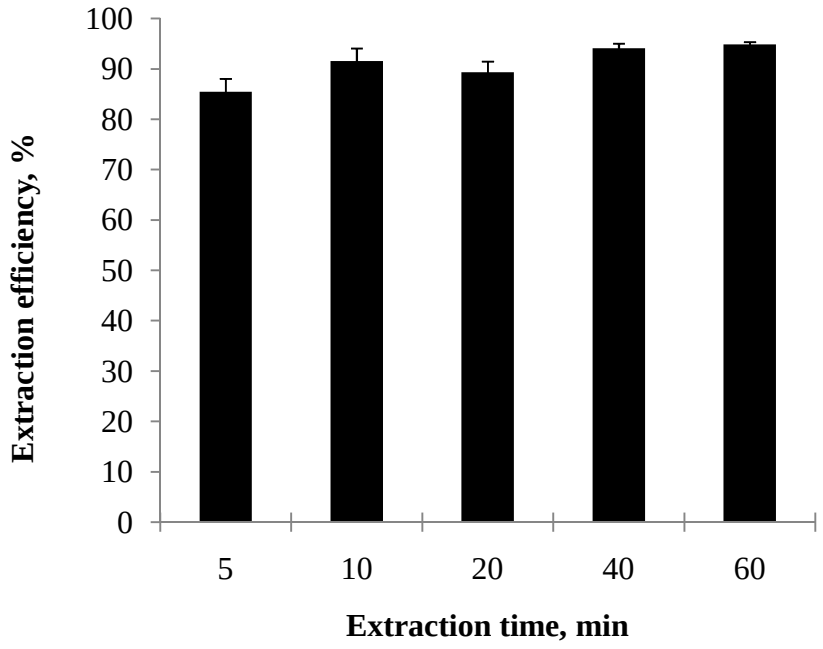


Figure 4.6. Effect of extraction time on oil extraction efficiency at 200 rpm shaking speed, solid-to-solvent ratio of 1:5 using the formulation of AOT/JBR/OA = 0.0125/0.0125/0.0125 M diesel-based reverse micellar microemulsion.

Effect of shaking speed

The effect of shaking speed on oil extraction efficiency was evaluated at 40 minutes of extraction time and solid-to-solvent ratio of 1:5. From the shaking speed range of 50 to 100 rpm, the extraction efficiency increased from 81.27 ± 4.46 % to 91.80 ± 0.61 %. However, for shaking speeds higher than 100 rpm, there is no

significant increase in the oil extraction efficiency. A different trend in the effect of shaking speed on oil extraction yield was found with the enzyme-assisted aqueous extraction [35]. For their system, it was found that at a shaking speed of 100 rpm or higher, emulsification occurs and reduces the amount of oil extracted [35]. In contrast, our extraction method using diesel-based reverse micellar microemulsions did not exhibit this emulsification problem.

Effect of extraction temperature

The study of the effect of extraction temperature on oil extraction efficiency shows statistically the same amount of oil extracted (about 93 %) at room temperature (23 ± 1 ^{o}C) and higher (up to 60 ^{o}C). The extraction was done at 150 rpm shaking speed and solid-to-liquid ratio of 1:5. The oil extraction efficiency at 10 and 40 minute extraction time is almost the same (about 93 %) at all studied temperatures, which falls in the range of values in Figure 4.6. With other oil extraction methods, high oil extraction efficiency (> 90%) was not observed until the extraction temperature reaches 40 ^{o}C or 60 ^{o}C [21, 31, 35].

Extracted Oil Blend Analysis

Peanut oil fraction and kinematic viscosity of extracted oil blend

Figures 4.7 and 4.8 plot the fraction of peanut oil in the extraction oil blend and the kinematic viscosity of the extracted oil blend at different solid-to-solvent ratios, respectively. It was found that the only extraction parameter that affects the peanut oil fraction and the viscosity of the extracted oil blends was solid-to-solvent ratio (data not shown). As the amount of extraction solvent increases or the solid-to-

solvent ratio decreases, the portion of peanut oil in the extracted oil blend decreases (Figure 4.7) as well as the viscosity of the extracted oil blend does (Figure 4.8).

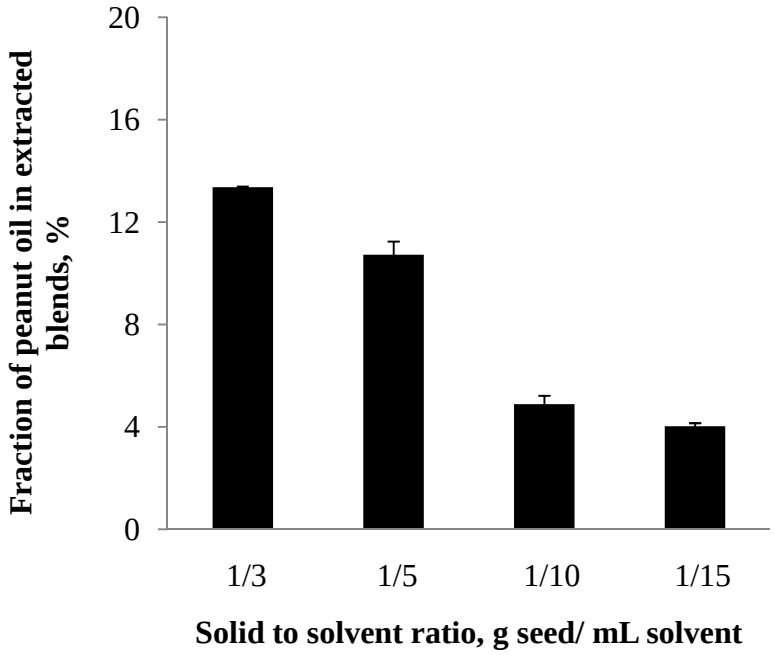


Figure 4.7. Fraction of peanut oil in extracted oil blend at various solid-to-solvent ratios and 200 rpm shaking speed for 40 minutes using the formulation of AOT/JBR/OA = 0.0125/0.0125/0.0125 M diesel-based reverse micellar microemulsion.

At all studied solid-to-solvent ratios, the fraction of peanut oil in the extracted oil blend is less than 15 %, which is desirable for alternative fuels used in diesel engine [6, 7, 9, 22]. The kinematic viscosity of the extracted oil blends was measured at two different temperatures of 25 and 40 ^{o}C. Lower viscosity was observed at higher temperature. At 25 ^{o}C, the viscosity decreases from 6.50 ± 0.24 cSt at solid-to-solvent ratio of 1/3 to 4.24 ± 0.19 cSt at solid-to-solvent ratio of 1/15. At 40 ^{o}C, the viscosity

decreases from 4.79 ± 0.17 cSt to 3.87 ± 0.14 cSt. These values meet the kinematic viscosity requirement for biodiesel, which ranges from 1.9 to 6.0 cSt at 40 ^{o}C [32].

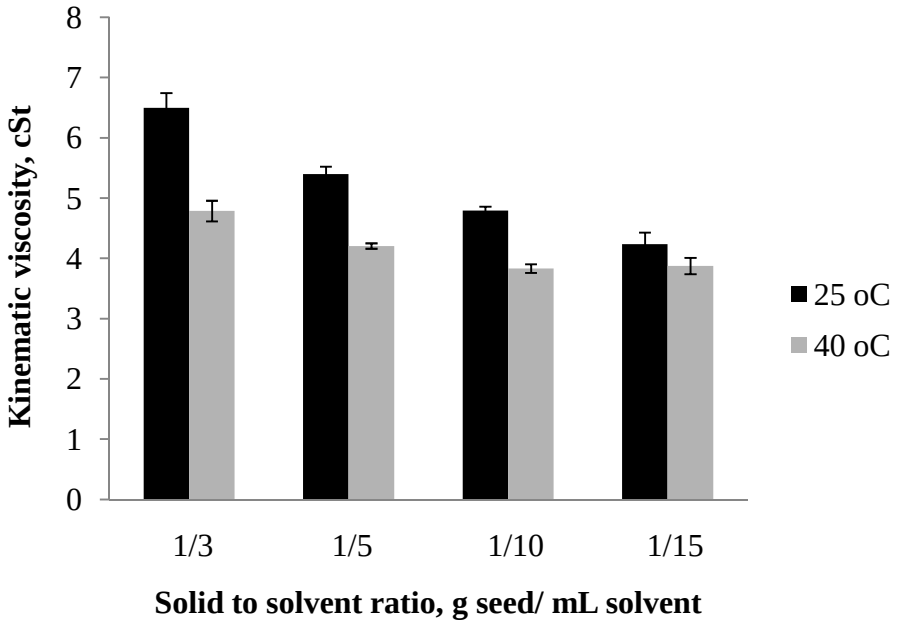


Figure 4.8. Kinematic viscosity of extracted oil blend at different solid-to-solvent ratios and temperatures, 200 rpm shaking speed and 40 minute extraction using the formulation of AOT/JBR/OA = 0.0125/0.0125/0.0125 M diesel-based reverse micellar microemulsion.

Cloud point and pour point of extracted oil blend

Since the extraction at solid-to-solvent ratio of 1/10 produces peanut oil/diesel blend with composition of less than 15 % peanut oil in the blend and kinematic viscosity within the typical viscosity range of diesel fuel No. 2, this extracted oil blend was selected to test the free fatty acid content, the cloud and the pour points. At 20 ^{o}F, the extracted oil blend was observed to be clear for all solid-to-solvent ratios. However, the pour points varied. At solid-to-solvent ratios of 1/10 and 1/15, the

extracted oil blend poured at -10 ^{o}F, but it only poured at temperature higher than 5 ^{o}F for solid-to-solvent ratios of 1/3 and 1/5. Thus at all studied conditions, the extracted oil blend meets the cloud point and pour point requirements for biodiesel, which typically are 40 ^{o}F for cloud point and 15-20 ^{o}F for pour point. In colder climate, the cloud point requirement for fuel can be as low as 10 ^{o}F and the pour point requirement can be -10 ^{o}F [32]. Therefore, depending on the climate, suitable extraction condition can be used to produce the biodiesel that meets the fuel requirement.

Conclusions

The data presented in this work demonstrate the feasibility of producing vegetable oil/diesel blends as biodiesel fuels through vegetable oil extraction using diesel-based reverse micellar microemulsions as extraction solvent. Various extraction parameters were studied, showing that at room temperature and short extraction time (10 minutes), almost 95% of extraction efficiency was obtained just by a single extraction step. Thus, an efficiency of almost 99% may be expected with a multistage extraction. The extracted peanut oil/diesel blend has the peanut oil fraction, viscosity, cloud point and pour point that meet the requirements for biodiesel fuel. The extraction efficiency using this method is higher than that when neat diesel or hexane was used under the same extraction condition and procedure.

Acknowledgement

The authors thank *Oklahoma Center for Advancement of Science and Technology (OCAST)* for financial support. Acknowledgement is also expressed to Dr. Richard Ashby from USDA-ARS for providing sophorolipid biosurfactant and undergraduate research assistants at the University of Oklahoma, Ashley Eleden and Bridgett Neighbors. Sponsors of the Oklahoma University Institute for Applied Surfactant Research (IASR) are acknowledged (http://cbme.ou.edu/iasr/index.htm).

References

1. Backer, L. F.; Jacobsen, L.; Olson, J. C. 1983. Farm-Scale Recovery and Filtration Characteristics of Sunflower Oil for Use in Diesel Engines. JAOCS, 60 (8), 1558-1560.
2. Peterson, C. L.; Auld, D. L.; Korus, R. A. 1983. Winter Rape Oil Fuel for Diesel Engines: Recovery and Utilization. JAOCS, 60 (8), 1579-1587.
3. Pryde, E. H. 1983. Vegetable Oils as Diesel Fuels: Overview. JAOCS, 60 (8), 1557-1558.
4. Ryan, T. W.; Dodge, L. G.; Callahan, T. J. 1984. The Effects of Vegetable Oil Properties on Injection and Combustion in Two Different Diesel Engines. JAOCS, 61 (10), 1610-1619.
5. Avella, F.; Galtieri, A.; Fiumara, A. 1992. Characteristics and Utilization of Vegetable Derivatives as Diesel Fuels. La Rivista dei Combustibili, 46 (6), 181-188.

6. Ergeneman, M.; Özaktas, T.; Ciğizoğlu, K. B.; Karaosmanoğlu, F.; Arslan, E. 1997. Effect of Some Turkish Vegetable Oil – Diesel Fuel Blends on Exhaust Emissions. Energy Sources, 19, 879-885.
7. Ma, F. and Hanna, M. A. 1999. Biodiesel Production: A Review. Bioresource Technology, 70, 1-15.
8. Neuma de Castro Dantas, T.; da Silva, A. C.; Neto, A. A. D. 2001. New Microemulsion Systems Using Diesel and Vegetable Oils. Fuel, 80, 75-81.
9. Rakopoulos, C. D.; Antonopoulos, K. A.; Rakopoulos, D. C.; Hountalas, D. T.; Giakoumis, E. G. 2006. Comparative Performance and Emissions Study of a Direct Injection Diesel Engine Using Blends of Diesel Fuel with Vegetable Oils or Bio-Diesels of Various Origins. Energy Conversion and Management, 47, 3272-3287.
10. Becker, W. 1978. Solvent Extraction of Soybeans. Journal of The American Oil Chemists' Society, 55, 754-761.
11. Johnson, L. A.; Lusas, E. W. 1983. Comparison of Alternative Solvents for Oils Extraction. JAOCS, 60 (2), 229-241.
12. Nieh, C. D.; Snyder, H. E. 1991. Solvent Extraction of Oil from Soybean Fluor I – Extraction Rate, a Countercurrent Extraction System, and Oil Quality. JAOCS, 68 (4), 246-249.
13. Bachmann, J. 2001. Small-Scaled Oilseed Processing. Appropriate Technology Transfer for Rural Area. 24 pages.

14. Hagenmaier, R.; Cater, C. M.; Mattil, K. F. 1972. Critical Unit Operations of the Aqueous Processing of Fresh Coconuts. JAOCS, 49, 178-379.

15. Cater, C. M.; Rhee, K. C.; Hagenmaier, R. D.; Mattil, K. F. 1974. Aqueous Extractions – An Alternative Oilseed Milling Process. JAOCS, 51, 137-141.

16. Nasuk, A.; Sabatini, D. A.; Tongcumpou, C. 2009. Microemulsion-Based Palm Kernel Oil Extraction Using Mixed Surfactant Solution. Industrial Crops and Products, 30 (2), 194-198.

17. Do. L. D., and Sabatini, D. A. 2009. Aqueous Extended-Surfactant Based Method for Vegetable Oil Extraction. Proof of Concept. Submitted to JAOCS in the area of Nonfood/Industrial Applications.

18. Chen, B.; Diosady, L. L. 2003. Enzymatic Aqueous Processing of Coconuts. International Journal of Applied Science and Engineering, 1 (1), 55-61.

19. Leser, M. E.; Luisi, P. L.; Palmieri, S. 1989. The Use of Reverse Micelles for The Simultaneous Extraction of Oil and Proteins from Vegetable Meal. Biotechnology and Bioengineering, 34, 1140-1146.

20. Ugolini, L.; Nicola, G. D.; Palmieri, S. 2008. Use of Reverse Micelles for the Simultaneous Extraction of Oil, Proteins, and Glucosinolates from Cruciferous Oilseeds. Journal of Agricultural and Food Chemistry, 56, 1595-1601.

21. Rhee, K. C.; Cater, C. M.; Mattil, K. F. 1972. Simultaneous Recovery of Protein and Oil from Raw Peanuts in an Aqueous System. Journal of Food and Science, 37, 90-93.

22. Lif, A. and Holmberg, K. 2006. Water-in-Diesel Emulsions and Related Systems. Advances in Colloid and Interface Science, 123-126, 321-329.

23. Rosen, M. J. 1989. Surfactants and Interfacial Phenomena. John Wiley & Sons, Inc., 2nd ed.

24. Bourrel, M., and Schechter, R. S. 1998. Microemulsions and Related Systems: Formulation, Solvency, and Physical Properties. Surfactant Science Series 30, 229-302.

25. Helvaci, Ş. Ş., Pecker, S., and Özdemir, G. 2004. Effect of Electrolytes on the Surface Behavior of Rhamnolipids R1 and R2. Colloids and Surfaces B: Biointerfaces 35, 225-233.

26. Ashby, R. D.; Solaiman, D. K. Y.; Foglia, T. A. 2008. Property Control of Sophorolipids: Influence of Fatty Acid Substrate and Blending. Biotechnol Lett, 30, 1093-1100.

27. Tat, M. E. and Gerpen, J. H. V. 2000. The Specific Gravity of Biodiesel and Its Blends with Diesel Fuel. JAOCS, 77 (2), 115-119.

28. Acosta, E. J.; Nguyen, T.; Witthayapanyanon, A.; Harwell, J. H.; Sabatini, D. A. 2005. Linker-Based Bio-compatible Microemulsions. Environmental Science and Technology, 39, 1275-1282.

29. Wan, P. J. and Wakelyn, P. J. 1997. Technology and Solvents for Extracting Oilseeds and Nonpetroleum Oils. AOCS Press, Champaign, Illinois.

30. Goodrum, J. W.; Kilgo, M. B. 1987. Peanut Oil Extraction using Compressed CO_2. Energy in Agriculture, 6, 265-271.

31. Sayyar, S.; Abidin, Z. Z.; Yunus, R.; Muhammad, A. 2009. Extraction of Oil from Jatropha Seeds-Optimization and Kinetics. American Journal of Applied Sciences, 6 (7), 1390-1395.

32. Gerpen, J. V.; Pruszko, R.; Clements, D.; Shanks, B.; Knothe, G. 2006. *Building a Successful Biodiesel Busines*, 2nd Ed. Biodiesel Basics. ISBN: 0-9786349-0-X.

33. ASTM method, D2500. 1995. ASTM Book of Standard Test Methods, 268-271, American Society for Testing Materials, Philadelphia, PA.

34. Lanzani, A.; Petrini, N. C.; Cozzoli, O.; Gallavresi, C.; Carola, C.; Jacini, G. 1975. On Use of Enzymes for Vegetable Oil Extraction, A Preliminary Report. Ital. Sostanze Grasse, 21, 226-229.

35. Sharma, A.; Khare, S. K.; Gupta, M. N. 2002. Enzyme-Assisted Aqueous Extraction of Peanut Oil. JAOCS, 79 (3), 215-218.

CHAPTER 5

Biocompatible Lecithin-Based Microemulsions with Rhamnolipid and Sophorolipid Biosurfactants: Formulation and Applications

Abstract

The objectives of this research are first to evaluate the hydrophilicity/hydrophobicity of sophorolipid biosurfactants relative to conventional synthetic surfactants and then to formulate and evaluate microemulsions of lecithin/rhamnolipid/sophorolipid biosurfactants with a range of oils (varying EACN values and oil types). We found that sophorolipid biosurfactants are more hydrophobic than sodium bis(2-ethyl) dihexyl sulfosuccinate (SBDHS), which is more hydrophobic than sodium dihexyl sulfosuccinate (SDHS) and rhamnolipid biosurfactant. Sophorolipid thus played an important role as the hydrophobic component in lecithin/rhamnolipid/sophorolipid biosurfactant formulation. This biosurfactant formulation was able to produce Winsor Type I, III and II microemulsions and the corresponding ultralow IFT for limonene, decane, isopropyl myristate and hexadecane. The phase behavior of this formulation with isopropyl myristate did not change significantly with changing temperature (10, 25, 40 ^{o}C) and electrolyte concentration (0.9 and 4.0% w/v), making it desirable for cosmetic and drug delivery applications. The hexadecane detergency performance of our biocompatible formulation was higher than that of a commercial liquid detergent at the same surfactant active concentrations.

Keywords: biocompatible, biosurfactant, microemulsion, phase behavior, detergency

Introduction

Microorganism-produced biosurfactants have diverse structures including glycolipids, phospholipids, polysaccharide-lipid complexes, lipopeptides and hydroxylated and cross-linked fatty acids [1, 2]. The most common glycolipid biosurfactants are rhamnolipids and sophorolipids, which are of interest in this research. The glycolipid species are generally composed of carbohydrate heads and lipid tails as shown in Figure 5.1 [3, 4].

Rhamnolipid biosurfactants have two hydrophilic head groups: carboxylate groups give rhamnolipids an anionic character and rhamnosyl groups contribute to the bulkiness of the head group. Rhamnolipid biosurfactants have two identical tails of C8 alkyl chains as shown in Figure 5.1 [5]. We have studied the characteristic and microemulsion formation of rhamnolipid extensively in our previous work [6, 7], which showed that rhamnolipid is a hydrophilic surfactant. The hydrophilicity – hydrophobicity balance (HLB) of rhamnolipid has been reported as 22 – 24 [5].

Sophorolipid has only one long tail of an unsaturated fatty acid. There are two conformations of sophorolipid during production: lactone form resulting from the esterification of the carboxylic acid group to the disaccharide ring (Figure 5.2a) and acidic form with two head groups of dimeric sugar sophorose and carboxylic acid (Figure 5.2b), in which the sophorose head is acetylated [4]. These acetyl groups have

been shown to lower the hydrophilicity of sophorolipid, and thus increase the hydrophobicity of sophorolipid [8].

Rhamnolipid and sophorolipid biosurfactants possess properties that make them attractive in many applications such as bioremediation, microbial enhanced oil recovery, food and cosmetic industries and pharmaceutical applications [9-14]. Due to their biocompatibility and low toxicity, the use of rhamnolipid and sophorolipid biosurfactants in cosmetic and pharmaceutical applications is of increasing interest [15]. Specifically, rhamnolipids have been shown to have a high antimicrobial activity against bacteria and fungi and immunological activity [16, 17]. Studies on sophorolipids have demonstrated that they show potential for use in cosmetic and pharmaceutical applications such as skin moisturizer, anti-human immunodeficiency virus and sperm-immobilizing activities [8, 15, 18].

Microemulsions are thermodynamically stable, isotropic dispersions of oil, water and surfactant [19]. Microemulsion systems produce high solubilization capacity and ultra-low interfacial tensions of oil and water, making them desirable in practical applications such as enhanced oil recovery (EOR), drug delivery, and food and cosmetic applications [20-25]. Microemulsions can exist in four forms of Winsor microemulsions [19, 20]. Type I and Type II microemulsions are two-phase systems. Type I microemulsions consist of oil solubilized in spherical normal micelles within the water-continuous phase in equilibrium with the free oil phase while Type II microemulsions consist of water solubilized in reverse micelles within the oil-continuous phase in equilibrium with the aqueous phase. Type III microemulsions

exhibit three-phase systems in which the middle phase microemulsions are in equilibrium with both excess oil and excess aqueous phases. Type IV microemulsions result from the expansion of the middle phase Type III microemulsions with increasing surfactant concentration such that all the excess oil and excess water is incorporated into a single phase system.

Lecithin-based microemulsions have proven to be desirable in biocompatible formulations due to their tendency to mimic the phospholipid nature of cell membranes [26]. Other studies have studies evaluated the applications of rhamnolipid and sophorolipid biosurfactants in cosmetics and pharmaceuticals [8, 9, 12, 15-18]. However, the microemulsion phase behavior of sophorolipid has not yet been studied and only limited research has evaluated the microemulsion phase behavior of rhamnolipid [5-7].

Therefore, the overall goal of this research is to evaluate the hydrophilicity/hydrophobicity of the sophorolipid biosurfactant and its microemulsion phase behavior in mixtures with rhamnolipid and lecithin using a range of oils. We hypothesize that sophorolipid is hydrophobic based on its lactone structure with two acetyl groups attached to the dimeric sugar sophorose head group. It is also hypothesized that, due to the dimeric sugar sophorose head, sophorolipid will be relatively insensitive to temperature even though it is a nonionic surfactant, and that consequently microemulsion formulations using lecithin, rhamnolipid and sophorolipid will be relatively insensitive to temperature. There are thus four objectives in this work: (1) to investigate the hydrophobicity of sophorolipid

biosurfactant; (2) to demonstrate the ability to produce alcohol free lecithin-based biocompatible microemulsions using sophorolipid for a range of oils (oil types and oil equivalent alkane carbon numbers (EACNs)), including limonene, decane, isopropyl myristate (IPM) and hexadecane; (3) to evaluate the effect of temperature and electrolyte on lecithin-based sophorolipid microemulsions; and (4) to compare the detergency power of lecithin-based sophorolipid formulation with commercial detergent for the removal of hexadecane. Among the four studied oils, the microemulsions of limonene and IPM are studied toward their applications in cosmetics and pharmaceutical and that of decane and hexadecane toward its application in detergency.

Materials and Methods

Materials

Rhamnolipid (JBR) biosurfactant was purchased from Jeneil Biosurfactant Co. (Saukville, Wisconsin) at 15.6 wt% active, which is roughly a blend of 50% monorhamnolipid (Figure 5.1a) and 50% dirhamnolipid (Figure 5.1b). Sophorolipid (SPL) biosurfactants (Figure 5.2) were synthesized and donated by the United States Department of Agriculture (USDA) with high purity (~ 100% active). Two types of SPLs were studied in this work, which were synthesized by *C. bombicola* from palmitic C16 fatty acid (SPL-P) and oleic C18 fatty acid (SPL-O) [4]. Thus, SPL-P has unsaturated C16 in the tail and SPL-O has unsaturated C18.

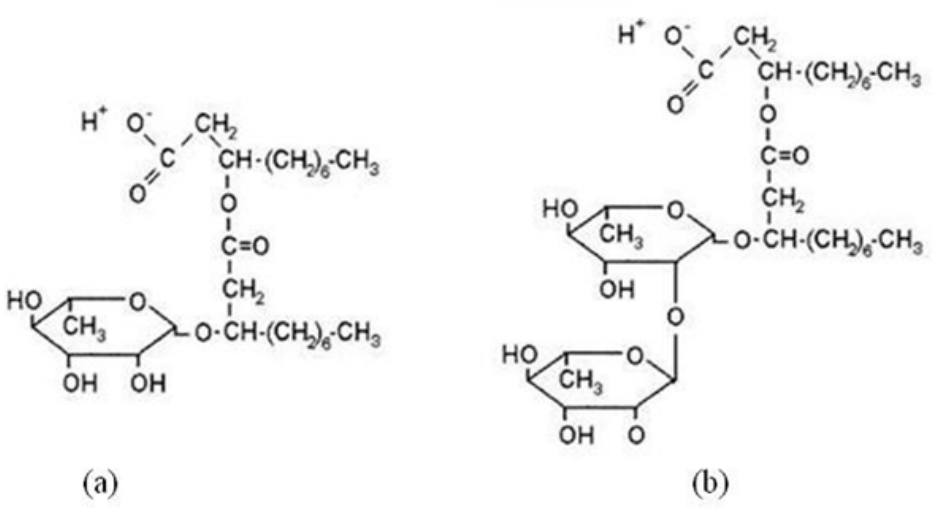


Figure 5.1. Structures of the rhamnolipids: (a) monorhamnolipid and (b) dirhamnolipid (adapted from ref. [3]).

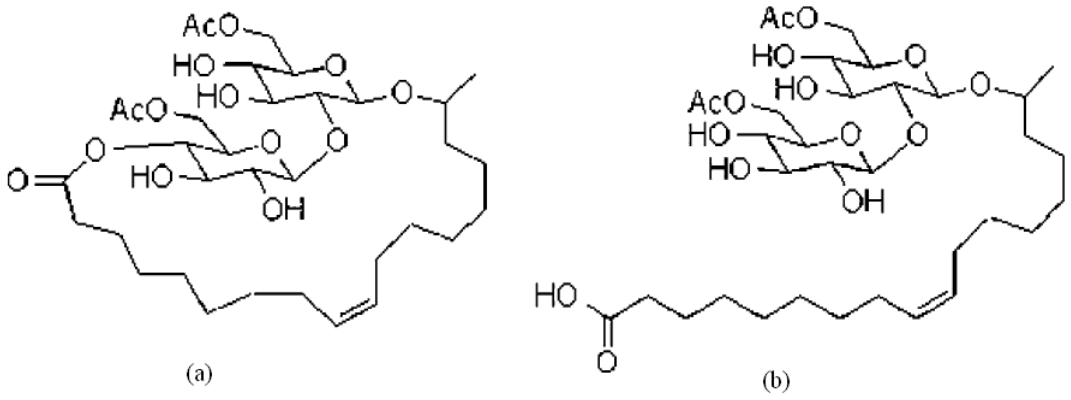
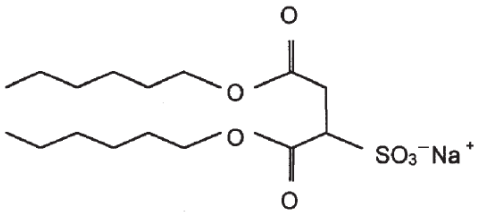
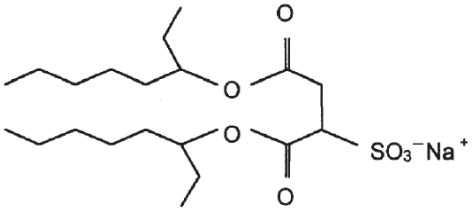
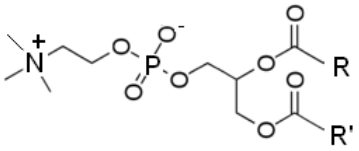


Figure 5.2. Structures of the sophorolipids (Ac = Acetyl): (a) lactone form and (b) acidic form (adapted from ref. [4]).

Soybean lecithin and sodium bis(2-ethyl) dihexyl sulfosuccinate (SBDHS) were purchased from Fisher Scientific as 100% active and sodium dihexyl

sulfosuccinate (SDHS, 80% wt. solution in water) was from Sigma Aldrich. Sodium chloride (NaCl, 99+%) was used as the electrolyte.

Table 5.1. Surfactants used in this work.

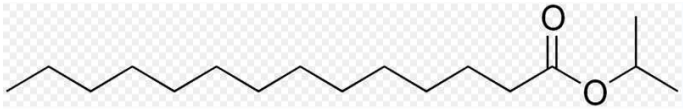
Surfactant	Mol. wt.	Molecular structure
Sodium dihexyl sulfosuccinate (SDHS)	376	
Sodium bis(2-ethyl)dihexyl sulfosuccinate (SBDHS)	432	
Lecithin	770[a]	
Rhamnolipid (JBR)	577[b]	Fig. 1
Sophorolipid - oleic acid (SPL-O)	688[c]	Fig. 2
Sophorolipid - palmatic acid (SPL-P)	660[c]	Fig. 2

[a]from ref [27], [b]from ref [3], [c]from ref [4]

The five oils studied were limonene (98%), isopropyl myristate (IPM, 98%), benzene, decane and hexadecane (99+%, anhydrous), which were purchased from

Sigma Aldrich. All chemicals were used without further purification. The fabric used in detergency tests was a standard unsoiled 65% polyester and 35% cotton blend.

Table 5.2. Oils used in this work.

Oil	EACN	Mol. wt.	Molecular structure
Benzene	0[a]	78	
Limonene	5.7[b]	136	
Decane	10[c]	142	
Isopropyl myristate	13[d]	270	
Hexadecane	16[c]	226	

[a]from ref. [20], [b]from ref. [27], [c]from ref. [28, 29], [d]from ref. [30]

Methods

Phase Study

Phase behavior studies were conducted by placing equal volumes of the aqueous and oil phase (5 mL of each phase) in 14 mL glass tubes (diameter of 13 mm). When benzene was used as the oil phase, Teflon® screw caps were used to minimize evaporation. The sample tubes were hand-shaken for one minute once a day

for the first three days, and then left to equilibrate at desired temperatures in a water bath for two weeks [30]. Microemulsions were identified visually and by passing a laser light through the phases.

Sophorolipid hydrophilicity/hydrophobicity study. In this study, rhamnolipid was used as the reference surfactant and mixed with SBDHS, SDHS, SPL-P and SPL-O individually. The total surfactant concentration was fixed at 0.1 M with varying surfactant ratio. For each surfactant ratio, salinity was scanned to determine the optimum formulation where equal amounts of oil and water were solubilized in the middle phase microemulsion. Benzene was used in this study as the oil. Thus the height of each phase in the middle phase microemulsion was measured after equilibrium to determine the phase volumes [30].

Microemulsion formulations of surfactant mixtures with various oils. Surfactant mixtures were studied using combinations of lecithin, SPL-O and JBR. The ratio of lecithin to SPL-O was kept constant at 1/1 by weight. The electrolyte concentration was fixed at 0.9 w/v % for most experiments since this is the maximum salinity concentration that does not cause irritation in human cosmetic and pharmaceutical products. The JBR concentration was varied for each lecithin concentration to delineate the transition between the different microemulsions types. For limonene and IPM, fish diagrams were constructed based on the varying lecithin concentration with varying JBR concentration. For decane and hexadecane, the lecithin/SPL-O concentration was fixed at 4/4% wt. and the JBR concentration was varied. The resulting interfacial tension values were measured with each oil. All these

phase studies were performed at room temperature of 23 ± 1 ^{o}C, except for those with IPM, which were also done at 10 and 40 ^{o}C.

Interfacial Tension

The interfacial tension value between the excess oil and excess water phases was measured using glass capillary tubes and a spinning drop tensiometer (Model 500 purchased from the University of Texas). The capillary tube is 2 mm in diameter and has a volume of 300 μl. The tube was filled with the excess water (the denser phase), and then 1-5 μl of the excess oil (the less dense phase) was injected into the aqueous solution to form a droplet [31]. The filled tube was then placed in the spinning drop tensiometer and the oil droplet size was measured.

Detergency Test

Detergency test was performed using a model 7243 Terg-O-Tometer US Testing machine (USA Testing Co., Inc., Hoboken, NJ) and ASTM standard D3050-98, "Standard Guide for Measuring Soil Removal from Artificially Contaminated Soils" [32]. Fabrics were cut into 3x4 in. pieces and artificially stained by immersing in a chloroform solution containing 20% by volume of hexadecane dyed with 200 ppm of oil red O. The stained fabrics were then dried under a ventilated hood [33, 34]. Detergency tests were conducted at an agitation speed of 120 rpm and room temperature with 20 minutes of washing with 1 L of surfactant formulation solution, followed by two rinse steps with deionized water: the first rinse was for three minutes and the second rinse was for two minutes [35]. Each detergency experiment was done in triplicate. The post wash fabrics were hung to dry overnight prior to determining

detergency efficiency, which was calculated based on the reflectance of the prewash and post wash stained fabrics. The reflectance was measured at 520 nm using the Ultra Scan Sphere Spectrophotometer (Hunter Lab). The detergency (%) was calculated based on the following equation:

$$\text{Detergency (\%)} = [(A - B)/(C_o - B)] \times 100 \qquad (5.1)$$

where A is the average reflectance of the soiled fabrics after washing, B is the average reflectance of the soiled fabrics before washing and C_o is the average reflectance of the unsoiled fabrics before washing [33]. For comparison purposes, a commercial liquid laundry detergent was also studied (2x Ultra Tide, manufactured by Procter & Gamble, Co., total active surfactant of 27.5% (P & G MSDS)).

Results and Discussions

Sophorolipid hydrophilicity/hydrophobicity

To access the hydrophilicity/hydrophobicity of the sophorolipid surfactant, we studied the optimum salinity of sophorolipids with benzene and compared it with that of conventional synthetic surfactants SDHS and SBDHS. Figure 5.3 plots the optimum salinity (S^*, the salinity at which the optimum formulation is obtained) for each surfactant mixture as a function of molar fraction of JBR, which is the common surfactant in all surfactant mixtures. It is observed that for all four surfactants studied, increasing the JBR mole fraction increases the optimum salinity for the mixture. Prior to further discussing the results presented in Figure 5.3, it is helpful to introduce the Winsor R-ratio concept. The Winsor R-ratio is defined as follows:

$$R = \frac{A_{CO}}{A_{CW}} \tag{5.2}$$

where A_{CO} and A_{CW} indicate the interaction between the surfactant adsorbed at the interface with the oil phase and water phase, respectively [36]. For R < 1, the water-surfactant interaction is stronger than the oil-surfactant interaction while the opposite is true for R>1; thus, systems with R <1 form Type I microemulsion system and systems with R > 1 form Type II microemulsion system. At R = 1, the water-surfactant and oil-surfactant interactions are balanced and optimum formulation (Type III microemulsion) is formed. A change in a tuning parameter such as salinity or temperature will result in a change in at least one of the interactions [37]. For example, as the salinity increases, the interaction between surfactant and water or A_{CW} will decrease and thus the R ratio will increase; as a result, a phase transition from Type I to Type III may occur. Another way of explaining the effect of salinity on the phase transition is that, as the salinity increases, the surfactant system becomes more hydrophobic and the surfactant-oil interaction increases, resulting in an increase in the R ratio. Therefore, for a given oil phase, a more hydrophilic surfactant system will require higher salinity to increase the R ratio to 1. In other words, the optimum salinity will be higher when using more hydrophilic surfactants to form microemulsions.

The Winsor concept can be used to interpret the trends observed in Figure 5.3. For any given molar fraction of JBR, the optimum salinity decreases in mixture with other surfactants in the following order: SDHS, SBDHS, SPL-P and SPL-O. Since JBR is the common surfactant in all mixtures, for a given molar fraction of JBR, the

optimum salinity value is dependent on the hydrophilicity/hydrophobicity of the other surfactant in the mixture. At 100% JBR, S* is at its highest (6.5%), indicating that JBR is the most hydrophilic surfactant among the surfactants studied.

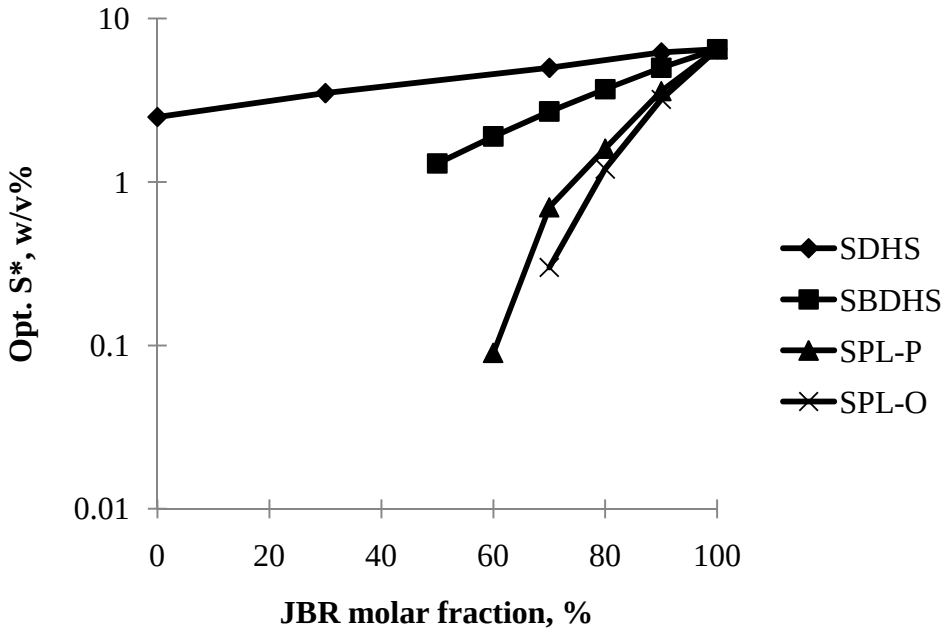


Figure 5.3. Optimum salinity (S^*) for varying fraction of rhamnolipid in mixtures with SDHS (♦), SDBHS (■), SPL-P (▲) and SPL-O (×) in microemulsion formulation with benzene. Total surfactant concentration is kept constant at 0.1 M for all mixtures and surfactant ratios.

Based on the discussion above, the hydrophilicity of other surfactants is as follows: JBR>SDHS>SBDHS>SPL-P>SPL-O (i. e., the most hydrophilic surfactant mixtures will result in the highest S^*). In addition, from Figure 5.3 we observed that an optimum middle phase microemulsion with benzene can be produced with SDHS

alone (no JBR), but the other surfactants require JBR to be present in order to form an optimum microemulsion. Higher molar fractions of the other three surfactants (SBDHS, SPL-P, SPL-O) results in only Type II microemulsions or no microemulsions because these surfactants are too hydrophobic for benzene and/or they form mesophases (e.g., liquid crystals) rather than microemulsions.

The optimum salinity values for mixtures of JBR with SPL-P and SPL-O show very similar results, which is expected due to the similarity in these surfactants (they differ only by two carbons in the tail). However, the optimum salinity of their mixture with JBR is an order of magnitude lower than that of SBDHS, which is in the same order of magnitude as that of SDHS. From this study, it can be concluded that sophorolipid biosurfactants are hydrophobic surfactants. In the following studies of microemulsion formulation, SPL-O was used throughout and abbreviated as SPL.

Effects of temperature and salinity on IPM-based biocompatible microemulsions

Changes in temperature or salinity are important considerations in microemulsion applications such as cosmetics and drug delivery [30]. Therefore, we studied the phase behavior of IPM-based biocompatible microemulsions at three temperatures (10, 25 and 40 ^{o}C – Figure 5.4A) and at two electrolyte levels (0.9 and 4% w/v – Figure 5.4B)) to evaluate the change in phase behavior of IPM-based microemulsions with these parameters. The phase behavior changed from Type II to III to I with increasing JBR/Lecithin weight ratio as observed in Figures 5.4A and 5.4B. At low JBR/lecithin weight ratios, Type II microemulsions were observed, indicating that the surfactant system has a Winsor R > 1; this suggests that the

interaction between the surfactant and the oil phase (A_{CO}) is stronger than that between the surfactant and the water phase (A_{CW}). As the JBR/lecithin weight ratio increases (the amount of JBR in the mixture increases), the Winsor parameter A_{CW} increases and the A_{CO} decreases due to the hydrophilic nature of JBR. This causes a transition from Type II to Type III microemulsions when the A_{CO} and A_{CW} values are balanced (R = 1). Further increases in JBR in the surfactant mixture cause the A_{CW} parameter to dominate and the R ratio becomes less than 1, causing Type I microemulsions to form.

With changing temperature the phase diagrams show only a slight change (see Figure 5.4A). All three types of microemulsions were produced at all three temperatures. However, the window of the middle phase microemulsions (Type III) at 10 ^{o}C is slightly narrower than that at 25 ^{o}C and 40 ^{o}C, which are very similar. This trend can be interpreted from the fact that at higher temperatures (i.e., 25 ^{o}C or 40 ^{o}C), the ionic surfactant becomes more hydrophilic, and the system requires a lower concentration of hydrophilic surfactant rhamnolipid to form a middle phase microemulsion [20]. As a result, the JBR to lecithin weight ratio decreases and the Type III window is narrower at 10 ^{o}C. In general, nonionic surfactants, SPL in this case, is affected by temperature to a greater extent than ionic surfactant [19]. However, the sugar head of SPL makes it less temperature-sensitive since the sugar head group hydration has been shown not to change significantly with temperature [38, 39]. This explains why the overall behavior of the IPM-based microemulsions is virtually temperature-insensitive.

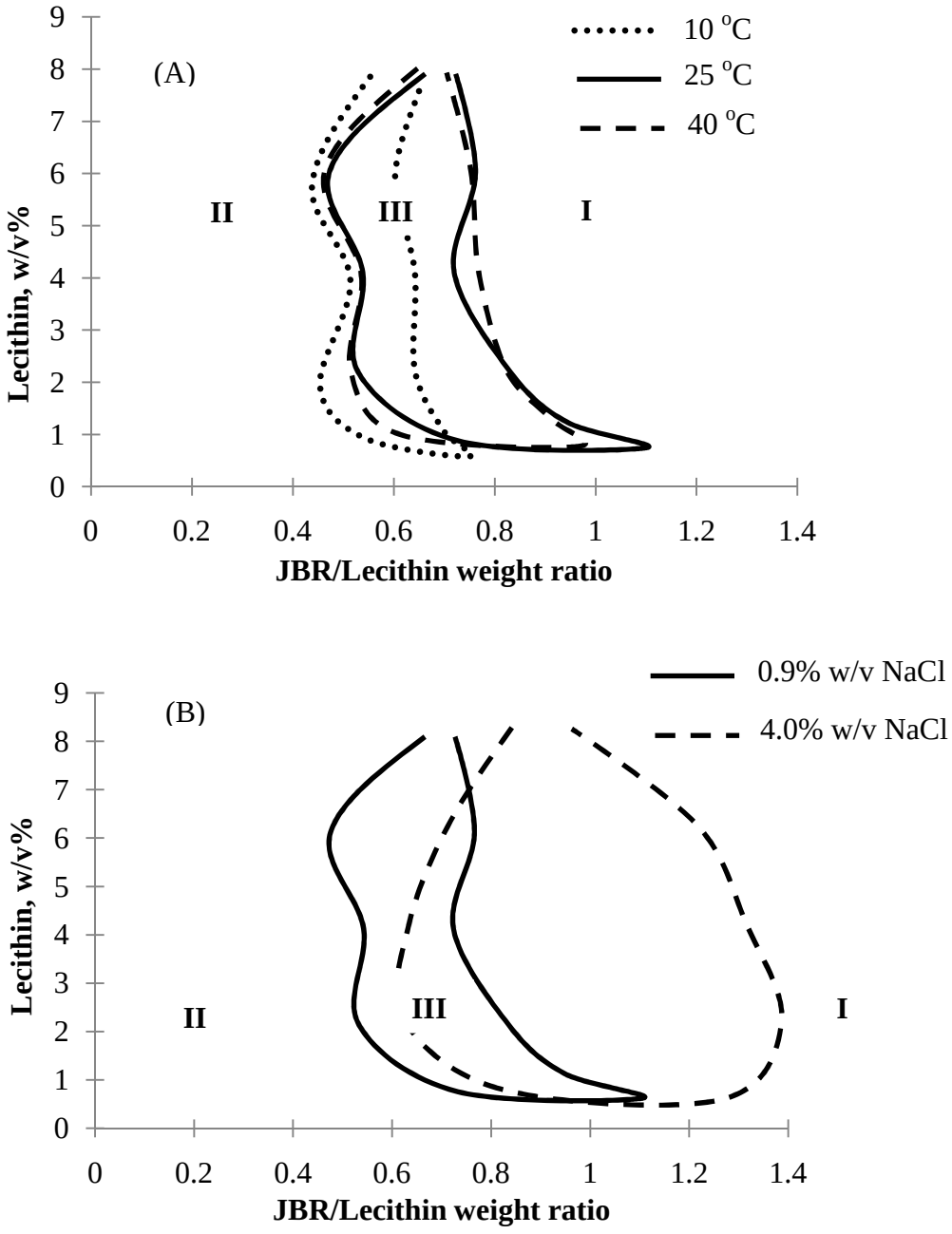


Figure 5.4. Phase behavior diagrams for biocompatible IPM-based microemulsions at different formulation conditions: (A) Effect of temperature (10 °C, 25 °C and 40 °C)

and (B) Effect of electrolyte concentration (0.9% and 4.0% w/v). Microemulsions were prepared at Lecithin/SPL weight ratio = 1/1.

Figure 5.4B presents the effect of electrolyte concentration on the phase behavior of IPM-based microemulsions. As the electrolyte concentration increases from 0.9% to 4.0%, the JBR to lecithin weight ratio slightly increases but the window of middle phase microemulsion (Type III) almost doubles due to the increasing hydrophobicity of the formulation at higher salinity.

The study of temperature and salinity effects thus indicates that Lecithin/SPL/JBR microemulsions are not significantly affected by changing temperature and electrolyte concentration, making these systems desirable in cosmetic and drug delivery applications.

IPM-based vs. Limonene-based biocompatible microemulsions

Figure 5.5 shows the phase diagram of IPM and limonene microemulsions using the biocompatible formulation of lecithin/SPL/JBR. It can be seen that the optimum JBR/Lecithin weight ratio is lower for IPM than limonene which is expected since IPM is the more hydrophobic oil (EACN of 13 versus 6 for limonene). As the oil becomes more hydrophilic, it requires more hydrophilic component in the formulation to balance the interaction between oil-surfactant and water-surfactant to form middle phase microemulsion [20]. Further, as the oil becomes more hydrophobic, the total surfactant concentration necessary to achieve a single phase microemulsion (Type IV) increases [20]. From Figure 5.5 we see that limonene, the less hydrophobic oil,

requires less total surfactant concentration to form Type IV single phase microemulsion, making its applications more economically viable.

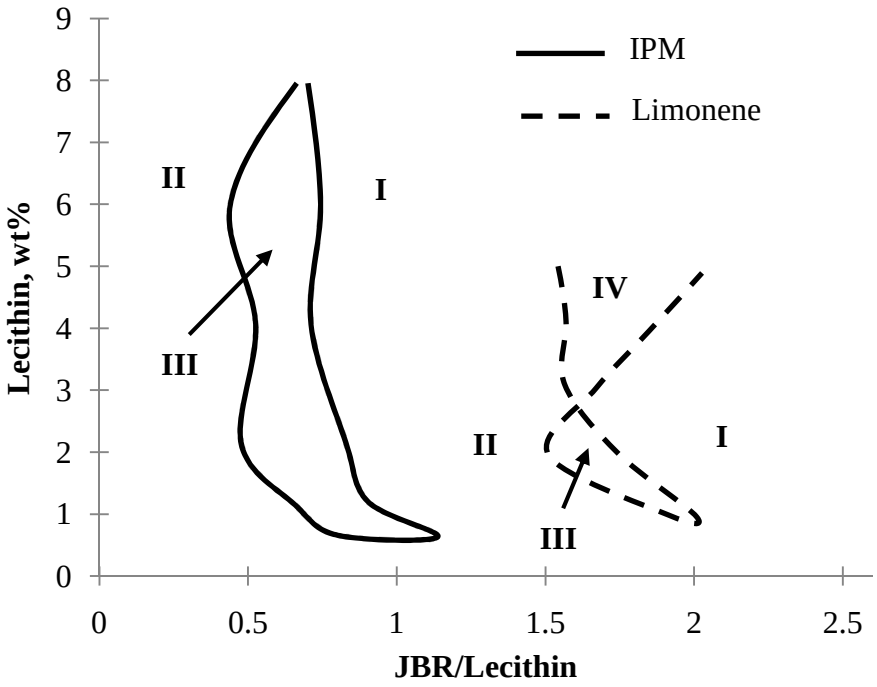


Figure 5.5. Phase behavior diagram for IPM and Limonene microemulsions at 25 ^{o}C, JBR/Lecithin weight ratio = 1/1, 0.9% w/v NaCl.

Biocompatible microemulsion formation for a range of oil types and oil EACNs

Lecithin/SPL/JBR mixtures were used to produce microemulsions with a range of oil (polar oils such as limonene and IPM and nonpolar oils such as decane and hexadecane) as well as oils with varying EACN (equivalent alkane carbon number, from 5.9 for limonene to 16 for hexadecane) (Table 5.2). More hydrophobic oils have a higher EACN value. We observed middle phase microemulsions for all the oils we studied. The single phase Type IV microemulsion was only observed with limonene

due to its hydrophilicity compared to the other three oils. For the same reason, the JBR to lecithin weight ratio is higher for limonene microemulsions. Ultralow interfacial tension (< 0.1 mN/m) was produced for microemulsions of all oils (Figure 5.6). These low IFT values are especially desirable in a wide variety of applications such as cosmetics and hard surface cleaners (limonene), cosmetics and pharmaceuticals (IPM) and detergents (hexadecane). The ultralow IFT values of lecithin microemulsions with hexadecane were also reported by Shinoda et al. [40].

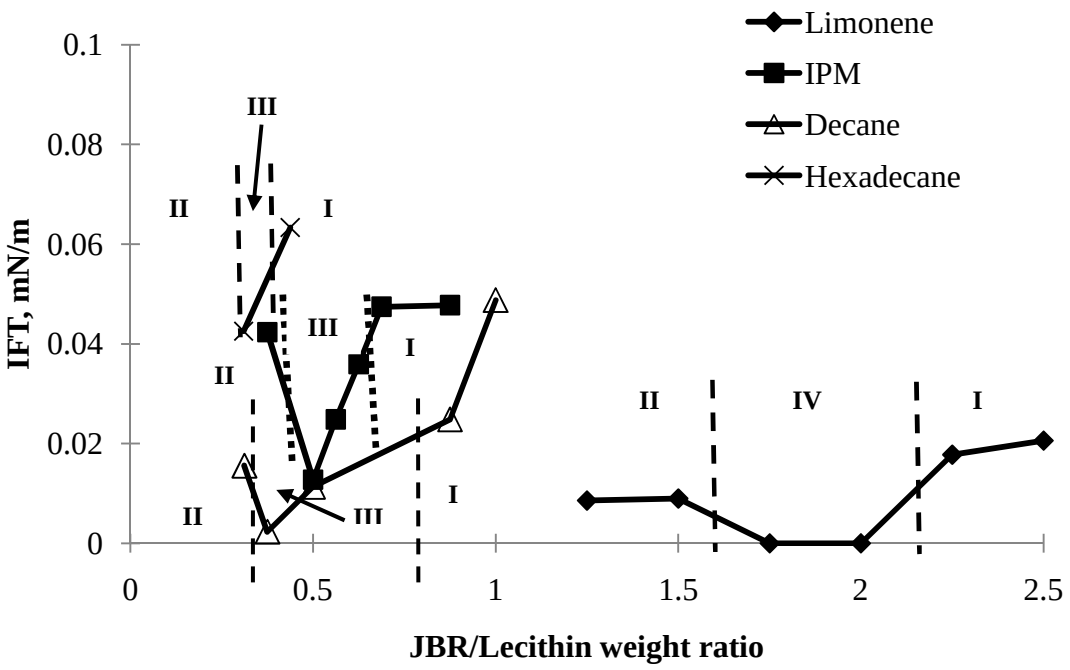


Figure 5.6. Interfacial tension and microemulsion for four different oils: limonene (♦), IPM (■), decane (Δ) and hexadecane (×). Formulations were prepared with Lecithin/SPL concentration of 4/4% w/v and 0.9% w/v NaCl.

Detergency performance on hexadecane removal using biocompatible formulation

To investigate the potential application of our biocompatible formulation (Lecithin/SPL/JBR) in detergency application, we performed detergency tests with this formulation and hexadecane. We chose hexadecane since it has been used in hydrophobic oily soil detergency tests [33, 42]. The detergency performance of our formulation was also compared to that of a commercial detergent (CD), namely liquid Tide.

In our detergency tests, total surfactant concentration was prepared at a range of concentrations (0 to 2000 ppm or 0.2% w/v) with formulation of Lecithin/SPL/JBR = 1.0/1.0/0.3 by weight ratio and 0.9% w/v NaCl. The concentration of CD was also prepared at the same surfactant active concentration range without electrolyte. Figure 5.7A shows the comparison of the detergency power for hexadecane removal at different total active concentrations of our formulation and the commercial liquid detergent (CD). Detergency performance increased as the total active concentration increased for both our formulation and the CD (Figure 5.7A) while the opposite trend was observed for dynamic IFT (Figure 5.7B). At all total active concentration, our formulation achieved higher detergency than CD. The highest detergency obtained with our formulation was 66 ± 1.8% at 1000 ppm or 0.1% w/v (IFT = 3.4×10^{-3} mN/m) while only 47 ± 4.3% (IFT = 2.6 mN/m) detergency was obtained with CD. The IFT values of prewash solutions against hexadecane are lower with our formulation than with CD. Detergency was found to be inversely proportional to IFT value for both our formulation and CD. This relationship was also found in other studies [41, 42].

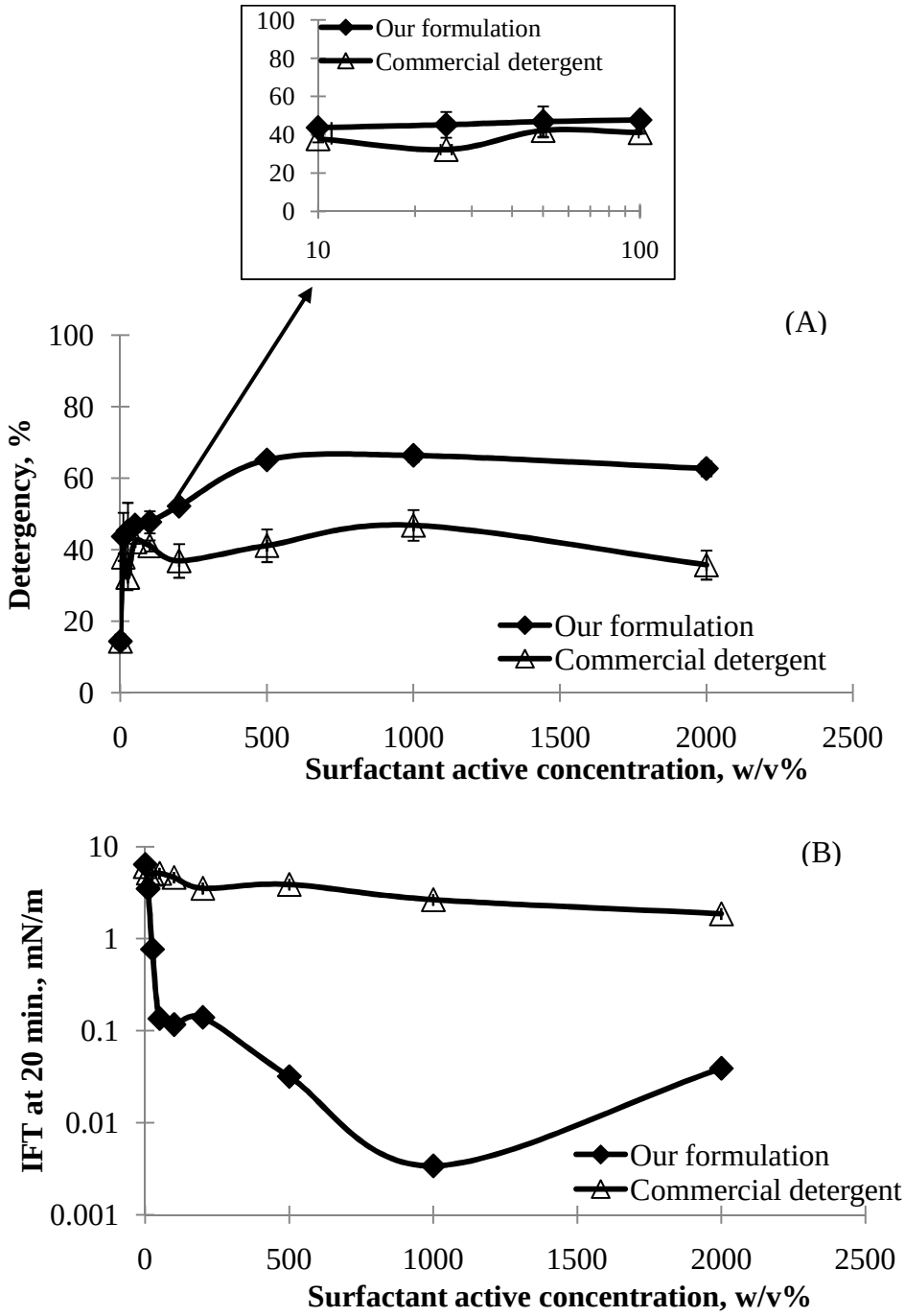


Figure 5.7. Detergency performance (A) and dynamic IFT (B) of our formulation vs. commercial detergent at different total surfactant active concentration. Our formulation has Lecithin/SPL/JBR = 1.0/1.0/0.3 by wt. ratio and 0.9% w/v NaCl.

Our detergency results are comparable to those reported by Tongcumpou et al. [42]. However, our formulation has desirable properties in terms of lower total active concentration and lower electrolyte concentration as compared to Tongcumpou [42]; for example, the same detergency power (~ 65%) was achieved at 0.1% w/v total active concentration and 0.9% w/v electrolyte concentration with our formulation as with 0.25% w/v total active concentration and 5% w/v electrolyte concentration with the formulation of Tongcumpou [42]. In addition, within the studied range of total surfactant active concentrations for household application, our formulation produced much better detergency performance than the commercial liquid detergent for hexadecane removal.

Conclusions

In this work, we compared the hydrophobicity of sophorolipid biosurfactants with conventional synthetic surfactants and rhamnolipid biosurfactant by evaluating the optimum salinity resulting from phase behavior study of these surfactants. Sophorolipid biosurfactants were found to be more hydrophobic than all the other surfactants and thus acted as the hydrophobic component in surfactant mixtures with lecithin and rhamnolipid in microemulsions with a range of oil EACNs and oil types.

We also evaluated the phase behavior of biocompatible microemulsions of lecithin/rhamnolipid/sophorolipid biosurfactant mixture at varying temperature and salinity as well as their potential applications in cosmetics, drug delivery and detergency. The phase behavior of these biocompatible microemulsions did not

change significantly with changing temperature and electrolyte concentration. They also formed microemulsions and produced ultralow IFT for all studied oils. Their detergency power on hexadecane removal was found to be better than commercial liquid detergent at the same surfactant active concentration and comparable with other reported formulations in literature at much lower total surfactant active concentration.

Acknowledgement

The authors thank Oklahoma Center for Advancement of Science and Technology (OCAST) for financial support, Dr. Richard Ashby from USDA-ARS for providing sophorolipid biosurfactants and undergraduate research assistants at the University of Oklahoma, Ashley Edelen and Bridgett Neighbors for helping with the experiments. Sponsors of the Oklahoma University Institute for Applied Surfactant Research (IASR) are also acknowledged (http://cbme.ou.edu/iasr/index.htm).

References

1. Lin, S. C.; Minton, M. A.; Sharma, M. M.; Georgiou, G. 1994. Structural and Immunological Characterization of a Biosurfactant Produced by *Bacillus lichenisformis* JF-2. Applied and Environmental Microbiology, 60 (1), 31-38.
2. Urum, K.; Pekdemir, T. 2004. Evaluation of Biosurfactants for Crude Oil Contaminated Soil Washing. Chemosphere, 57, 1139-1150.

3. Helvaci, Ş. Ş., Pecker, S., and Özdemir, G. 2004. Effect of Electrolytes on the Surface Behavior of Rhamnolipids R1 and R2. Colloids and Surfaces B: Biointerfaces 35, 225-233.

4. Ashby, R. D.; Solaiman, D. K. Y.; Foglia, T. A. 2008. Property Control of Sophorolipids: Influence of Fatty Acid Substrate and Blending. Biotechnol Lett, 30, 1093-1100.

5. Xie, Y., Li, Y., Ye, R. 2005. Effect of Alcohols on the Phase Behavior of Microemulsions Formed by a Biosurfactant – Rhamnolipid. Journal of Dispersion Science and Technology. 26, 455-461.

6. Nguyen, T. T.; Youssef, N. H.; McInerney, M. J.; Sabatini, D. A. 2008. Rhamnolipid Biosurfactant Mixtures for Environmental Remediation. Water Research, 42 (6-7), 1735-1743.

7. Nguyen, T. T.; Sabatini, D. A. 2009. Formulating Alcohol-Free Microemulsions Using Rhamnolipid Biosurfactant and Rhamnolipid Mixtures. Journal of Surfactants and Detergents, 12 (2), 109-115.

8. Van Bogaert, I. N. A.; Saerens, K.; De Muynck, C.; Develter, D.; Soetaert, W.; Vandamme, E. J. 2007. Microbial Production and Application of Sophorolipids. Applied Microbiol Biotechnology, 76, 23-34.

9. Maier, R. M. and Soberón-Chávez , G. 2000. *Pseudomonas Aeruginosa* Rhamnolipids: Biosynthesis and Potential Applications. Appl Microbiol Biotechnol, 54, 625-633.

10. Banat, I. M.; Makkar, R. S.; Cameotra, S. S. 2000. Potential Commercial Applications of Microbial Surfactants. Appl Microbiol Biotechnol, 53, 495-508.

11. Desai, J. D. and Banat, I. M. 1997. Microbiol Production of Surfactants and Their Commercial Potential. Microbiology and Molecular Biology Reviews, 61 (1), 47-64.

12. Rodrigues, L.; Banat, I. M.; Teixeira, J.; Oliveira, R. 2006. Biosurfactants: Potential Applications in Medicine. Journal of Antimicrobial Chemotherapy, 57, 609-618.

13. Brown, M. J. 1991. Biosurfactants for Cosmetic Applications. International Journal of Cosmetic Science, 13, 61-64.

14. Makkar, R. S. and Cameotra, S. S. 2002. An Update on the Use of Unconventional Substrates for Biosurfactant Production and Their New Applications. Appl Microbiol Biotechnol, 58, 428-434.

15. Mulligan, C. N. and Gibbs, B. F. 2004. Types, Production and Applications of Biosurfactants. Proc. Indian natn Sci Acad, B70 (1), 31-55.

16. Kitamoto, D.; Isoda, H.; Nakahara, T. 2002. Functions and Potential Applications of Glycolipid Biosurfactants – from Energy-Saving Materials to Gene Delivery Carriers. Journal of Bioscience and Bioengineering, 94 (3), 187-201.

17. Piljac, G. and Piljac, V. 1996. Immunological Activity of Rhamnolipids. US Patent 5,514,661.

18. Shah, V.; Doncel, G. F.; Seyoum, T.; Eaton, K. M.; Zalenskaya, I.; Hagver, R.; Azim, A.; Gross, R. 2005. Sophorolipids, Microbial Glycolipids with Anti-

Human Immunodeficiency Virus and Sperm-Immobilizing Activities. Antimicrobial Agents and Chemotherapy, 49 (10), 4093-4100.

19. Rosen, M. J. 1989. Surfactants and Interfacial Phenomena. John Wiley & Sons, Inc. 2nd ed.
20. Bourrel, M. and Schechter, R. S. 1998. Microemulsions and Related Systems: Formulation, Solvency, and Physical Properties. Surfactant Science Series 30, 229-302.
21. Lawrence, M. J. and Rees, G. D. 2000. Microemulsion-Based Media as Novel Drug Delivery Systems. Advanced Drug Delivery Reviews 45, 89-121.
22. Vandamme, T. F. 2002. Microemulsions as Ocular Drug Delivery Systems: Recent Developments and Future Challenges. Progress in Retinal and Eye Research 21, 15-34.
23. Kogan, A. and Garti, N. 2006. Microemulsions and Transdermal Drug Delivery Vehicles. Advances in Colloid and Interface Science 123-126, 369-385.
24. Yuan, J. S.; Ansari, M.; Samaan, M.; Acosta, E. J. 2008. Linker-Based Lecithin Microemulsions for Transdermal Delivery of Lidocaine 349 (1-2), 130-143.
25. Komesvarakul, N.; Sanders, M. D.; Szekeres, E.; Acosta, E. J.; Faller, J. F.; Mentlik, T.; Fisher, L. B.; Nicoll, G.; Sabatini, D. A.; Scamehorn, J. F. 2006. Microemulsions of Triglycerides-Based Oils: The Effect of Co-oil and Salinity on Phase Diagrams. J. Cosmet. Sci. 55, 309-325.
26. Malmsten, M. 1999. In *Handbook of Microemulsion Science and Technology.* Kumar, P., Ed.: Marcel Dekker: New York.

27. Witthayapanyanon, A.; Harwell, J. H.; Sabatini, D. A. 2008. Hydrophilic-Lipophilic Deviation (HLD) Method for Characterizing Conventional and Extended Surfactants. Journal of Colloid and Interface Science 325, 259-266.

28. Salager, J. L.; Morgan, J.; Schechter, R. S.; Wade, W. H.; Vasquez, E. 1979a. Optimum Formulation of Surfactant/Water/Oil Systems for Minimum Interfacial Tension or Phase Behavior. Soc. Petrol. Eng. J. 19, 107-115.

29. Salager, J. L.; Morgan, J.; Schechter, R. S.; Wade, W. H. 1979b. Mixing Rules for Optimum Phase Behavior Formulations of Surfactants/Water/Oil Systems. Soc. Petrol. Eng. J. 19, 271-278.

30. Acosta, E. J.; Nguyen, T.; Witthayapanyanon, A.; Harwell, J. H.; Sabatini, D. A. 2005. Linker-Based Biocompatible Microemulsions. Environ. Sci. Technol. 2005, 39, 1275-1282.

31. Childs, J. D., Acosta, E., Knox, R., Harwell, J. H., Sabatini, D. A. (2004) Improving the Extraction of Tetrachloroethylene from Soil Columns Using Surfactant Gradient Systems. J Contam Hydrol, 71, 27-45.

32. ASTM, *Annual Book of ASTM Standards*, Vol. 15.04, ASTM International, West Conshohocken, PA, 2003, Method D3035-98.

33. Tongcumpou, C.; Acosta, E. J.; Quencer, L. B.; Joseph, A. F.; Scamehorn, J. F.; Sabatini, D. A.; Chavadej, S.; Yanumet, N. 2003. Microemulsion Formation and Detergency with Oily Soils: I. Phase Behavior and Interfacial Tension. Journal of Surfactants and Detergents 5 (2), 1-13.

34. Acosta, E.; Mai, P. D.; Harwell, J. H.; Sabatini, D. A. 2003. Linker-Modified Microemulsions for a Variety of Oils and Surfactants. Journal of Surfactants and Detergents 6 (4), 353-363.

35. Phan, T. T.; Witthayapanyanon, A.; Harwell, J. H.; Sabatini, D. A. Microemulsion-based Vegetable Oil Detergency using Extended Surfactant. *Submitted to Journal of Surfactants and Detergents, 2009.*

36. Winsor, P. 1954. Solvent Properties of Amphiphilic Compounds. Butterworth, London.

37. Salager, J. L.; Antón, R. E.; Sabatini, D. A.; Harwell, J. H.; Acosta, E. J.; Tolosa, L. I. 2005. Enhancing Solubilization in Microemulsions – State of the Art and Current Trends. Journal of Surfactants and Detergents 8 (1), 3-21.

38. Söderberg, I.; Drummond, C. J.; Furlong, D. N.; Godkin, S.; Matthews, B. 1995. Non-ionic Sugar-Based Surfactants: Self Assembly and Air/Water Interfacial Activity. Colloids and Surfaces A: Physicochemical and Engineering Aspects 102, 91-97.

39. Soderman, O.; Johansson, I. 2000. Polyhydroxyl-Based Surfactants and Their Physico-chemical Properties and Applications. Curr. Opin. Colloid Interface Sci. 4 (6), 391-401.

40. Shinoda, K.; Shibata, Y.; Lindman, B. 1993. Interfacial Tensions for Lecithin Microemulsions Including the Effects of Surfactant and Polymer Addition. Langmuir 9, 1254-1257.

41. Thompson, L. 1994. The Role of Oil Detachment Mechanisms in Determining Optimum Detergency Conditions. Journal of Colloid and Interface Science 163, 61-73.

42. Tongcumpou, C.; Acosta, E. J.; Quencer, L. B.; Joseph, A. F.; Scamehorn, J. F.; Sabatini, D. A.; Chavadej, S.; Yanumet, N. 2003. Microemulsion Formation and Detergency with Oily Soils: II. Detergency Formulation and Performance. Journal of Surfactants and Detergents 6 (3), 205-214.

CHAPTER 6

Conclusions

This chapter summarizes the knowledge gained from each section of this dissertation and highlights some significant findings from this work. The overall purpose of this dissertation is to explore the properties of biosurfactants and their ability to formulate microemulsions with a wide range of oils and to discuss the potential use of biosurfactants in replacing conventional synthetic surfactants in practical applications.

Chapter 2 evaluated the hydrophilicity/hydrophobicity of rhamnolipid biosurfactant based on the optimum salinity resulting from rhamnolipid-toluene microemulsion phase diagram. It was found that this microemulsion system possessed a high optimum salinity range (10-16 % w/v), which indicates that rhamnolipid was relatively hydrophilic. Thus, mixtures of rhamnolipid with more hydrophobic surfactant were needed to formulate microemulsions for more hydrophobic oils. With these mixtures, ultralow interfacial tension (< 0.1 mN/m) was achieved for all hydrocarbon oils such as hexane, decane and hexadecane. This chapter also served as a guideline in formulating microemulsions with hydrocarbons or mixtures of hydrocarbons that have different hydrophobicity.

Chapter 3 further studied the hydrophilicity of rhamnolipid biosurfactant by determining the characteristic curvature (Cc) of rhamnolipid using the hydrophilic-lipophilic deviation (HLD) model. Knowing the Cc value of rhamnolipid, we were able to quantitatively compare its hydrophilicity with conventional synthetic

surfactant. Surfactants with more positive Cc values are more hydrophobic while those with more negative Cc values are more hydrophilic. The Cc value of rhamnolipid biosurfactant was determined to be -1.41. Thus, rhamnolipid is more hydrophobic than sodium dodecyl sulfate (Cc = -2.34), but more hydrophilic than sodium dodecyl benzene sulfonate (Cc = -0.91). This finding serves as a helpful guideline when rhamnolipid biosurfactant is considered to replace conventional synthetic surfactants in microemulsion formulation.

Chapter 4 demonstrates the feasibility of the vegetable oil extraction technique using diesel-based reverse-micellar microemulsions for biofuel application. Diesel-based microemulsions were produced using environmentally friendly biosurfactant/biorenewable surfactant mixtures. This extraction technique was proposed based on the “like dissolves like” principle and the resulting product was the blend of diesel and vegetable oil. This blend was then evaluated for use as biofuel. The results showed that the oil extraction efficiency was ~ 95% with only single step extraction and the blending product met the requirements of biodiesel in terms of the viscosity, composition, cloud point and pour point.

In chapter 5, hydrophobicity/hydrophilicity of sophorolipid biosurfactants was evaluated and compared to conventional synthetic surfactant and rhamnolipid. Two types of sophorolipids were studied, oleic acid sophorolipid (SPL-O, C18 tail) and palmatic acid sophorolipid (SPL-P, C16 tail). SPL-P was found to be slightly more hydrophilic than SPL-O, as expected. However, both sophorolipid biosurfactants showed higher hydrophobicity than conventional hydrophobic surfactant sodium

bis(2-ethyl)dihexyl sulfosuccinate. Again, this finding can serve as a useful guide in replacing synthetic surfactants by sophorolipid biosurfactants in microemulsion formulations. This chapter also demonstrated the potential properties of biocompatible lecithin-based microemulsions using sophorolipid and rhamnolipid biosurfactants in cosmetic and drug delivery applications. These biocompatible microemulsions formed with limonene and isopropyl myristate were found to be quite insensitive to changes in temperature and electrolyte concentration, making them desirable in cosmetics and drug delivery. In addition, the hexadecane detergency performance of these biocompatible formulations were investigated and found to be better than that of commercial detergent and comparable with other formulations reported in literature.

APPENDIX A

Rhamnolipid Biosurfactant Mixtures for Environmental Remediation (Chapter 2)

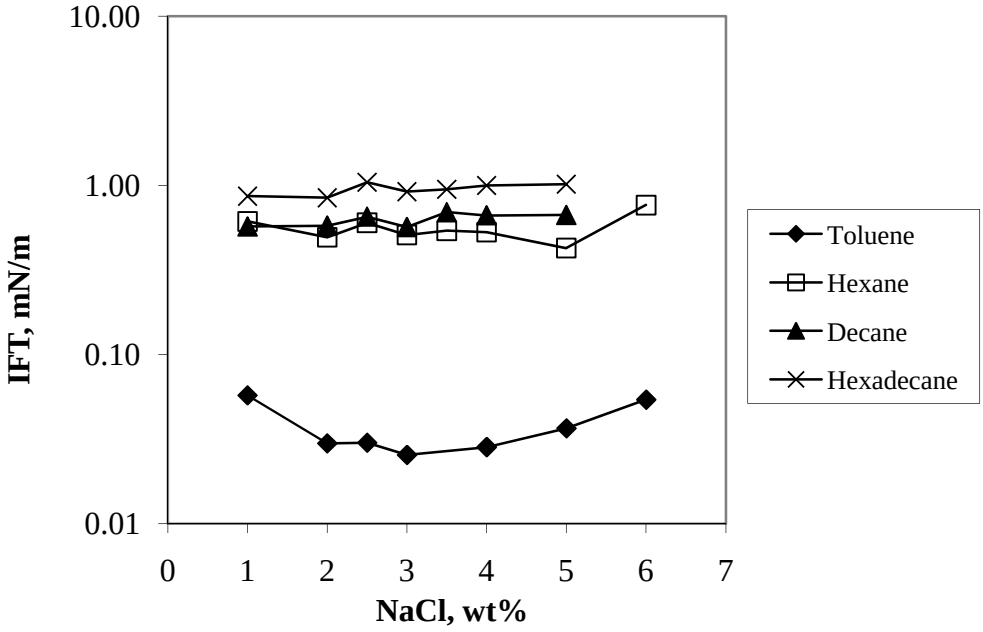


Figure A1. Dynamic IFTs at 15 minutes of rhamnolipid biosurfactant at 0.01 wt% for four oils versus salinity

APPENDIX B

Formulating Alcohol-Free Microemulsions Using Rhamnolipid Biosurfactant and Rhamnolipid Mixtures (Chapter 3)

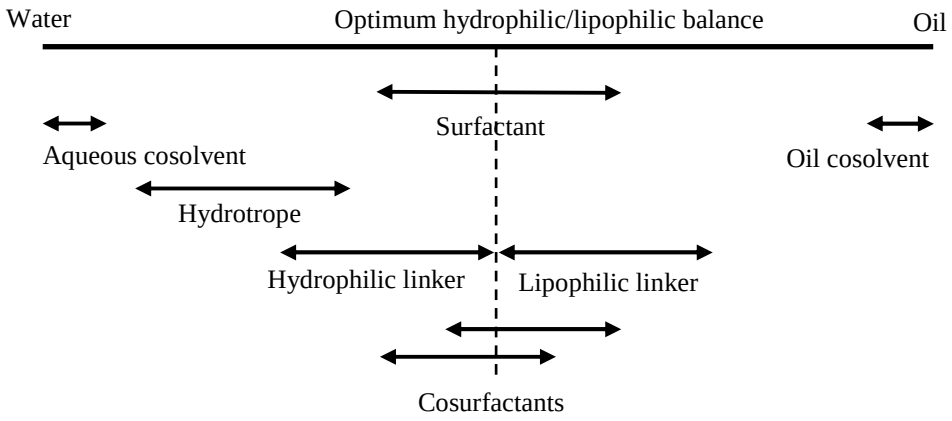


Figure B1. Relative hydrophilicity/lipophilicity of microemulsion additives

APPENDIX C

Biocompatible Lecithin-Based Microemulsions with Rhamnolipid and Sophorolipid Biosurfactants: Potential Applications (Chapter 5)

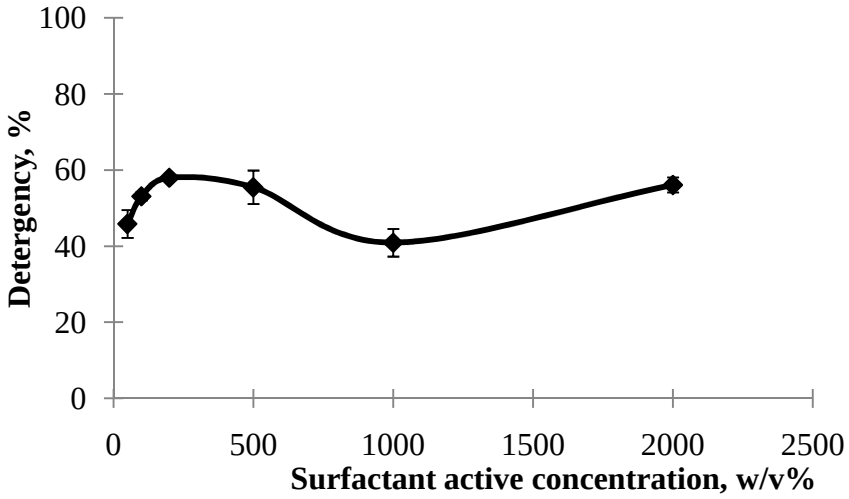


Figure C1. Detergency performance on hexadecane removal using our formulation that forms Type I microemulsions with hexadecane.

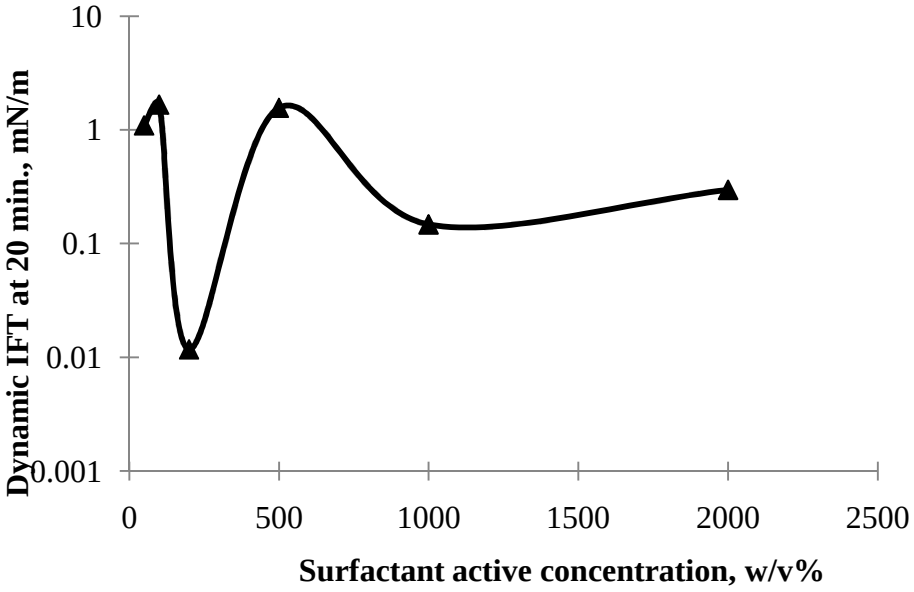


Figure C2. IFT at 20 minutes of our Type I formulation against hexadecane